Improving breast cancer therapy through oestrone analogue and glycolysis inhibitor synergism

By
Roxette Dianne Anderson

(29003238)

Submitted in fulfillment of part of the requirements for the degree
Masters of Science (Pharmacology)
In the faculty of Health Sciences
University of Pretoria
Pretoria
November 2015

Supervisor: Prof AD Cromarty
Co-supervisors: Prof AM Joubert and A van Tonder

i

Declaration

University of Pretoria

Faculty of Health Sciences

Department of Pharmacology

I, Roxette Dianne Anderson

Student number: 29003238

Subject of project: Improving breast cancer therapy through oestrone analogue and glycolysis inhibitor synergism

Declaration

1. I understand what plagiarism is and am aware of the University's policy in this regard.
2. I declare that this project is my own original work. Where other peoples work has been used (either from a printed source, internet or any other source), this has been properly acknowledged and referenced in accordance with departmental requirements.
3. I have not used work previously produced by another student or any other person to hand in as my own.
4. I have not allowed, and will not allow, anyone to copy my work with the intention of passing it off as his or her own work.

Signature

…………………………

ii

Acknowledgements

I would like to acknowledge the following people for their contribution and support throughout the duration of the study:

iii

- My boyfriend JP. Hulley for being my rock of strength and for his support, patience, motivation, understanding and help throughout this study as well as the comical relief during weekends and holidays in the lab

- To my late father who provided me with the opportunity to study and chase my goals. I am forever grateful for what you did for me and the inspiration and motivation with which you left me.

iv

Abstract

Introduction: In South Africa, breast cancer has the highest prevalence with a life time risk of 1 in every 9 women being diagnosed annually. There are four sub-types of breast cancer and according to the stage of the cancer, various treatment regimens are prescribed. A major obstacle is that majority of cancers have developed multi-drug resistance and new treatment regimens need to be developed in order to obtain therapeutic efficacy. Cancer cells use aerobic glycolytic metabolism for energy generation and inhibition of this pathway increases sensitivity of the cells to anti-neoplasic treatments. 2-Deoxyglucose (2-DG) competes with and inhibits glucose uptake inhibiting the glycolytic pathway which can result in depolarisation of the mitochondrial membrane potential releasing cytochrome *c*. Two 2-Methoxyestradiol (2-ME) derivatives, ESE-15-ol and ESE-16 have shown to be promising anti-cancer agents and combination therapy could allow the use of these compounds with a decreased side effect profile. The combination of these compounds with 2-DG was therefore investigated.

Aim: To investigate combinations of two oestrone analogues and the glycolysis inhibitor 2-deoxyglucose for potential synergistic effects using a cell enumeration assay, mitochondrial membrane potential and cell cycle analysis, on breast cancer cells in an *in vitro* setting. Cell apoptosis, necrosis and autophagy pathways were assessed to indicate the mechanism of cytotoxicity.

Methods: The breast cancer MCF-7 and non-tumorigenic MCF-12A cell line were used. Cells were exposed to ESE-15-ol, ESE-16 and 2-DG alone and in combination. Mechanistic studies were performed using the various research methodologies including the sulforhodamine B assay for cell enumeration, Annexin-V FITC and propidium iodide labeling for apoptosis/necrosis studies, PlasDIC and light microscopy for morphological analysis, propidium iodide staining for cell cycle progression, JC-1 for mitochondrial membrane potential studies, transmission electron microscopy and western blotting for the analysis of autophagy.

Results: A GI_{50} of 34.1 nM was reported for MCF-7 cells after treatment with ESE-15-ol, 141 nM for ESE-16 and 1.3 mM 2-DG. The GI_{50} of ESE-15-ol treated MCF-12A cells was 141 nM, 140.1 nM for ESE-16 treated cells and 1.7 mM for 2-DG. ESE-16 had the greatest effect on cell viability in MCF-7 cells and a shift from an inhibitory effect to the initiation of cell death was evident after treatment of 100 nM of ESE-15-ol and ESE-16. 2-DG had a lower cytotoxic effect than the oestrone analogues. The MCF-12A cell line was less susceptible to the experimental compounds. The combination of the oestrone analogues with 2-DG elicited a greater effect on

v

cell enumeration than each of the compounds alone with a less pronounced effect on the MCF-12A cell line in comparison to the MCF-7 cells. The experimental compounds initiated apoptosis with ESE-16 eliciting a greater effect than ESE-15-ol. The combination of the oestrone analogues with 2-DG resulted in increased apoptosis in contrast to the compounds alone. ESE-16 alone and in combination with 2-DG lead to the most prominent morphological changes, with ESE-15-ol decreasing cell density slightly. The combination of ESE-15-ol with 2-DG decreased cell density with membrane blebbing apparent. The MCF-12A cell line was less susceptible to morphological changes after treatment of ESE-15-ol with 2-DG however ESE-16 and the combination with 2-DG resulted in similar attributes seen in MCF-7 treated cells. ESE-15-ol resulted in accumulation of cells in the G2 cell cycle phase which was further amplified after the combination of 2-DG. A sub-G1 accumulation was observed after treatment with ESE-16 with a shift to a G2 accumulation after the combined treatment of ESE-16 with 2-DG. After 48 hours, ESE-15-ol alone and in combination with 2-DG on MCF-7 cells resulted in depolarisation of the mitochondrial membrane. A slight decrease in the membrane potential was observed after treatment with ESE-16 and this was further increased after the combined treatment of ESE-16 with 2-DG. The MCF-12A were less susceptible after 24 hour treatment than 48 hour exposure of the experimental compounds. The presence of autophagic-like vacuoles were apparent in all treatment groups as well as the increased expression of LC3-II.

Conclusion: The combined treatment of synthetic oestrone analogues with 2-DG displayed greater therapeutic efficacy than each of the compounds alone. As a result, the apoptotic and autophagic pathways were induced and a shift in cell cycle progression was observed. Mitochondrial involvement was apparent and the compounds significantly affected cell viability. This suggests that the combinations between the antimitotic oestrone analogues and glycolysis inhibitor 2-DG act synergistically to induce apoptosis and autophagy in MCF-7 breast cancer cells.

Keywords: Breast cancer, combination therapy, glycolysis inhibitors, oestrone analogues, mechanisms, synergism, cell death, *in vitro*, MCF-7, MCF-12A.

vi

Contents

viii

ix

Glossary of abbreviations

%	Percentage
ABC	ATP-binding cassette
ADP	Adenosine diphosphate
Akt	Protein kinase B
Apaf-1	Apoptotic protease activating factor 1
ASA	Adherent state apoptosis assay
ATCC	American Type Culture Collection
Atg	Autophagy related
ATP	Adenosine tripohosphate
Bad	Bcl-2-associated death promoter
BAEC	Bovine aortic endothelial cells
BAK	Bcl-2 homologous antagonist/killer
BAX	Bcl-2-like protein 4
Bcl-2	B-cell lymphoma protein 2
Bcl-xL	B-cell lymphoma-extra large
BRCA1/2	Breast cancer associated gene ½
CARD	Adaptor proteins binding to the caspase activation and recruitment domain
Caspase	Cysteinyl aspartic acid-protease
CAT	Cationic amphiphilic tracer
CDK	Cyclin dependent kinase
CI	Combination index
c-Myc	Transcription factor
CO_2	Carbon dioxide
Complex I	NADH: ubiquinone oxioreductase
Complex III	Ubiquinol: cytochrome c oxioreductase; cytochrome bc complex
DCA	Dichloro acetate
DCIS	Ductal carcinoma *in situ*
DIC	Differential interference contrast

x

DISC	Death-inducing signaling complex
2-DG	2-Deoxyglucose
DMEM	Dulbecco's Modified Eagles Medium
DMSO	Dimethyl sulfoxide
DMEM/Ham's F12	Dulbecco's Modified Eagles Medium/ Nutrient mixture F-12 Ham's, Kaighn's Modification
DNA	Deoxyribonucleic acid
E2F	Elongation factor 2
EMBS	(8R, 13S, 14S, 17S)-2-Ethyl-13-methyl-7,8,9,11,12,13,14,15,16,17-decahydro-6H-cyclopenta[a]-phenanthrene-3, 17-diyl bis(sulfamate)
ERK1	Extracellular signal-related kinase 1
ESE-15-ol	2-ethyl-3-O-sulphamonyl-estra-1,3,5(10),15-tetraen-17-ol
ESE-15-one	2-ethyl-3-O-sulphamoyl-estra-1,3,5(10),15-tetraen-17-one
ESE-16	2-ethyl-3-O-sulphamoyl-estra-1,3,5(10)16-tetraene
ETC	Electron transport chain
FADD	Apoptosis stimulating factor associated protein with death domain
FAS	Apoptosis stimulating factor
FCS	Foetal calf serum
G	Gram
G	Relative centrifugal force
GFP-LC3	Green fluorescent protein microtubule-associated protein 1 light chain 3
GI_{50}	50% Growth inhibitory concentration
G0	Quiescence
G1 phase	First gap or growth phase
G2 phase	Gap phase two
GFP	Green fluorescent protein
GLUT	Glucose transporter
GSH	Glutathione

xi

H	Hour
HeLa	Human epithelial cervical cancer cell line
HepG2	Hepatocarcinoma cell line
HER-2	Human epidermal growth factor receptor 2
HIF-1	Hypoxia-induced factor 1
HPV	Human papilloma virus
HT29D4	Colonic cell line
IC_{50}	Concentration at which cell proliferation is reduced by half
IGROV1-R10	Head cancer cell line
INK 4	Inhibition of cyclin dependent kinase 4
JC-1	5, 5', 6, 6'-tetrachloro-1, 1', 3, 3'-tetraethylbenzimidazolyl carbocyanine iodide
L	Litre
LC3	Microtubule-associated protein 1 light chain 3
LC3-II	Microtubule-associated protein II light chain 3
LCIS	Lobular carcinoma *in situ*
LC-MS/MS	Liquid chromatography tandem mass spectrometry
LKB1	Liver kinase B1
LN-229	Human brain glioblastoma cell line
LNCaP	Human prostate cancer cell line
M	Molar (moles/litre)
2-ME	2-Methoxyestradiol
M phase	Mitotic phase
MCF-7	Estrogen receptor positive breast cancer cell line
MCF-12A	Non-tumorigenic breast cell line
MDA-MB-231	Estrogen receptor negative breast cancer cell line
MDR	Multidrug resistance
MEF	Mouse embryo fibroblast cells
mg	Milligram
mL	Millilitre

xii

mM	Millimolar
MPF	Maturation promoting factor
MSTO-211H	Mesothelioma cell line
MtDNA	Mitochondrial DNA
mTORC1	Mammalian target of rapamycin complex 1
MTT	3-(4,5-dimethylthiazol-2-yl)-2,5-diphenyltetrazolium bromide
N	Number of observations in sample
NaCl	Sodium chloride
NAD	Nicotinamide-adenine-dinucleotide
NADH	Nicotinamide-adenine-dinucleotide (reduced form)
nM	Nanomolar
OxPhos	Oxidative phosphorylation
P	P-value
PARP	poly (ADP-ribose) polymerase
PBS	Phosphate buffered saline
PC3	Human androgen insensitive prostate cancer cell line
PCD	Programmed cell death
PDK	Pyruvate dehydrogenase kinase
PE	Phosphatidylethanolamine
pH	Negative log of hydrogen ion concentration
PI	Propidium iodide
PI3(K)	Phosphatidylinositol 3- kinase
PlasDIC	Polarization optical differential interference contrast microscopy
pRb	Retinoblastoma protein
PS	Phosphatidylserine
PTEN	Phosphatase and tensin
PVDF	Polyvinylidene difluoride
p53	Cellular tumor antigen p53
R	Restriction point

xiii

Raf-1	Raf-1 proto-oncogene serine/threonine kinase
Ras	Small GTPase protein
Rho123	Rhodamine 123
RNA	Ribonucleic acid
RNAse	Ribonuclease
ROS	Reactive oxygen species
RSA	Republic of South Africa
SCC12B2	Neck squamous cancer cell line
SCC61	Neck squamous cancer cell line
SDS	Sodium dodecyl sulphate
SDS-PAGE	Sodium dodecyl sulphate polyacrylamide gel electrophoresis
SEM	Standard error of the mean
Ser	Serine
SkBr3	Breast adenocarcinoma cell line
SKOV3	Head cancer cell line
SQ2OB	Neck squamous cancer cell line
S-phase	Synthesis phase
SNO	Oesophageal carcinoma cell line
SRB	Sulforhodamine B
STX140	2-Methoxyoestradiol-3,17-O,O-bis-sulphamate
Sub-G1 phase	Fractional DNA content (apoptosis)
T98G	Human brain glioblastoma cell line
TCA	Tricarboxylic acid
TEM	Transmission electron microscopy
TIGAR	TP53-induced glycolysis and apoptosis regulator
TRADD	Tumour necrosis factor receptor type 1 associated death domain
TRAIL R1/2	Tumour necrosis factor related apoptosis inducing ligand receptor type ½
U937	Human monocytic leukemia cell line
UK	United Kingdom
ULK1	Unc-51 like autophagy activating kinase

xiv

USA	United States of America
XTT	2,3-bis[2-methoxy-4-nitro-5-sulfophenyl]-2H-tetrazolium-5-carboxanilide inner salt
°C	Degree Celsius
µl	Microlitre
µM	Micromolar
µm	Micrometer

List of figures

List of tables

Chapter 1: Introduction

1. Literature review

1.1 The prevalence of cancer

Cancer is a worldwide health problem with 14 million new cases being reported in 2012 of which 8.2 million resulted in death (Stewart and Wild, 2015). In the UK approximately 1 685 000 new cases of cancer were estimated to occur resulting in 595 690 deaths in 2016 (Siegel *et al.*, 2016). .It has been hypothesised that the number of new cases will increase by approximately 70% over the next 20 years (Stewart and Wild, 2015).

The growth of the population in Africa is estimated to result in 1.28 million new cases of cancer by 2030 (Blecher *et al.*, 2008). Annually in South Africa, more than 100 000 people are diagnosed with this deadly disease and only 6 out of 10 people will survive if treatment regimens are optimised and the patient enters remission. In South Africa, breast cancer has the highest prevalence with a life time risk of 1 in every 9 females being diagnosed annually (www.cansa.org.za, 2010). The average age at which breast cancer is diagnosed is decreasing and due to this, women have an increased chance of developing cancer by the age of 60. Breast cancer presented with the highest incidence of all cancers between 1975 and 2009 and in 2013, resulting in approximately 40 030 deaths of which only 410 were male patients (Siegel *et al.*, 2013). It has been estimated that an increase of 78% in the number of cancer cases will occur in South Africa by 2030 (Bray *et al.*, 2012).

Estimates for 2016 reveal that breast cancer will present with the highest number of new cancer cases of approximately 2600 cases of breast cancer reported in men and 246 600 cases in women. Out of the 595 690 deaths that were estimated to occur last year as a result of cancer, 40 890 were estimated to be as a result of breast cancer in both female and male patients with breast cancer ranking as the second highest cause of cancer deaths in women. It has been hypothesised that 61 000 *in situ* breast cancer cases would be diagnosed in 2016 (Siegel *et al.*, 2016).

Estimates revealed that breast cancer accounted for approximately 29 % of the reported cancer cases in 2013. Statistics showed that up until the age of 39 years, females have a 1 in 202 chance of developing this form of invasive cancer and throughout their lifetime this increases to a 1 in 8 chance (Siegel *et al.*, 2013). The death rate as a result of cancer in men has decreased

1

since 1991 by 23% due to the increased early diagnosis and treatment of prostate cancer, however, in women the trends remain stable (Siegel *et al.*, 2016). Early diagnosis of breast cancer and increased treatment regimens have significantly decreased mortality rates (Siegel *et al.*, 2016).

1.2 The risk of developing cancer

Age is a contributing factor in the development of cancer with approximately 86% of diagnosed cancers in people over the age of 50 years (Siegel *et al.*, 2016). Behavioural factors such as smoking, unhealthy diets and a sedentary lifestyle are also contributing factors (www.who.int, 2015). The probability that a person will die after a confirmed cancer diagnosis has been estimated to 1 in 2 men and 1 in 3 women (Siegel *et al.*, 2016). Family history is linked to genetic risk factors in the development of cancer with women being twice as likely to develop breast cancer if there is a family history of breast cancer. Genetic predisposition accounts for 10% of breast cancer in western countries and is inherited through an autosomal dominant gene (McPherson *et al.*, 2000).

The precise number of breast cancer genes remains unknown however the breast cancer associated gene 1 (BRCA1) and breast cancer associated gene 2 (BRCA2) have been identified to contribute to genetic predisposition. These genes are located on the long arm of chromosomes 17 and 13 and have been reported to easily undergo mutations.

A common risk factor in the development of breast cancer is excessive weight gain after the age of 18 years. Common risk factors include but are not limited to the use of replacement hormone therapy after menopause, alcohol consumption, recent use of oral contraceptives, never having children or having the first child after the age of 30 as well as high plasma levels of sex hormones (McPherson *et al.*, 2000).

1.3 Staging of cancer at the time of diagnosis

At the time of diagnosis, cancers need to be staged in order to determine the extent of the cancer growth and whether metastasis has occurred. This staging is essential in order for optimal treatment regimens to be initiated. The stage of cancer is based on whether or not the tumour is localised or has metastasised, as well as the size of the primary tumour. *In situ* is the term used for cancer cells that are present in the layer of cells in which they initially developed and have not spread to other target areas. If however the tumour penetrates this layer it is termed

2

invasive and is further categorised as local, regional or distant. Within a clinical setting, the TNM system is used to assess the extent of the primary tumour (T), whether or not lymph nodes are involved within the region (N) as well as whether or not metastases are involved (M). Following this, a stage is assigned such as stage 0 (in situ), stage I (early), stage III (intermediate) and stage IV (advanced disease) (Siegel *et al.*, 2016).

There are two forms of stage 0 breast cancer namely ductal carcinoma *in situ* (DCIS) and the less prevalent lobular carcinoma *in situ* (LCIS) (Pravettoni *et al.*, 2016). DCIS is diagnosed by the presence of abnormally growing cells in the milk ducts of the breasts in contrast to LCIS where abnormal cells are apparent in the milk gland lobules of the breast (Foote Jr and Stewart, 1941, Holland *et al.*, 1994). When cancer cells have not spread beyond the primary site or have spread to a minimal number of lymph nodes stage I cancer is diagnosed. Stage II cancer is characterised by the tumour at the primary site of growth and sometimes apparent in nearby lymph nodes (Greenough, 1925). Tumour progression from the primary site to other sites including nearby lymph nodes is characteristic of stage III cancer. This stage is an advanced primary cancer and is marked by local and regional extensions (Hortobagyi *et al.*, 1988). A large number of lymph nodes are observed to be cancerous and often the tumour increases in size and grows into the wall of the chest or skin of the breast. Stage IV cancer is characteristic of the cancer spreading to other parts of the body often including the brain, bones, liver or lungs (Greenough, 1925).

1.4 Breast cancers

The majority of cancers develop in the terminal duct lobular units which are the secretory units of the breast (Tavassoli and Devilee, 2003). Tumour cells in the breast are characterised by the lack of organisation of the tissue. A characteristic of benign tumours of the breast are the tumour cells remaining localised within the basement membrane of the ductal lobular system of the breast (Gusterson *et al.*, 1982). Malignancy is observed once the tumour cells break through the basement membrane (Ronnov-Jessen *et al.*, 1996). Malignancy of the breast is marked by a decrease in myoepithelial cells (Gudjonsson *et al.*, 2005) and an increase in myofibroblasts and general increased vascularisation of the tumour (Bissell and Radisky, 2001). Histologically, breast cancers can be classified into 18 different subtypes based on patterns of growth and the characteristics of the tumour cells (Tavassoli and Devilee, 2003). Breast cancers are divided into two groups which are characteristic of the presence or absence of the nuclear oestrogen receptor. This classification of mammary tumours allows for the

3

prediction of the effect that chemotherapeutic agents will elicit on the tumour. Metastases can be detected at all stages of the disease but is more dominant in stages III and IV (Harris *et al.*, 2012)

A useful marker is the expression of oestrogen receptors in order to predict the reaction that will be initiated in response to the treatment administered (Hayes *et al.*, 1996). These phenotypes of breast cancer include oestrogen receptor positive, oestrogen receptor negative and triple negative breast cancer. These tumour markers have a significant role in cancer research due to their impact on survival rates, prognosis, treatment as well as relation to the subtypes of breast cancer (Bauer *et al.*, 2007). Responses initiated due to endocrine therapy have previously been described to be attributed to the expression of the oestrogen receptor (Lumachi *et al.*, 2013). Oestrogen receptor positive breast cancer features an abundant expression of cyclin D1 which is involved in regulating cell cycle progression through G1/S phase transition. This transition is a prerequisite for oncogenesis (Agarwal *et al.*, 2009, Yu *et al.*, 2001). Oestrogen receptor positive breast cancer is stimulated by higher oestrogen levels (Henderson *et al.*, 1988). Patients with oestrogen receptor positive breast cancer elicit a predictable response to endocrine therapies (Bauer *et al.*, 2007).

Currently five subtypes of breast carcinoma have been identified namely luminal A, luminal B, normal breast-like, basal like and human epidermal growth factor receptor 2 (HER2) over-expressing (Perou *et al.*, 2000). The basal like subtype is characterised by the triple negative breast cancer showing low levels of oestrogen, and progesterone receptors and normal levels of HER2-cell surface receptors (Foulkes *et al.*, 2003, Livasy *et al.*, 2006, Sørlie *et al.*, 2001). Breast cancers without the absence of a detectable oestrogen receptors form the remainder of breast cancers and are seldom responsive to hormonal therapy (Katzenellenbogen, 1991). The two main subtypes of the negative oestrogen receptor breast cancer are the basal-like and HER-2 subtype. Oestrogen receptor positive tumours are characterised by the luminal A and B subtypes (Sørlie *et al.*, 2001, Sørlie *et al.*, 2003). Higher expression of the oestrogen receptor is displayed in luminal A and has been linked to increased patient response to anti-hormone treatment (Sørlie *et al.*, 2003).

1.5 Detection of breast cancer

Early detection is essential for the successful treatment of many types of cancers including breast cancer (www.who.int, 2015). A common method for the detection of breast cancer is through a low-dose x-ray known as a mammogram. This technique is usually effective,

4

however false negative and false positive diagnosis is possible with the majority of women with an abnormal mammogram not having cancer. The average guideline for mammography is annually for women above the age of 40 years. From the age of 30 years, the combination of mammography with magnetic resonance imaging is suggested if the patient has a high risk factor (Saslow *et al.*, 2007).

Due to the fact that cancer is such a prevalent disease and affects more of the population each year, it is extremely important that the treatment offered is significantly improved. Moreover it is essential that better prevention strategies, as well as new treatment regimens are developed.

1.6 Current treatment regimens

Cancer treatment has significantly transformed over the years and there has been a shift from high dose non-specific chemotherapy to targeted treatment that maximises anti-tumour activity with minimal adverse side effects (Abou-Jawde *et al.*, 2003).

There are currently several approaches that aim to target cancer and to prevent further metastasis. These approaches include treatment procedures such as surgery, radiotherapy, chemotherapy including hormone therapy, immunotherapy, combined modality therapy, as well as prevention measures. Therapy utilizing monoclonal antibodies as well as vaccines against cancer are a growing paradigm and arose as an approach to target solid and haematologic tumours (Abou-Jawde *et al.*, 2003). The aim of a vaccine as a line of therapy is to enable the immune system to identify antigens that are associated with tumours and that are displayed on the surface of malignant cells. Once these antigens have been recognised, the ultimate goal of the treatment is to induce a cytotoxic response to these cancerous cells (Boon *et al.*, 1997).

Endocrine therapy for hormone receptor-positive breast cancer has been utilized but, conversely in many cases, the residual tumour tissue becomes resistant to the therapy and grows to form a new tumour. Studies on the origin of human breast cancer have linked increased oestrogen levels and therefore treatments are aimed at decreasing oestrogen synthesis, as well as preventing oestrogen from binding to its receptors thereby inhibiting the induced response (Seeger *et al.*, 2003).

Treatment regimens differ considerably depending on the stage of malignant tumour growth (Table 1.1). According to webmd, typically for stage 0 DCIS tumours, surgery to remove the abnormal cells is preferred and is known as a lumpectomy with a complete mastectomy

5

involving removal of the entire breast preferred in some cases. Following a lumpectomy, radiation therapy is often performed in order to target any abnormal cells that were not removed. Webmd states that hormonal therapy is often used in the treatment of LCIS in order to decrease the risk of survival and growth of invasive cancer cells. Stage I, II and III cancer are typically treated with surgery followed with post-treatment radiation therapy. In some cases, generally after the removal of a large tumour, webmd refers to the administration of chemotherapy to decrease the risk of the cancer returning. Hormone therapy is a good option after removal of the tumour as cancer cells utilise hormones to grow and the use of drugs can starve tumours of growth stimulating hormones. Such treatments described on webmd, include tamoxifen and in post-menopausal women the use of anastrozole.

Targeted therapy is a newer approach for triple negative breast cancer in addition to treatment following removal of the tumour (Www.Breastcancer.Org, 2015). According to webmd, Trastuzamab targets the HER2 receptor and prevents it from binding growth stimulating ligands aiding in the effectiveness of other chemotherapy treatments.

Due to the fact that stage IV cancer treatment involves multiple target sites, a combination of treatments is essential (www.breastcancer.org, 2015). Webmd states that treatment cannot cure cancer at this advanced stage, however it can shrink the cancer and inhibit the progression associated with increased morality. Patients with stage IV cancer can live for years however at some point this disease will become life threatening (www.breastcancer.org, 2015). The main treatment regimen for stage IV cancer as described by webmd, is to slow the progression of the cancer via chemotherapy and it is often used in combination with hormone therapy. The stages of cancer and the appropriate treatment regimens are further summarised in Table 1.1 below.

The most widely used endocrine drug is the anti-oestrogenic compound, tamoxifen. This compound was thought to be an ideal treatment in the management of oestrogen dependent tumours. This drug, however, presented adverse effects including cataracts, occlusion of blood vessels, increased risk of developing cancer of the uterus, hot flushes, as well as sexual dysfunction.

It was established that 15-20 % of the patients are more inclined to respond well to second-line therapy with a different endocrine agent than previously administered (Seeger et al., 2003). Despite the variety of chemotherapeutic agents available, multi-drug resistance has proven problematic in the effective targeting of malignant tumours.

6

Table 1.1: Summary of the stages of breast cancer with the characteristics and treatment options

	Stage 0	Stage I	Stage II	Stage III (operable)	Stage III (inoperable)	Stage IV
Description	Cancer cells at primary site no neighbouring tissue invasion	Cancer cells at primary site No lymph nodes involved Tumour < 2 cm	Tumour <2 cm and in lymph nodes Tumour >2 cm and not in lymph nodes Tumour >2 cm<5 cm	Tumour >5 cm and in lymph nodes Tumour and > 10 lymph nodes infected	Tumour that has spread to tissues near breast Inflammatory breast cancer Spread to lymph nodes in or near breast and to neck	Tumour spread to other organs
Treatment to the breast	Lumpectomy alone Lumpectomy and radiation Total mastectomy	Lumpectomy alone (rare) Lumpectomy and radiation Total mastectomy and radiation	Total mastectomy and radiation Lumpectomy and radiation	Total mastectomy and radiation Lumpectomy and radiation Followed by chemotherapy	Chemotherapy Followed by total mastectomy Radiation after mastectomy	Surgery Radiation
Treatment to the lymph nodes		Biopsy of lymph node	Biopsy of lymph node Radiation to lymph nodes	Removal of axillary lymph nodes Radiation to lymph nodes	Removal of axillary lymph nodes Radiation to lymph nodes	Treatment of enlarged lymph nodes
Chemotherapy		Often given to reduce risk of reoccurrence	Recommended	Always recommended	Always recommended	Always recommended
Hormonal therapy	Treatment of hormone-receptor positive breast cancer	Used to treat patients with hormone-receptor positive breast cancer	Used to treat patients with hormone-receptor positive breast cancer	Used to treat patients with hormone-receptor positive breast cancer	Used to treat patients with hormone-receptor positive breast cancer	Used to treat patients with hormone-receptor positive breast cancer
Targeted therapy		Used for cancers with particular characteristics such as HER2 expression	Used for cancers with particular characteristics such as HER2 expression	Used for cancers with particular characteristics such as HER2 expression	Used for cancers with particular characteristics such as HER2 expression	Used for cancers with particular characteristics such as HER2 expression
Treatment of distant sites						Radiation Surgery

1.7 Characteristics of malignant cells

Cancer cells form heterogeneous tissues that undergo various interactions (Hanahan and Weinberg, 2011). These cells need to obtain the traits that allow them to become carcinogenic and invasive. The genetic makeup of tumours must be understood through examining and assessing the acidic microenvironment with which these cells are associated. The 'seed and soil' hypothesis was described by Paget in 1889 and describes that tumour cells (seeds) need to find an appropriate environment (soil) in order to grow aiding in metastatic development (Paget, 1889).

Tumours originate from normal cells by genetic altering systems within the cell that are responsible for cellular growth. Hanahan and Weinberg described the classical 'six hallmarks of cancer' which refers to the characteristics that a cell acquires in order to differentiate into the many types of human malignancies (Hanahan and Weinberg, 2000, Hanahan and Weinberg, 2011). These 'six hallmarks of cancer' describe changes found in neoplastic diseases and describes the transition of normal cells to this neoplastic state. Cancer cells are capable of providing their own growth signals, are not sensitive to normal antigrowth signals, are capable of evading apoptosis, contain unlimited replication potential, have continuous angiogenesis and lastly, are capable of invading tissues and metastasising (Hanahan and Weinberg, 2000, Hanahan and Weinberg, 2011, Pietras and Östman, 2010).

There is a close correlation between the adenosine tripohosphate (ATP) produced and how aggressive the tumour is (Simonnet *et al.*, 2002). Cancer cells generally use aerobic glycolysis for energy production from glucose however this is an less efficient pathway to produce ATP (Warburg, 1956). For every mole of glucose, only four moles of ATP are produced using aerobic glycolysis (Vander Heiden *et al.*, 2009). This suggests the altered metabolism of cancer cells requires the increased uptake of nutrients for cell proliferation (DeBerardinis *et al.*, 2008). This altered metabolism forces cancer cells to assimilate and metabolise nutrients less efficiently producing less ATP per glucose molecule (Warburg, 1956). Glutamine has also been described as a source of energy in cancer cells. Glutamine is metabolised to lactate through the process of glutaminolysis and this is considered to be a hallmark of metabolism in tumour cells (Mazurek *et al.*, 2005).

The metastatic process involves the detachment of cells from the tumour at its primary neoplasm (Weiss and Ward, 1983). A characteristic of tumour cells is that in contrast to normal cells they can separate from the solid tumour mass with greater ease (Nicolson, 1988). Tumours

8

are also capable of stimulating the deposition of fibrin around the malignant cells and the implantation into cells from the vasculature is linked to their platelet aggregating and thromboplastic properties (Gasic *et al.*, 1977, Tanaka *et al.*, 1977).

The determination of the location of the malignant secondary tumour involves close consideration to the fact that a tumour cell circulates through the blood and lodges itself in the first capillary bed that it encounters (Sella and Ro, 1987). By examining the patterns of venous circulation as well as lymph drainage, the metastasis of regional tumours can be explained (Sugarbaker, 1981). In contrast to this, distant metastases are more challenging to explain as tumour cells establish their own pattern of metastasis and patterns are not dependent on the first organ that was encountered (Nicolson, 1988).

A vital characteristic of cancer cells is their ability to maintain chronic proliferation. There are many different signals produced and used by a healthy cell that induces cellular division through the cell cycle in order to maintain homeostasis. Cancer cells however, deregulate these signals (Hanahan and Weinberg, 2011). Apoptosis is normally initiated in response to a cell undergoing physiological stress which can be a result of anti-cancer therapy. Cancer cells will respond to these various strategies in order to avoid or limit the induction of apoptosis. It is therefore essential that treatments be adapted and developed in order to target these hallmarks and ultimately stop the progression of this deadly disease.

1.8 Cancer cell metabolism

A rapidly developing research paradigm involves the exploration of the metabolism of cancer cells as a therapeutic target. A number of oncologic signalling pathways merge and support the growth and survival of cancer cells through adaption of tumour metabolism. For this reason, cancer cell metabolism and its alterations are proposed to be a key characteristic of cancer cells. Cellular metabolism is altered through the convergence of intrinsic and extrinsic mechanisms in order to provide rapid production of ATP, the increased synthesis of macromolecules as well as homeostasis of the redox state (Vander Heiden *et al.*, 2009). This is accomplished in cancer cells through alteration to protein, carbohydrate, lipid and nucleic acid metabolism.

Otto Warburg predicted in the 1920's metabolic pathway targeting by observing the way cancer cells utilize glucose in comparison to that of normal cells (Warburg, 1956). The first tumour-specific alteration includes increased aerobic glycolysis and as a result of this, cancer cells use more glucose and are more dependent on aerobic glycolytic metabolism than they are on

9

mitochondrial metabolism for the production of ATP (Figure 1.1). The glycolytic pathway yields two ATP molecules from each glucose molecule in contrast to that of oxidative phosphorylation which yields 34 ATP molecules (Stein *et al.*, 2010). The shift seen in energy production demands an abnormally high rate of glycolysis in order to meet the energy demands (Semenza *et al.*, 2001). There is a close correlation between the ATP produced and how aggressive the tumour appears to grow (Simonnet *et al.*, 2002). An explanation of the use of glycolysis in tumour cells is that it occurs in an adaptive mechanism to hypoxic conditions (Gatenby and Gillies, 2004). During early phases of tumour development, avascular conditions result in the production of ATP via anaerobic conditions (Gillies *et al.*, 2008). Another possibility for the use of glycolytic metabolism is due to the production of excess lactate resulting in adaptation of the malignant cells metabolism (Gatenby and Gillies, 2004, Gillies *et al.*, 2008). The PI3K pathway is activated via the stimulation of tumour suppressor genes such as phosphatase and tensin homolog (*PTEN)* (Figure 1.1)*.* The activation of this pathway provides a strong basis for tumour cell growth, survival and alters the metabolism of tumour cells (Wong *et al.*, 2010).

The utilization of the aerobic glycolysis pathway enables cells to exert their oncogenic effects and for this reason, tumour cells will be prone to sensitivity to chemotherapeutic agents when the glycolytic pathway is inhibited. The increased dependency of tumour cells on the glycolytic pathway therefore provides a foundation to preferentially kill malignant cells through glycolytic inhibition (Sahra *et al.*, 2010).

10
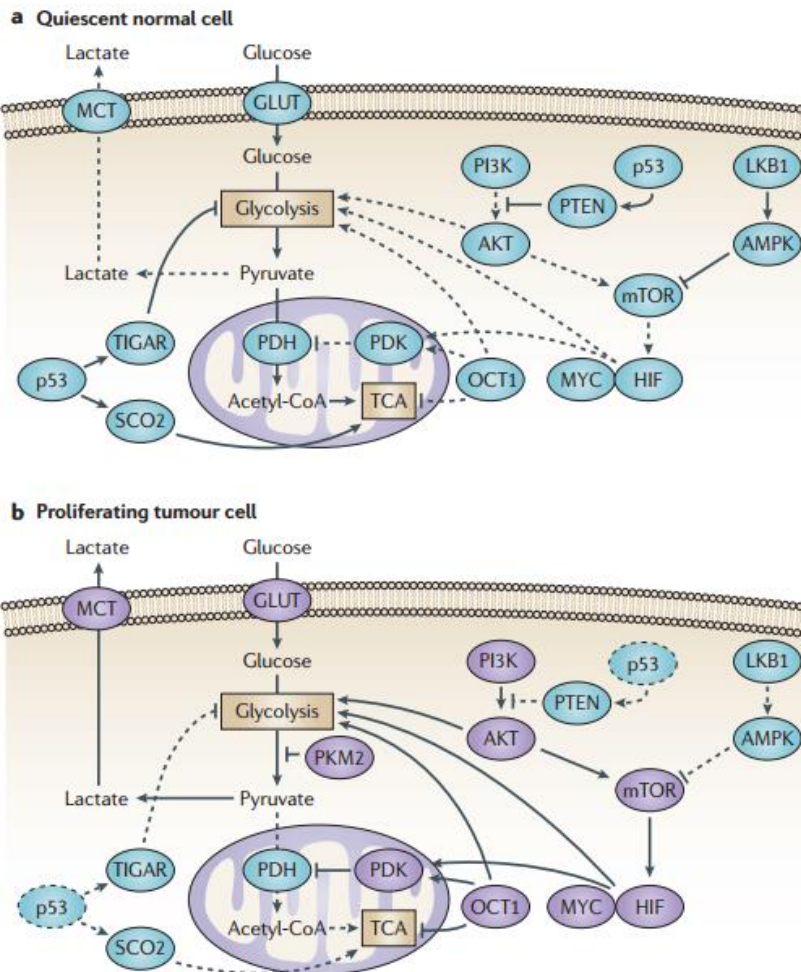
Figure 1.1: A schematic overview of the mechanisms involved in the Warburg effect. Various signalling pathways are involved in the transition of oxidative phosphorylation seen in normal cells (a) to aerobic glycolysis in tumour cells (b). The activation of mTOR occurs through the induction of the PIK3 pathways which activate AKT and glycolytic enzymes. The tumour suppressor liver kinase B1 (LKB1) inhibits mTOR and opposes glycolytic metabolism. mTOR enhances the hypoxia induced factor 1 (HIF1) which in turn increases glucose transporter (GLUT) expression, glycolytic enzymes, pyruvate dehydrogenase kinase (PDK) and then blocks entry into the tricarboxylic acid (TCA) cycle. The tumour suppressor protein p53, inhibits glycolysis TP53-induced glycolysis and apoptosis regulator (TIGAR) therefore stimulating mitochondrial function. Used with permission. (Cairns *et al.*, 2011).

1.9 The immune system and cancer

The initiation and progression of tumour development is closely linked to the role of the innate immune systems cells. These cells of the immune system can prevent the progression of malignant cells but can assist in the transformation of malignant cells and development of the tumour (Hagerling *et al.*, 2015). The hallmarks of cancer are influenced by the inflammatory microenvironment of a malignant tumour (Hanahan and Weinberg, 2011, Mantovani, 2009).

11

The clinical outcome of cancer patients is affected by whether tumour progression is triggered, prevented or promoted by cells of the innate immune system. Most cancers have been linked to a status of chronic inflammation which aids the metastatic process of tumours (Colotta *et al.*, 2009). Nearly 100 % of cervical cancers can be linked to chronic infection by human papilloma virus (HPV) (Jemal *et al.*, 2010).

The perturbation of tissue triggers a first line response from cells of the innate immune system including macrophages, innate lymphoid cells, neutrophils and dendritic cells (Hagerling *et al.*, 2015). This response ultimately determines the fate of the tumour where initiation or prevention of tumour progression is established. Tumour cells are capable of acquiring characteristics in order to be resistant to immune attack by pro-inflammatory macrophages (Jinushi *et al.*, 2012). Cells of the innate immune system play an essential role in the general inflammatory response and are directly linked to cancer-related inflammation (Hagerling *et al.*, 2015). Therefore, understanding the role that the innate immune system plays in tumour development is essential in the treatment of cancer.

1.10   Cancer and multi-drug resistance

Cancer therapy has significantly advanced and improved in recent times, however there are no chemotherapeutic agents that are completely effective at targeting malignant cells (Gottesman, 2002). The effectiveness of a number of anti-cancer compounds has been limited by the development of drug resistance and serious side effects. Tumour cells often display intrinsic resistance which makes them more challenging to target effectively. Some malignant cells show initial sensitivity to chemotherapeutic agents but often develop resistance, not only to the treatment administered but to other treatments using similar targeting mechanisms that they have not been exposed to (Tsuruo *et al.*, 2003).

A link to drug resistance and sensitivity is related to the pro- and anti-apoptotic pathways (Gottesman *et al.*, 2002, Tsuruo *et al.*, 2003). Previous data has reported that the initiation of apoptosis plays a vital role in tumour cell death induced by chemotherapeutic agents (Igney and Krammer, 2002). It has been suggested that a mechanism for multidrug resistance (MDR) is through inhibition of the apoptotic pathway (Tsuruo *et al.*, 2003). MDR can also result from various mechanisms including increased drug efflux, decreased drug uptake, detoxifying systems being activated or DNA repair mechanisms that are activated (Gottesman *et al.*, 2002). MDR is associated with the increased efflux of the drug from the cell which is mediated by mechanisms that are energy dependent. The MDR phenotype can sometimes be reversed

12

through inhibition of the drug transporters that are generally ATP-binding cassette (ABC) efflux transporter proteins (Coley, 2010).

Resistance to a number of chemotherapeutic drugs including vinblastine, vincristine and doxorubicin results from overexpression of P-glycoprotein (P-gp) (Hamada and Tsuruo, 1988). This glycoprotein is upregulated on the surface of resistant tumour cells and is capable of binding and transporting chemotherapeutic agents out of the cell in an ATP-dependent manner (Hamada and Tsuruo, 1986). A calcium channel blocker that also blocks the P-glycoprotein transport, verapamil inhibits efflux of the drug and restores drug sensitivity therefore restoring cytotoxic activity of some chemotherapies (Tsuruo *et al.*, 1981).

Due to increasing MDR, novel treatment regimens are essential to target rapidly proliferating tumorigenic cells in order to obtain the necessary anti-cancer therapeutic outcome.

1.11   2-Methoxyestradiol

2-Methoxyestradiol (2-ME) was developed as an anti-cancer treatment due to its anti-carcinogenic, anti-proliferative and anti-angiogenic properties demonstrated *in vitro* (Carothers *et al.*, 2002, Dahut *et al.*, 2006, Lakhani *et al.*, 2003, Pribluda *et al.*, 2000). Oestrogens are metabolised by cytochrome P450 into catechol oestrogens and then via *O*-methlytransferase into 2-methoxyestradiol. 2-ME is thus an endogenous metabolite of oestrogen that is a 17-β oestradiol derivative. 2-ME possesses little oestrogenic activity but initiates apoptosis aimed at rapidly proliferating tumour cells. This compound was considered promising as it does not interact with oestrogen receptors, as demonstrated by the low affinity that it possesses for both the alpha- and beta oestrogenic receptors. Thus it can be assumed that this compound should not be influenced by oestrogen receptor antagonists or agonists (Lakhani *et al.*, 2003).

Although the mechanism of action is not precisely known, 2-ME has been demonstrated to interfere with microtubule dynamics by interacting with the colchicine binding site (Lakhani *et al.*, 2003, StanderJoubert *et al.*, 2011). Reports have indicated sensitivity of breast cancer, as well as other cancer cell lines including colon and lung cancer to the effects of 2-ME (Binkhathlan and Alshamsan, 2012, Lakhani *et al.*, 2003). It has been reported that 2-ME induces apoptosis via both the intrinsic and extrinsic pathways in cancer cells (Mooberry, 2003). 2-ME has proven to be effective when used as primary anti-cancer treatment however it also sensitises cells that are resistant to conventional treatments including radiation therapy (Amorino *et al.*, 2000).

13

When examining the anti-proliferative and anti-metastatic effects that this compound has *in vivo*, 2-ME inhibited the growth of tumours in the lung by 60% by not only targeting the tumour directly but reduced the vasculature supplying the tumour. Clinical studies have shown that 2-ME is tolerated at doses as high as 1200 mg/day when administered daily for a period of 28 days (Lakhani *et al.*, 2003). This compound was therefore deemed a promising anti-cancer agent due to its protection against tumour growth (Lakhani *et al.*, 2003, Seeger *et al.*, 2003, StanderJoubert *et al.*, 2011).

However, 2-ME lacks oral bioavailability *in vivo* since 17-hydroxysteroid dehydrogenase targets the 17-hydroxy group of 2-ME for metabolism which results in the rapid breakdown of this compound (Newman *et al.*, 2006). This results in low bioavailability related to a high hepatic first pass effect. 2-ME has undergone a phase one clinical trial which resulted in no significant adverse effects and led to an overall decrease in bone related pain, as well as a reduction in the use of analgesic medications (Lakhani *et al.*, 2003). Following this it was reported that this compound possesses a short half-life and an elimination half-life of 10 hours (James *et al.*, 2007). A phase II randomized double blind trial was carried out on hormone refractory prostate cancer patients and it was concluded that doses of 400 and 1200 mg/day were well tolerated. Minor grade 2 and 3 abnormalities of liver function were observed in phase II clinical trials , however, liver function returned to normal on cessation of administration of 2-ME (James *et al.*, 2007, Lakhani *et al.*, 2003). From this it was established that 2-ME is an orally active compound and suggested to be an effective treatment regimen to treat cancers. Despite the promising anti-tumour activity, the short half-life of this compound and low bioavailability resulted in the development of structural analogues of 2-methoxyestradiol to effectively target cancer.

1.12   Combination therapy and novel oestrone analogues as a new approach

Significant progress has been made in the management and survival of patients diagnosed with cancer due to the use of better imaging and diagnostic techniques. Knowledge of treatments using combination therapy will further contribute to the increased survival rate. The survival rate has not been significantly improved with the current treatment regimens of chemotherapy and radiation especially in that of patients diagnosed with malignant tumours in the pancreas, liver and brain (Chu *et al.*, 2004). Following a mastectomy, radiation therapy was not observed to significantly reduce mortality rates (Group, 2000). For this reason, alternate routes need to

14

be established in order to complement curative apoptotic induction and overcome multi-drug resistance. Combination therapy is thought to be the most effective way to improve the survival rates of cancer patients.

An ideal anti-cancer drug is one which is able to selectively target cancer cells and have little toxicity towards normal healthy cells even after prolonged periods of exposure. Many current chemotherapies and treatment regimens have very narrow therapeutic indexes and do not possess these ideal characteristics. Combination therapy is a useful technique to improve therapeutic efficacy of compounds and lead to improved side effect profiles. The active compounds can be used at a lower concentration in the combination therapy than if single compound treatment was used. This is favourable as the risk of non-selective cytotoxicity is significantly reduced. The combination of two compounds can be described as antagonistic where the combination of two compounds has less of an overall effect than the sum of their individual effects, additive where the compounds efficacy is equal to the sum of the effects of each of the compounds alone, or synergistic, where the combination is more effective than the sum of each of the compounds in isolation (Arnold *et al.*, 2013).

Previous studies made use of 2-ME in combination with tamoxifen and results showed that these two compounds show an additive effect on breast cancer cells *in vitro* (Seeger *et al.*, 2003). Further studies were aimed at combining 2-ME with docetaxel in order to assess whether there is a beneficial effect by using the combination therapy. However, the use of these compounds in combination resulted in grade 3 fatigue, as well as hand and foot syndrome (Lakhani *et al.*, 2003). From clinical trials previously performed it appears that 2-ME possesses desirable anti-cancer traits, but the short half-life and low bioavailability are factors which needed to be improved.

Antimitotic compounds are most widely used in chemotherapeutic anti-cancer drugs and it was therefore proposed to develop novel 2-ME derivatives with an enhanced half-life and bioavailability that is equally effective in terms of the potency of the anti-cancer agent (Stander *et al.*, 2012). The aim of the development of novel analogues is to enhance the reported anti-angiogenic and anti-mitotic properties of the parent compound, 2-ME (Leese *et al.*, 2004). The preservation of anti-tubulin and cytotoxic characteristics is attainable through the dehydration of position 17 of the compound resulting in a decreased metabolic breakdown (Edsall *et al.*, 2004, LaVallee *et al.*, 2008).

15

Several derivatives were developed by the addition of a sulphamate group at position 3 of the oestradiol structure of the parent compound, 2-ME (Stander *et al.*, 2012). The sulphamate group improved the compound's biological half-life and bioavailability due to reduced hepatic first pass metabolism (Elger *et al.*, 1995). The improvement in bioavailability is further improved by the compound reversibly binding to carbonic anhydrase II (CAII) within the red blood cells, which then follows the slow release of the compound back into the circulatory system (Elger *et al.*, 1995, Ho *et al.*, 2003).

CAII is a catalytic zinc based enzyme aiding in the production of carbonic acid through the combining of carbon dioxide and water. A unique characteristic of a cancerous cell is that it creates an extracellular pH that is lower than that of a normal cell. This increased acidic environment promotes important factors involved in the progression of a tumour growth including inducing growth factors and proteases to become more active. An enzyme commonly overexpressed in a tumour is carbonic anhydrase IX (CAIX) and by selectively inhibiting this enzyme metastasis can be abrogated (Pastorekova *et al.*, 2008)

A number of 2-ME derivatives were designed *in silico* at the Bioinformatics and Computational Biology Unit at the University of Pretoria. These compounds were then synthesized by iThemba Pharmaceuticals (Pty) Ltd (Modderfontein, Gauteng). *In vitro* testing of several of these 2-ME derivatives have shown increased apoptosis due to a mitotic blockade initiated by the compound interfering with the microtubule dynamics of the cell (Stander *et al.*, 2011). The most promising derivatives from the initial *in vitro* cytotoxic testing when using breast cancer cell lines, namely 2-ethyl-3-O-sulphamonyl-estra-1, 3, 5 (10),15-tetraen-17-ol (ESE-15-ol) and 2-Ethyl-3-O-sulphamoyl-estra-1, 3, 5(10)16-tetraene (ESE-16) (Figure 1.2) were used for this study due to their unique characteristics and potential.

16
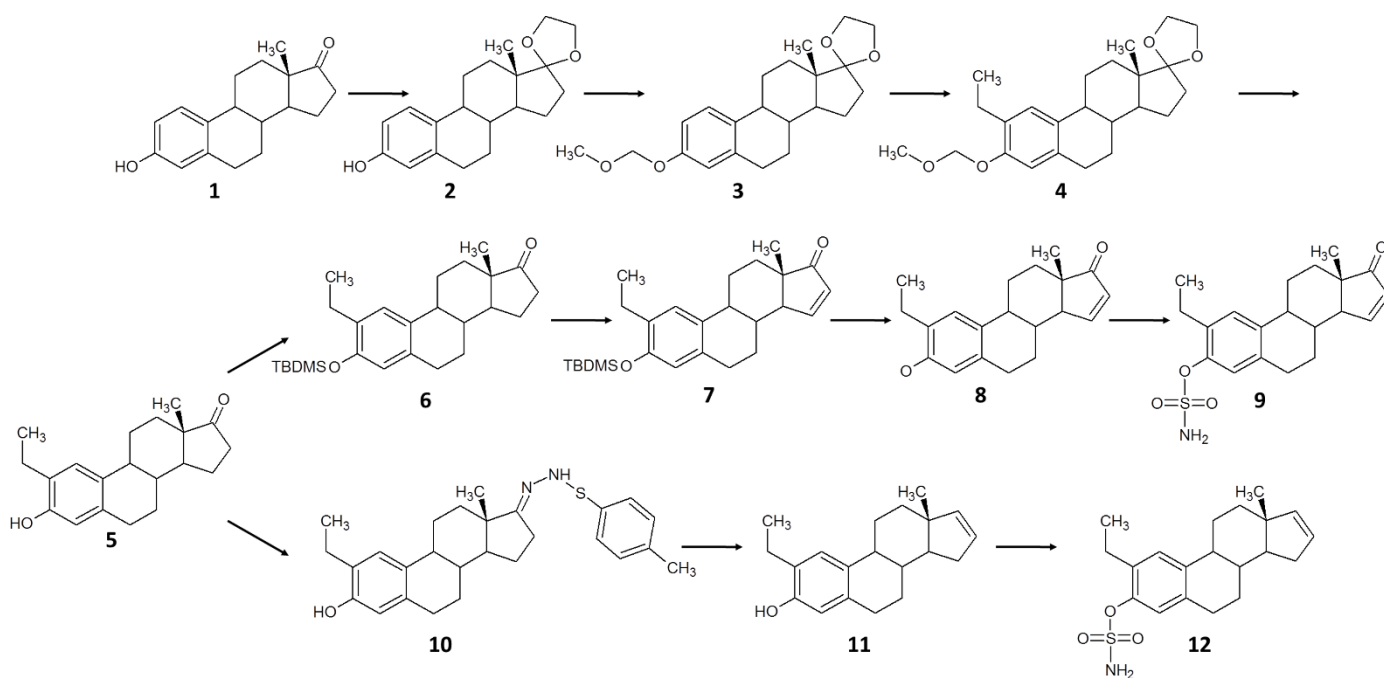
Figure 1.2: The synthetic pathways and structures of the oestrone analogues. The chemical structure of ESE-16 is shown as number 12, ESE-15-ol is represented by number 9. Used with permission (Stander *et al.*, 2011).

Kinetic and docking studies performed *in silico* describe that ESE-15-ol and ESE-16 show antimitotic effects and are capable of inhibiting CAIX. *In vitro* experimentation with ESE-16 has previously shown that it influences the expression of genes and proteins, the shape of cells, the production of reactive oxygen species and ultimately the induction of apoptosis and plays a role in mitochondrial membrane potential as well as caspase 3 and 7 activation (Stander *et al.*, 2013). The 2-ME derivatives have been reported to show potential cytotoxicity at low concentrations which decrease risk of unselective toxicity and further warrant their use in combination therapy.

Extensive research has previously been done on several analogues of 2-ME including (8R, 13S, 14S, 17S)-2-Ethyl-13-methyl-7,8,9,11,12,13,14,15,16,17-decahydro-6H-cyclopenta[a]-phenanthrene-3, 17-diyl bis (sulfamate) (EMBS), 2-ethyl-3-O-sulphamoyl-estra-1,3,5(10),15-tetraen-17-one (ESE-15-one) and 2-Methoxyoestradiol-3,17-O,O-bis-sulphamate (STX140). Due to the similarity between these compounds and ESE-15-ol and ESE-16 used in the present study, these compounds will be referred to throughout the discussion.

17

1.13   Glycolysis inhibitors

2-Deoxyglucose (2-DG) (Figure 1.3) is an analogue of glucose that competitively inhibits the metabolism of glucose upon entering the cell. following the initial ATP dependent phosphorylation of position 6 of the glucose, no further metabolic reactions can occur (Kaplan *et al.*, 1990). The phosphorylated form, 2-deoxyglucose-6-phosphate (DG-6-P) inhibits hexokinase, the first enzyme involved and the rate limiting step of the glycolytic pathway (Kaplan *et al.*, 1990, Sahra *et al.*, 2010). This pathway blockade results in reduced ATP within the cell which may induce autophagy, a cell survival process in response to cell starvation. Due to the malignant cells being more dependent on glucose metabolism, 2-deoxyglucose has been suggested as a potential anti-cancer agent (Sahra *et al.*, 2010). N-linked glycosylation is also altered by 2-DG and this results in disrupted protein responses in a cell treated with 2-DG (Kurtoglu *et al.*, 2007). These alterations induces downstream alterations in the phosphorylation of proteins that are involved with the control of the cell cycle, signalling pathways, gene expression and DNA repair, the influx of calcium as well as cell death via the initiation of apoptosis (Lin *et al.*, 2003).
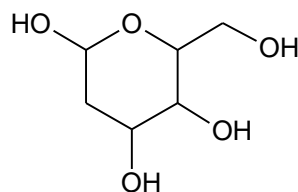
Figure 1.3: **T**he structure of 2-deoxyglucose. Drawn with Chemsketch 12 (Freeware) (www.acdlabs.com).

Clinical side effects of 2-DG treatment have been reported with majority being intracellular glucose deprivation resulting in glucopenia. Neurotransmitter systems are often activated in order to compensate for the decreased glucose. This results in the increased secretion of adrenalin, glucagon and growth hormone (Dwarakanath *et al.*, 2009). Through the process of glycogenolysis, glucose for use by the cells is released from the liver and muscle stores (Brodows *et al.*, 1975). The side effects noted after treatment with 2-DG have been short lived lasting for approximately 4-6 hours and can be alleviated by the administration of glucose. In general, no significant changes in vital signs are observed after administration of 2-DG (200-300 mg/kg) and only slight increases in heart rate and slight decreases in systolic blood pressure have been observed after treatment with 50 mg/kg (Fagius and Berne, 1989). Vagus nerve

18

stimulation occurs after treatment with this glycolytic inhibitor resulting in increased gastric and pepsin secretion (Duke *et al.*, 1965).

Studies conducted previously where 2-DG was administered intravenously to patients with various carcinomas ranging from renal and bronchogenic carcinomas to leukaemia used doses ranging from 50 to 200 mg/kg 2-DG for 25 to 60 minutes. Post-administration, glucose levels in the blood increased following the onset of drowsiness, hypothermia, diaphoresis and increased warmth. The nature of the side effects induced by 2-DG were low in severity and symptom cessation occurred 90 minutes after treatment (Landau *et al.*, 1958). From clinical reports, it is suggested that high doses of 2-DG need to be administered for a long period of time in order to obtain therapeutic efficacy in cancer treatment (Dwarakanath *et al.*, 2009). Studies have also pointed out that short exposure (a few hours) to 2-DG sensitises cells to radiation therapy and aids in decreases damage to normal cells thereby inducing a protection function (Jain, 1996). It has been suggested that treatment with 2-DG weekly is sufficient to induce the therapeutic response required and is a cost effective and convenient treatment scheme for patients with cerebral gliomas (Dwarakanath *et al.*, 2009).

The inhibition of glycolytic metabolism occurs in cancer cells after treatment with approximately 20 mM of 2-DG (Wu *et al.*, 2009). Clinical evidence demonstrates that, when 2-DG is used as a treatment in isolation, it will favour anti-cancer effects. It has also been noted that the treatment of glioma with 2-DG at high concentrations is limited in its efficacy due to systemic toxicity (Dwarakanath *et al.*, 2009). Due to the side effects elicited, it was suggested that this compound should be tested in combination to reduce the concentration of 2-DG required to achieve the desired therapeutic effect (Kaplan *et al.*, 1990).

Hypersensitisation of tumour cells has been achieved through the combination of 2-DG with mitochondrial inhibitors such as oligomycin (Liu *et al.*, 2001). This dual targeting of glycolytic and mitochondrial pathways has introduced a promising strategy for chemotherapeutic treatment of malignant cells (Pathania *et al.*, 2009). 2-DG has previously been combined with metformin, an anti-diabetic drug that inhibits the release of glucose from the liver. Combining these two compounds, the two sources of energy for a cell are targeted and a stronger deleterious effect is seen which leads to a shift from cell survival to apoptotic cell death. This shift could create a greater advantage in the treatment of cancer compared to traditional chemotherapies (Sahra *et al.*, 2010). 2-DG has been used in the testing of adriamycin resistant human breast cancer cells and resulted in the inhibition of glycolysis, as well as accumulation

19

of the compound within the cancer cells. This again reiterates that the use of 2-DG in combination regimes is favourable in anti-cancer treatment (Kaplan *et al.*, 1990).

The cytotoxicity after treatment with adriamycin and paclitaxel in sarcomas of the bone, as well as in a lung cancer xenograft model was enhanced after combination treatment with 2-DG and when used in combination with 2-ME, the cytotoxicity was enhanced. These promising *in vivo* results motivated for a phase one clinical trial where the safety and efficacy of this drug, as well as the dosing required for an optimal outcome were determined. Doses of 30, 45 and 60 mg/kg 2-DG were administered to patients with solid tumours. These doses were well tolerated with third and fourth grade toxicities observed (Stein *et al.*, 2010). First and second grade toxicities were apparent and patients reported that they experienced dizziness as well as fatigue. The cardiac QT interval describes the depolarization and then the repolarisation of the ventricles and is represented electrically via an ECG (Electrocardiography) (Goldenberg *et al.*, 2006). At a dosing concentration of 60 mg/kg, patients were observed to suffer from a Grade 3 toxicity with the QT interval prolonged, however, no further symptoms were reported (Stein *et al.*, 2010). From this it was established that a concentration of 45 mg/kg should be used to continue into a phase II clinical trial which was reported to be well tolerated by patients. A follow up phase III multicentre trial was then implemented to evaluate the efficacy of 2-DG in combination with radiotherapy (Dwarakanath *et al.*, 2009).

Future prospective studies should focus on an improved tolerance of 2-DG at high doses accompanied by reduced toxicity and increased cancer cell sensitivity which could be accomplished by combination therapy. It is therefore important to describe the mechanistic properties of the synergistic combination of the oestrone analogues and 2-DG on various cell lines in order to determine if these compounds have a greater therapeutic application in comparison to that of presently used breast cancer therapy.

1.14   2-Deoxyglucose in combination with oestrone analogues

An analogue of 2-ME, 2-ME-3,17-O,O-bis-sulphamate (STX140) elicited similar yet improved properties to 2-ME similar to the experimental compounds ESE-15-ol and ESE-16 (Leese *et al.*, 2006). The oestrone analogues of 2-ME are advantageous as they can be administered orally and have been reported to be efficient in targeting many human cancer cell lines *in vitro* (Chander *et al.*, 2007). STX140 like ESE-15-ol and ESE-16 interferes with microtubule dynamics by acting at the colchicine binding site (Stengel *et al.*, 2014). The combination of STX140 and 2-DG synergistically decreases tumour mass. It was also hypothesised that

20

STX140 may increase tumour sensitivity to glycolytic inhibition (TaggFosterLeese *et al.*, 2008). This suggests that due to similar mechanistic properties of STX140 and ESE-15-ol and ESE-16 there is a possibility that the combination of ESE-15-ol, ESE-16 and 2-DG would synergistically target cancer cells in a similar manner. The combination of a glycolytic inhibitor with a steroid-like compound containing a sulphamate substituted ring system has been shown to improve activity towards malignant cells (TaggFosterNewman *et al.*, 2008). The combination of ESE-15-ol and ESE-16 with 2-DG therefore warrants investigation to assess potential of synergistically targeting breast cancer cells.

1.15 Background to cell viability assay

Chemosensitivity testing has been used for many decades and continues to expand. In 1983 the 3-(4,5-dimethylthiazol-2-yl)-2,5-diphenyltetrazolium bromide (MTT) assay was introduced by Mosmann (Mosmann, 1983) as a simplified cell enumeration assay to be used for cytotoxicity testing. The dehydrogenase enzymes in the mitochondrion reduces the tetrazolium ring to give a highly coloured formazan product that serves as a useful surrogate colorimetric assay for enumerating living cells as this reaction only occurs within a viable, metabolically active cell. Many different tetrazolium-based assays have been established but all suffer from cell activity dependence.

An alternative colorimetric assay that is used is the sulforhodamine B assay (SRB). The SRB assay, has been extensively used for cellular enumeration for drug-induced cytotoxicity assays that results from treatment with a specific test compound (Kitamura *et al.*, 2013, Voigt, 2005). The SRB assay, developed by Skehan *et al.* is used for the quantification of total protein within a cell (Papazisis *et al.*, 1997, Skehan *et al.*, 1990). Sulforhodamine B is a dye that under acidic conditions will bind to basic amino acids within cellular proteins, (Henriksson *et al.*, 2006, Papazisis *et al.*, 1997). Under basic conditions, the dye can be released from the cell for colorimetric quantification giving an indication of cell number. In contrast to that of the tetrazolium-based assays, the SRB assay exhibits similar yet improved aspects of improved linearity, increased sensitivity, stability in the end point which is not time sensitive as well as being more cost effective (Papazisis *et al.*, 1997). Previous studies assaying ESE-15-ol and ESE-16 generally utilized the MTT assay or crystal violet assay for cell enumeration studies.

21

1.16 Background to programmed cell death

Programmed cell death (PCD) occurs through three diverse pathways including apoptosis, autophagy and necrosis. In the development of organisms, apoptosis plays a crucial role and is also significantly involved in regulating the immune system and acts as a defence response to various infectious stimuli (Chaabane *et al.*, 2013). Typical characteristics of an apoptotic cell include cell shrinkage, cytosolic condensation, membrane blebbing, the formation of apoptotic bodies, nuclear condensation, protein cross-linking, nuclear DNA fragmentation, and phosphatidylserine exposure on the outer surface of the cell (Chaabane *et al.*, 2013, Henry *et al.*, 2013, Radi *et al.*, 2014). Necrotic cells display swelling of cells and intracellular organelles, cell rounding and the sudden collapse of the plasma membrane which result in the leaking of intracellular contents and initiation of inflammation (Darzynkiewicz *et al.*, 1992)

Apoptosis can be initiated as a mechanism of cell death through four different pathways namely the intrinsic, extrinsic, perforin or endoplasmic reticulum stress-induced pathways (Sun *et al.*, 2009). Apoptosis is a mechanism of controlled cell death dependant on the sequential action of a series of caspase enzymes. Caspases cleave target proteins, many of which are involved in cell structure. It is essential that caspase activity is normally inhibited and this occurs via the storage as pro-caspases which need to be activated by proteolytic cleavage prior to their involvement in apoptotic cell death (Boatright and Salvesen, 2003).

There are various points of entry into the apoptotic cascade and the caspases are classified according to the initiation point of entry. Caspases are also structurally classified. Group 1 consists of long pro-domains caspases 1, 2, 4, 5, 8, 9, 10, 11 and 12 and Group 2 of short pro-domains namely caspases 3, 6, 7 and 14 (Troy and Jean, 2015). Group 1 is further divided into the initiator caspases of apoptosis (caspases 2, 8, 9 and 10) and the inflammatory caspases 1, 4, 5, 11 and 12. Group 2 is commonly termed the executioner caspases. Executioner caspases are located in their inactive form within the cytosol of the cell (Boatright *et al.*, 2003).

Caspases 8 and 9 have been reported to cleave and thereby activate the executioner caspases (Slee *et al.*, 1999). Adaptor proteins bind to the caspase activation and recruitment domain (CARD) involving caspases 1, 2, 4, 5, 9, 11 and 12 or binding occurs to the death effector domain comprising caspases 8 and 10 (Boatright and Salvesen, 2003, Troy and Jean, 2015).

Apoptosis is sensitive to the function of the mitochondria as well as reactive oxygen species (ROS) in the mitochondria via the signalling pathway of the intrinsic apoptotic pathway (Wang

22

and Youle, 2009). Caspases 3, 6, 7 and 9 are involved in this pathway. The intrinsic pathway functions in response to many chemotherapeutic anti-cancer compounds, ionising radiation, mitochondrial damage and is responsible for the apoptosis involved following stress parameters. This pathway involves regulation of the activation of caspase-9 through the mitochondrial leakage of cytochrome c (Troy and Jean, 2015).

The initiation of apoptosis is determined via the balance between the pro and anti-apoptotic B cell lymphoma protein 2 (Bcl-2) family members (Kluck *et al.*, 1999). Healthy cells contain the phosphorylated Bcl-2-associated death promoter (Bad) protein in the cytoplasm. Bcl-2 and B-cell lymphoma-extra-large (Bcl-xL) (anti-apoptotic) bind to the proteins Bcl-2-like protein 4 (BAX) and Bcl-2 homologous antagonist/killer (BAK) (pro-apoptotic) (Kluck *et al.*, 1999, Tait and Green, 2010). This in turn inhibits apoptosis. Bcl-2 and Bcl-xL bind to excess free Bad present in the cytoplasm and release BAX and BAK (Kluck *et al.*, 1999). These proteins then bind to the mitochondrial membrane resulting in loss of membrane integrity. This then results in the depolarisation of the mitochondrial membrane and increases mitochondrial membrane permeability (regulated by Bcl-2 family proteins) (Tait and Green, 2010). This results in release of cytochrome *c* (Figure 1.4).

Released cytochrome *c* in the cytoplasm is recruited into the apoptosome complex where activation of pro-caspase 9 is triggered (Boatright and Salvesen, 2003, Slee *et al.*, 1999, Zou *et al.*, 1999). The apoptosome also contains an apoptotic protease activating factor 1 (Apaf-1) which in turn activates caspase 9 and initiates the intrinsic apoptotic pathway. The initiator caspases cleave and activate a cascade of executioner caspases, caspase 3 and 7 (Chinnaiyan, 1999) that results in the cleavage and disassembly of the target cell cytoskeleton.

The extrinsic pathway's role is the removal of unwanted cells during periods of development, education of the body's immune system as well as immuno-surveillance (the removal of tumours mediated through the immune system). This pathway (Figure 1.4) is initiated when the trans-membrane death receptor is activated by ligand binding. Common death receptors include apoptosis stimulating fragment (Fas), TNF related apoptosis inducing ligand receptor type 1/2 (TRAIL R1/2) TRAIL not only rapidly induces apoptosis but can result in selective cancer cell death while eliciting a protective effect on normal cells due to the protection of decoy receptors (Chicheportiche *et al.*, 1997, Ning *et al.*, 2013). Activation of Fas results in micro-aggregate formation at the surface of the cell and in turn recruits Fas-associated protein with death domain (FADD) or Tumour necrosis factor receptor type 1 associated death domain

23

(TRADD) to its cytosolic tail. FADD is responsible for the recruitment of pro-caspase 8 and 10 molecules. Pro-caspase 8 is then cleaved to form activated caspase 8 within the death-inducing signalling complex (DISC) located at the cell surface. Executioner caspases are then recruited which leads to programmed cell death of the target cells (Hsu *et al.*, 1995).
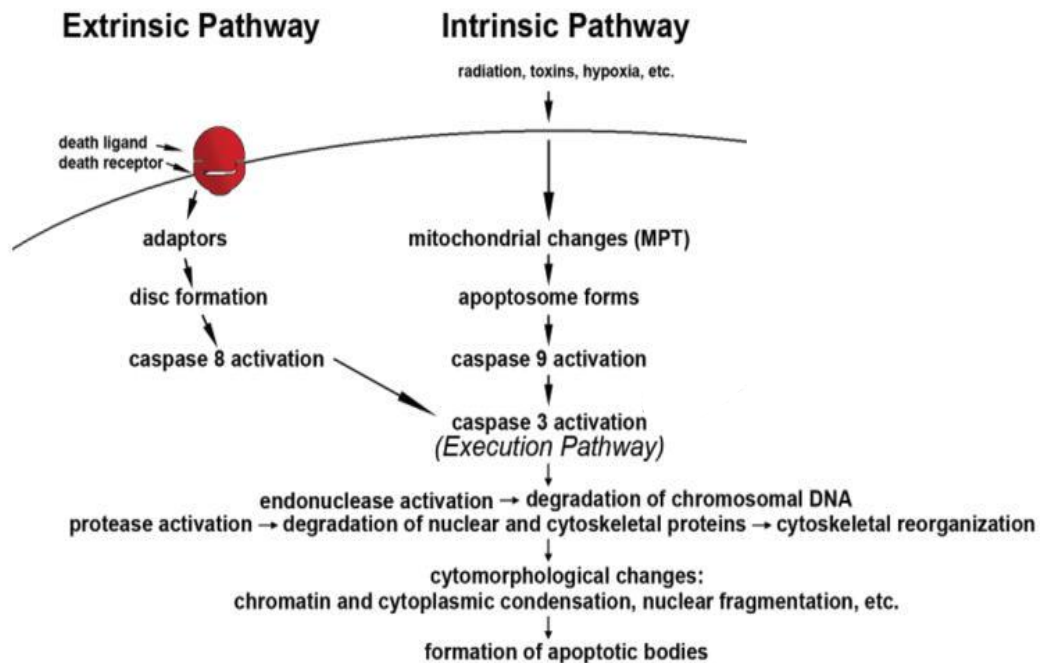
Figure 1.4 A schematic overview of the extrinsic and intrinsic apoptotic pathway. The extrinsic pathway is activated through the ligation of the death receptor which interacts with the DISC activating caspase 8. The intrinsic pathway releases cytochrome c after mitochondrial membrane depolarization. This results in the activation of caspase 9. Caspases 8 and 9 activate caspase 3 for the initiation of the execution pathway and cell death. Used with permission (Elmore, 2007).

Many different assays are available to detect apoptotic cell death. These include but are not limited to the adherent state apoptosis assay (ASA) (Emamzadeh *et al.*, 2014), APOPCYTO Caspase-3 Colorimetric Assay Kit (Takano *et al.*, 2014) or the apoptosis kit (Tong *et al.*, 2015). Annexin-V FITC staining was used as the assay of choice in this study to detect the presence of early apoptotic cells. During apoptosis phosphatidylserine (PS) in the plasma membrane relocates from the inner to the outer leaflet of the plasma membrane of the cell. The translocation of this PS provides an extracellular binding site for Annexin V. Annexin-V conjugated to the fluorochrome FITC allows for the flow cytometric identification of early or

24

late phase apoptosis as well as necrosis (Sawai and Domae, 2011, Span *et al.*, 2002, Visagie *et al.*, 2015). Loss of membrane integrity allows the uptake of the membrane impermeable propidium iodide (PI) dye which was used to detect the presence of necrotic cells (Hurrell and Outhoff, 2013, Sawai and Domae, 2011, Span *et al.*, 2002).

A new and emerging paradigm suggests that cell death related to tumour specific alterations in metabolism links several different aspects. This elucidates to the unlikelihood of classifications into a single mechanism. It has been proposed that cell death is a greater integration of different mechanisms (Huo *et al.*, 2017).

1.17   Background to PlasDIC and light microscopy

Cellular function is an important requirement for cell growth and proliferation. Live cell imaging using light microscopy enables cellular functions to be observed as they are occurring. It is essential that the cells environment is kept constant through the monitoring of temperature, humidity and carbon dioxide levels. Light microscopy is routinely used to count cells but is also used for live cell imaging during the different phases of the cell growth (Stephens and Allan, 2003).

Two sets of interlaced planes of polarised light play a role in image enhancement when using DIC (Murphy, 2002). The Kohler illumination method described in 1893 by August Kohler (Köhler, 1893) is used in light microscopy and involves a bright, uniform illumination of the specimen being observed. PlasDIC is a method that was commercialised by Zeiss (Carl Zeiss AG, Germany) and produces images that have decreased contrast when illuminated as well as a lower degree of coherence (Esslinger and Gross, 2015). This contrast method is used to observe the morphology of cells on a three dimension level (Visagie *et al.*, 2012) and is an extension of differential interference contrast (DIC) microscopy that provides high imaging of a variety of cells including individual cells, clusters of cells as well as thick individual cells maintained in cell culture flasks. PlasDIC is used to observe morphological changes typical of apoptosis or necrosis as well as chromosomal changes, cell membrane integrity and cell density (Visagie *et al.*, 2014). PlasDIC imaging eliminates the 'halo' effect that is observed in certain cells that are imaged under polarised light microscopy. PlasDIC allows for the enhanced observation of living cells, providing increased contrast in thick specimens and enables cell morphology to be observed (Mehta and Sheppard, 2008).

25

The principle of PlasDIC is based on linearly polarised light (Mehta and Sheppard, 2008). An advantage of this method is the adjustability of contrast that can be adapted relevant to the specimen being observed (Zeiss). PlasDIC combines coherence and polarisation that the entire sample area lays outside of the area that is sensitive to polarisation. This method is the first polarisation-optical DIC method that allows for the use of plastic dishes and therefore cells can be imaged in flat bottom clear plates while maintaining ideal environmental cell conditions. PlasDIC is advantageous as it is operator friendly, the diaphragm doesn't need to be changed, stability is present with the basic setting, cost effective, standard objectives can be used and live cells can be imaged without staining (Wehner, 2003).

1.18   Background to cell cycle

Control of the balance between cell proliferation and cell death is essential in order to maintain tissue homeostasis (Danial and Korsmeyer, 2004). If regulation fails and the balance is disrupted, unwanted cell growth or cell death can occur. Cell cycle is closely linked to apoptosis through the detachment of cells and chromatin condensation (Israels and Israels, 2000).

The cell cycle is a process of ordered events that allows for the replication, transferral of genetic information and division of cells identical to the parent cell. During cell cycle progression, the DNA of a cell is accurately replicated and identical genetic information is divided between two daughter cells. The cell cycle is divided into four phases (Figure 1.5) namely the G1 (gap phase 1), S (DNA synthesis phase) the G2 (gap phase 2) and M (mitosis phase). During the G1 phase the cell grows larger and prepares for division due to exposure to growth factors and extracellular mitogens. Following this the cell enters into the S phase where DNA replication occurs to form an exact copy of the DNA resulting in double the DNA in a single cell where the chromosomes are reordered and aligned for separation. This is the G2 phase. During the M phase that follows, mitotic spindles are generated, and sister chromatids are pulled towards opposite poles of the cell after which cell division rapidly occurs. Cells that are not actively dividing are either temporarily or permanently arrested in the G0 (quiescent) phase (Israels and Israels, 2000).

Cells are activated by external stimuli and phosphorylation with up-regulation of cyclins and cyclin-dependent kinases (CDKs) that allows the cell to begin proliferation. Protein kinases drive the cell cycle. Kinases activate the regulatory cyclin unit attached to the catalytic CDK partner via phosphorylation. Increased expression of cyclin D (D1, 2, 3) initiates the start of the G1 phase of the cell cycle. The family of cyclin D's associate with the kinases CDK4 or

26

CDK6. The association of the cyclin with the CDK activates the CDKs through phosphorylation and in turn activates retinoblastoma protein (pRb) (Grandori *et al.*, 2000, Israels and Israels, 2000). This protein regulates the progression of the cell through the restriction point in the G1 phase.

In late G1 progression, cyclin E is up-regulated (Israels and Israels, 2000). Cyclin E forms a complex with CDK2 and allows the transition from the G1 into the S phase. At the G1/S transition, cyclin A/CDK2 complex is up-regulated allowing the cell to progress through the S phase. Cyclin A associates with CDK1 in the G2 phase. The transition of the cell into the mitotic phase is regulated by the cyclin B1/Cdk1 complex (Hunt, 1989). This complex aids in the breakdown of the nuclear membrane and in the separation of the centrosomes (Takizawa and Morgan, 2000). Cyclin B forms a complex with p34 to form the Maturation Promoting Factor (MPF). Entry into mitosis is induced via activation of MPF while the inactivation induces the exit of the cell from the mitotic phase (Murray, 1992).

Pathways that regulate cell cycle in respect to the timing and transitions from one phase to another are controlled via cell cycle checkpoints. These checkpoints ensure the completion of DNA replication and the segregation of chromosomes (Elledge, 1996). Damage to the cell, incorrect DNA replication or unfavourable conditions are monitored and according to the extent of the damage, the cell will either be repaired or mitosis will be terminated (Israels and Israels, 2000).

The most essential checkpoint in the cell cycle is the restriction point (R) located in the last third of G1. The G1 checkpoint ensures that the DNA of a cell is not damaged. If DNA damage occurs, CDK inhibitors which are induced by increased levels of p53 mediate a G1 arrest. The G2 checkpoint is responsible for checking the DNA prior to entrance into mitosis (Murray, 1994). Both damaged as well as unreplicated DNA can inhibit entry of the cell into the mitotic phase of the cell cycle. The transition of the cell from metaphase to anaphase is monitored by the metaphase checkpoint (Tyson *et al.*, 2002). Once a cell enters into mitosis it is essential that the attachment of sister chromatids to microtubules occurs ensuring chromosome segregation. This is monitored by the spindle assembly checkpoint. The arrest of a cell at a checkpoint allows for the repair of the cell or the initiation of cell death. Cell death, specifically apoptosis can be initiated if the DNA of the cell is damaged, unreplicated or depolymerisation of the spindles occur (Murray, 1994).

27
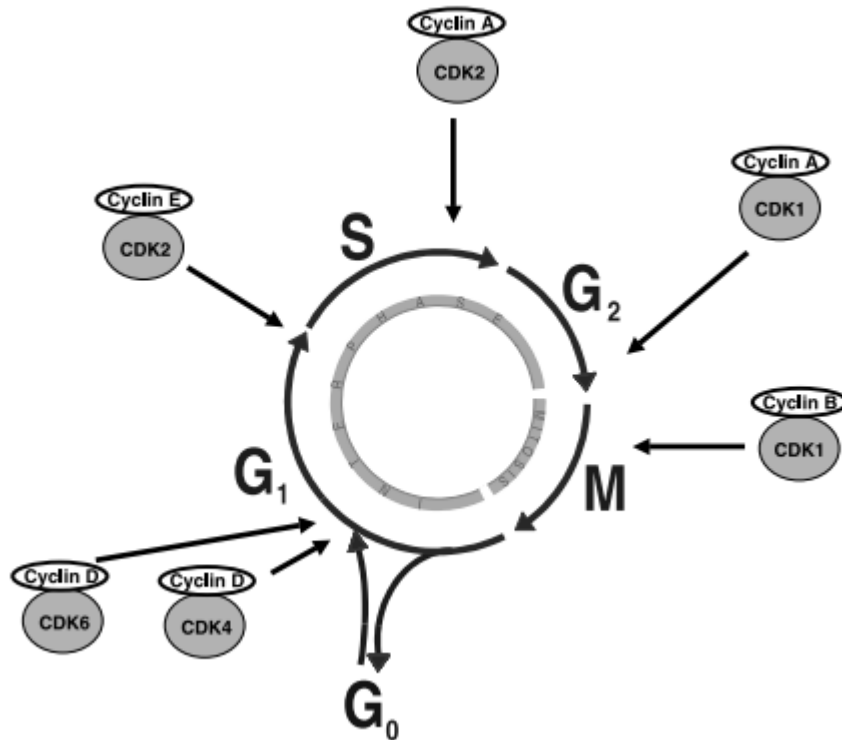
Figure 1.5: Schematic overview of the cell cycle. The interphase stage of the cell cycle is divided into the G0, G1, S and G2 phases. The mitotic or M phase follows during which the cell divides. The regulatory cyclins, CDK's and their points of control during the cell cycle are indicated. Used with permission (VermeulenVan Bockstaele *et al.*, 2003).

The cell cycle is further regulated by CDK inhibitors known as the Cip/Kip family which includes p21 and p27. These proteins target CDK2, 4 and 6 and function at various sites of the cycle. Inhibitors of Cyclin Dependent Kinase 4 (INK4) form the second family of cell cycle inhibition.

Many different proteins are linked to cell cycle progression. An oncogenic phospho-protein in the nucleus, c-Myc stimulates the progression of cell cycle (Facchini and Penn, 1998, Spencer and Groudine, 1991). The induction of signals for mitosis stimulates c-Myc to direct cells into the G_1 phase. The effect on the cell cycle can occur via the transcription of cell cycle genes such as cyclins D1, D2, E, A, CDK1, 2, 4 and elongation factor 2 (E2F) (Beier *et al.*, 2000). Cellular damage results in cell cycle arrest so that the cell can be repaired prior to replication and division (Elledge, 1996). Cell cycle arrest is induced by the tumour suppressor protein p53 (Sionov and Haupt, 1999). Cell cycle progression is also inhibited by the pRb which interacts with E2F in a complex (VermeulenBerneman *et al.*, 2003). Cell proliferation is stimulated

28

through the phosphorylation of pRb with subsequent release of E2F. The apoptotic protein Bcl-2 plays a role in cell cycle progression and can result in a 30-60% increase in the length of the G1 phase (Linette *et al.*, 1996). Bcl-2 is responsible for the exit of cells into quiescence and stops cells from re-entering a new division cycle (Adams and Cory, 1998).

1.19 Background to the mitochondria

Warburg described the traits of cancer with one being the dependence on aerobic glycolysis (Warburg, 1956). From this it was suggested that one of the possibly aetiologies of cancer was attributed to impaired metabolism in the mitochondria. Cancerous cells could therefore be targeted through inhibition of mitochondrial oxidative phosphorylation. Mitochondria are the most efficient energy supplying organelles of all living organisms. Their main function is to oxidize fatty acids and the glycolytic product, pyruvate, as well as many other substrates for the production of ATP (Dröse *et al.*, 2009). The production of reactive oxygen species (ROS) on the inner mitochondrial membrane is associated with superoxide anion that is generated within the mitochondria but is not able to exit into the cytosol (Gao *et al.*, 2008).

Mitochondrial membrane potential drives three essential functions including the generation of ATP through oxidative phosphorylation, the uptake and storage of calcium, as well as the detoxification of ROS. During the process of apoptosis, apoptotic signals are initiated as a result of disruption of the mitochondrial membrane potential followed by trans-membrane leakage of cytochrome *c* into the cytosol where the intrinsic apoptotic pathway is activated (Nicholls, 2004). Mitochondrial membrane potential is therefore indicative of the function of the mitochondria, as well as the health of the cell.

Four complexes of enzymes constitute the electron transport chain (ETC) of the mitochondria (Birsoy *et al.*, 2015). These chains are responsible for the transport of electrons from donors such as NADPH to electron acceptors such as oxygen. A proton gradient across the inner mitochondrial membrane is generated through the pumping of protons from the ETC into the inter-membrane space (Mitchell, 1961). This in turn drives the synthesis of ATP. Electron donors that drive the ETC are often obtained through glycolysis (Birsoy *et al.*, 2015). The ETC has an impact on many different processes including the redox state, ROS, mitochondrial membrane potential (Chen *et al.*, 2014), apoptosis and cellular signalling. An impairment in the ETC can lead to many effects but has been specifically linked to impaired cell proliferation (Fendt *et al.*, 2013). This anti-proliferative effect has been linked to but not confirmed to changes in ATP or ROS levels (Wallace, 1999).

29

Alteration of the mitochondrial metabolism of tumour cells can initiate cell death. The respiratory chain consists of complexes I, III and IV. These complexes guide the electrons through a series of redox reactions which use free energy in order to create a proton gradient that will initiate complex V to produce ATP through ATP synthase. Complexes I (NADH: ubiquinone oxioreductase) and III (ubiquinol: cytochrome c oxioreductase; cytochrome bc_1 complex) of the ETC have been considered the major source of intracellular ROS (Dröse and Brandt, 2012). The release of superoxides (ROS) occurs through complex I which in turn causes mitochondrial DNA damage or the opening of the mitochondrial permeability pore (Figure 1.6) (Costa *et al.*, 2011). The generation of superoxide is regulated mainly by the $NADH/NAD^+$ ratio and when in reverse form, regulation is dominated by the membrane potential (Kussmaul and Hirst, 2006). Complex III is regulated by a balance between membrane potential, reduced and oxidized ubiquinone availability as well as the redox state of the complex (Dröse *et al.*, 2009).

The production and accumulation of intracellular ROS activates the mitochondrial permeability pore to open resulting in a possible leakage of the mitochondrial membrane (Figure 1.6) (Chen *et al.*, 2012, Shrotriya *et al.*, 2014). This leads to depolarisation of the membrane and leakage of cytochrome c into the cytosol where the apoptosome is assembled followed by the initiation of apoptosis. Previous studies have shown that inhibition of these trans-membrane complexes result in mitochondrial ROS accumulation (Shrotriya *et al.*, 2014). Insufficient ATP during oxidative phosphorylation has been linked to deficient complex III activity in the mitochondria (Wen and Garg, 2010). The rate of ROS production by the mitochondria is inversely proportional to the amount of ADP that is available in the cytosol. Therefore by decreasing ADP levels, the mitochondrial membrane potential will increase resulting in a decreased respiratory rate and an increase in ROS generation due to the ETC undergoing reduction (Cadenas and Davies, 2000). In contrast to this, a small decrease in the membrane potential results in a large decrease in hydrogen peroxide (ROS).

Mitochondria

↓

ROS

DNA damage

↓

PARP

GSH ⬇ NADPH ⬇   OXPhos ⬇

↓

NAD ⬇ ATP ⬇

Redox status collapse

⊥

Glycolysis → Energetic collapse

↓
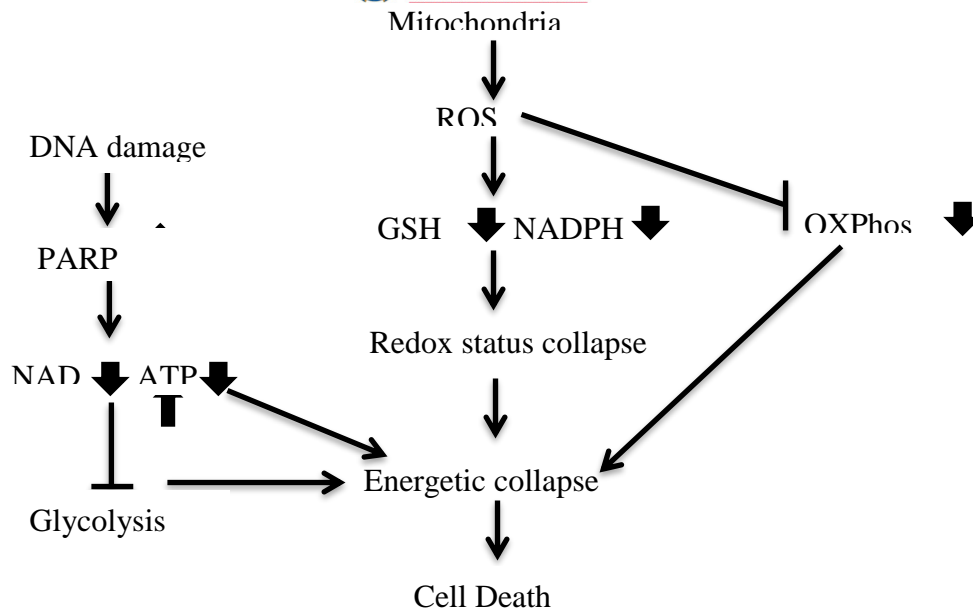
Cell Death

Figure 1.6 The process of cell death via mitochondrial involvement. The production of ROS via the mitochondria results in the damage of DNA inhibiting glycolysis. It can also lead to downstream events where NADPH levels are decreased with a subsequent collapse in both redox status and energy. ROS further inhibits oxidative phosphorylation. These events results in the death of the cell. Legend: Adenosine tripohosphate (ATP), glutathione (GSH), Nicotineamide-adenine-dinucleotide (NAD), Nicotineamide-adenine-dinucleotide (reduced form) (NADPH), oxidative phosphorylation (OXPhos), poly (ADP-ribose) polymerase (PARP), reactive oxygen species (ROS).

1.20   Background on autophagy

Autophagy is a cellular process that utilizes lysosomal activity for the degradation of material in the cytoplasm (Eskelinen, 2008). Autophagy plays a role in regulating the biology of mammalian cells and recycles nutrients that are produced during the process of autophagy (Jing and Lim, 2012). The main function of autophagy is the degradation of long-lived proteins as well as intracellular (IC) organelles that are damaged (Nedelsky *et al.*, 2008). The survival of cells is dependent on organelle turnover as well as the breakdown of protein. The disruption of autophagy can result in cells growing abnormally or undergoing cell death which can result in the progression of various diseases (Klionsky and Emr, 2000). There is increasing evidence that autophagy is not a non-selective degradation process of the engulfment of cytoplasm but that selective autophagy occurs through the degradation of mitochondria (mitophagy), endoplasmic reticulum (reticulophagy), aggregated proteins (aggrephagy) as well as microorganisms (xenophagy) (Johansen and Lamark, 2011). The outcome of autophagy can either be cell survival or cell death depending on the contents of the cell as well as the different stimuli (Jing and Lim, 2012). Under unfavourable conditions, the role of autophagy is claimed

31

to be a protective role as it primarily functions to eliminate damaged organelles and provide nutrients to the cell. Autophagy can also be triggered by cytotoxic drugs, and when inhibited, it has been reported to potentiate anti-cancer drug induced apoptosis (Song *et al.*, 2008). Autophagy can enhance cell death via the degradation of factors that are essential in the survival of a cell (Yu *et al.*, 2006). This effect on cell death could also be attributed to the effect autophagy has on the maintenance of energy as ATP is required for apoptosis and necrosis (Qu *et al.*, 2007).

Cells that avoid autophagy are characterised by abnormal accumulation of protein as well as disorganised mitochondria (Ebato *et al.*, 2008). This suggests that cells utilize the process of autophagy for intracellular homeostasis. In addition, autophagy plays a role in the regulation of rapid changes responsible for cellular differentiation in the cell as well as in the removal of infectious agents from the cell. Due to the vital role of autophagy in mammalian cells, the inhibition of this process could contribute to disease progression including neurodegenerative disorders, diabetes mellitus as well as diseases such as cancer (Jing and Lim, 2012).

The autophagic process is induced by various stimuli such as the starvation with respect to amino acids and autophagy is initiated when a flat membrane cistern (phagophore) entraps a portion of the cytoplasm forming a double-membrane vacuole (Figure 1.7) (Arstila and Trump, 1968). The expansion of the phagophore and completion of the vesicle is regulated via the conjugation of microtubule-associated protein 1 light chain 3 (LC3) (Jing and Lim, 2012). The vacuole contains cytosol as well as organelles and is known as an autophagosome. The autophagosome fuses with an endosome or a lysosome which transfers essential enzymes such as hydrolases for the degradation of cytoplasmic components (Eskelinen, 2005). The fused autophagosome with the lysosome/endosome is termed an autolysosome and amphisome (Ylä-Anttila *et al.*, 2009). Once the entrapped components have been degraded they are transported back to the cytoplasm via pumps that are located within the limiting membrane of the lysosome (Jing and Lim, 2012).

An important analytical tool in the observation and study of the internal structure of a cell is transmission electron microscopy. This technique is used to study complex ultra-structures and need to be analysed in thin sections. TEM preparation includes cell fixation, processing of samples for thin sectioning, embedding of samples into resin for sectioning, sectioning of samples with an ultra-microtome and specific heavy metal staining for visualisation (Burghardt and Droleskey, 2006). TEM is advantageous as images can be observed at higher resolution,

32

however a disadvantage is the small sample size examined (Ylä-Anttila *et al.*, 2009). This technique makes use of ultra-thin sections of cells usually 70-80 nm in thickness. TEM has been routinely used as the most accurate ultra-structural cellular analysis where autophagy characteristics can be confirmed (Eskelinen, 2008, Ylä-Anttila *et al.*, 2009). Various biological methods such as western blot analysis have been employed to monitor and identify autophagy however, morphological techniques such as TEM are often needed to strengthen and support findings (Eskelinen, 2008). A method that is suitable for cultured adherent cells uses osmium tetraoxide which provides excellent contrast for the membranes of autophagosomes (Ylä-Anttila *et al.*, 2009).

Autophagy can be confirmed through TEM by identification of membrane-bound vesicles which contain organelles or degraded material from the cytoplasm (Eskelinen, 2005). Autophagic compartments can further be morphologically classified into early or initial compartments which contain intact organelles, and into late compartments which contain degraded autophagic compartments (Dunn, 1990). Using TEM the limiting membrane often appears as multiple layers which have been speculated to be caused by chemical fixation during sample preparation. Poor contrast of autophagosome limiting membranes has been attributed to lipid extraction during sample preparation. At low magnifications, the narrow empty space between the two membranes can be used to identify autophagosome formation (Ylä-Anttila *et al.*, 2009). Another useful identification is the presence of rough endoplasmic reticulum located near either side of the autophagosome. TEM allows for ultrastructural analysis with excellent sensitivity and it does not require the use of antibodies in contrast to other imaging techniques such as fluorescent microscopy. One of the disadvantages however is the incorrect interpretation of the images produced due to lack of experience (Eskelinen, 2008).

33
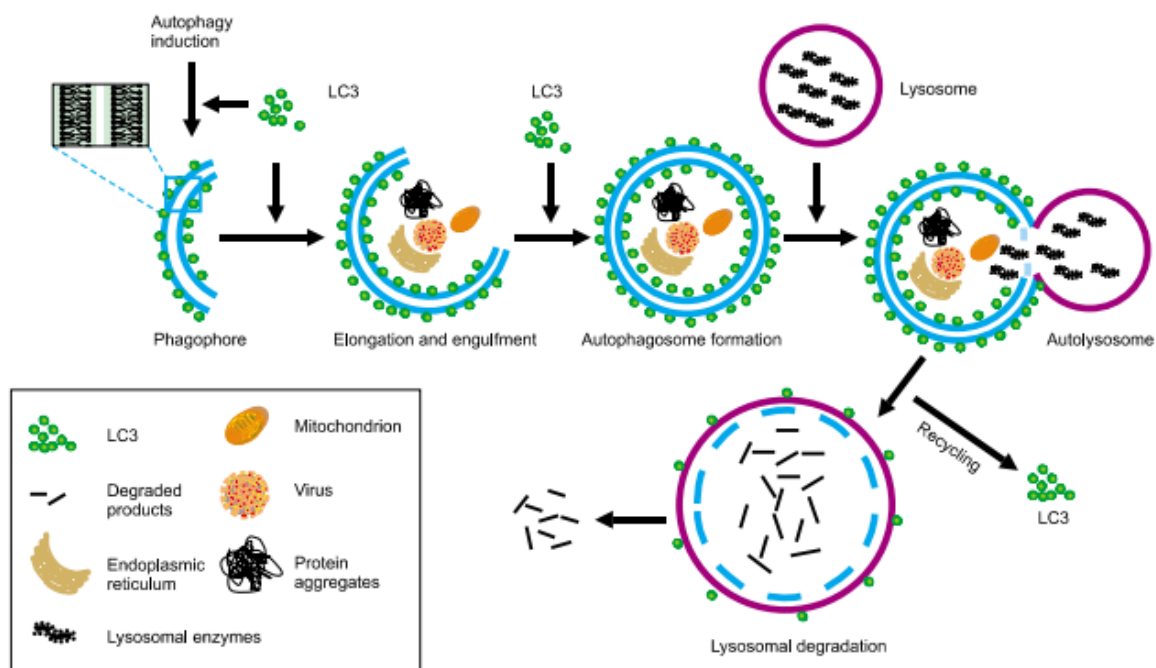
Figure 1.7 Schematic overview of the process of autophagy. Autophagy induction signals result in the formation of a membrane known as a phagophore. The conjugation of LC3-I (cytosolic) to the membrane occurs, regulating elongation of the phagophore. The complete phagophore contains cytoplasmic constituents such as endoplasmic reticulum, mitochondria as well as foreign organisms. The closure of the membrane result in the formation of double-membrane bound autophagosome. Fusion of the autophagosome with a lysosome forms an autolysosome for the degradation of cellular compartments. Lysosomal enzymes degrade the engulfed material and LC3-II (membrane bound) as well as the autophagic-derived nutrients are re-cycled. The autophagic process can be used for cellular homeostasis or can result in cell death either directly or indirectly. Used with permission (Jing and Lim, 2012).

Identification of autophagosomes is often mistaken for normal vacuole formation and an important criterion for autophagic compartments is the presence of cytoplasmic compartments such as ribosomes within it (Eskelinen, 2008). In TEM, autophagosomes are often observed fused with an endosome/ lysosome.

Autophagosome membranes have been described to contain a high content of unsaturated lipids which has been observed by darker staining in comparison to autolysosomes and amphisomes which display less contrast (Ylä-Anttila *et al.*, 2009). Although there is a basic protocol for identifying autophagic compartments, using TEM alone, certain structures cannot be defined as being an amphisome or autolysosomes without the use of specific markers. The use of the terms initial autophagic vacuole and degradative autophagic vacuole are therefore more appropriate in TEM analysis (Eskelinen, 2008).

34

TEM imaging can also provide basic quantitation of autophagy via establishing the accumulation of either early or late autophagic compartments (Eskelinen, 2005). Early autophagosomes prevailing could be due to an increase in their formation or a defect in their ability to mature into autolysosomes. If late autophagic compartments predominate, a defect in degradation in the autolysosome could be apparent. Autophagic accumulation kinetics can be studied through the addition of compounds such as leupeptin or pepstatin that inhibit the breakdown of lysosomes (Klionsky *et al.*, 2012).

Cancer cells up-regulate autophagy as a mechanism for survival. Autophagy is responsible for intracellular homeostasis through the degradation and recycling of damaged organelles and misfolded proteins (Alayev *et al.*, 2015). This cellular process functions during periods of nutrient deprivation where the cell reuses proteins within the cell until amino acids from outside the cell become available again. Autophagy plays an important role in cancer by functioning to either induce cell death or to promote cell survival (Baehrecke, 2005). Cell survival in cancer cells occurs through the recycling of components within the cell allowing for survival in nutrient deprived or stress induced conditions. The balance in autophagy is essential as excessive autophagic damage can result in cell death. Autophagy is a protective process which is commonly utilized in breast cancer cells and may be a contributing factor to acquired drug resistance (Rabinowitz and White, 2010). Tumours are often located in environments deprived of growth factors, nutrients, vascularization as well as oxygen. Due to this, the process of autophagy may inhibit some cancers or support the growth of the tumour (White and DiPaola, 2009). Cancer cells are capable of deregulating autophagic pathways and some chemotherapeutic agents aim to target these pathways to induce autophagy. A hypothesis was that synergistic combinations of chemotherapeutic agents with autophagy inhibitors exist as a possible mechanism to target cancer cells due to the fact that autophagy could favour tumour survival.

The process of autophagy has many different roles including those of mammalian development, cell death and cell survival. Autophagy also plays an essential role in adult starvation and increased autophagy is observed after 24 hour starvation in renal, hepatic, pancreatic, cardiac and skeletal muscle thereby protecting the brain (Mizushima *et al.*, 2004). The metabolites produced from autophagy provide substrates for the production of energy as well as biosynthesis (Rabinowitz and White, 2010).

35

The formation of autophagosomes is controlled by autophagy related (Atg) gene products such as Atg1 or Unc51-like autophagy activating kinase (ULK1) and the process is inhibited via the binding of ULK1 to the mammalian target of rapamycin complex 1 (mTORC1) (Kuma and Mizushima, 2010). Under nutrient deprived conditions, mTORC1 dissociates from ULK1. The dissociated ULK1 nucleates and elongates the autophagosome for the induction of autophagy. The recruitment of class III phosphatidylinositol 3-kinase (PI3K) occurs via an Atg6 or Beclin 1 complex and generates phosphatidylinositol 3-phosphate (PI3) which results in nucleation of the autophagosome. Autophagosome expansion occurs through an ubiquitin-like reaction of Atg12 and Atg8 which in mammals are known as LC3. LC3 is cleaved by Atg4 and 3 and conjugates with phosphatidylethanolamine (PE) to form the lipidated LC3-II protein. LC3-II in association with new autophagosome membranes remains in mature autophagosomes monitoring the process of autophagy until binding of the lysosome to the membrane (Funderburk *et al.*, 2010).

Many different techniques to evaluate the induction of autophagy have been utilized with one of the more frequently used technique being immunoblotting for the detection of LC3-II (Klionsky *et al.*, 2007). The marker LC3-II contains several homologs including LC3A, LC3C as well as LC3B which is the homolog used in many autophagic studies (Barth *et al.*, 2010). LC3 is detected as two distinct bands after SDS-PAGE and immunobloting onto a membrane. The lower band from the SDS gel is the LC3-II and the second band of higher mass is the cytosolic LC3-I protein which is present on the membrane of autophagosomes (Kabeya *et al.*, 2000). LC3-II (14 kDa) is more hydrophobic than LC3-I (16 kDa) and migrates faster than LC3-I (Barth *et al.*, 2010). The quantity of autophagosomes can be closely related with the amount of LC3-II present and therefore this is a good marker to show activation of the autophagy process (Kabeya *et al.*, 2000).

Due to the fact that LC3 plays an essential role in the formation and functioning of the autophagosome, antibodies that are specific for LC3-I and LC3-II have been widely used in western blot analysis to monitor autophagy in cells (Karim *et al.*, 2007, Tanida *et al.*, 2008). Multiple samples can be analysed for the presence of these markers of autophagy through western blot analysis (Kaufmann *et al.*, 1987).

1.21   Research aim

The aim of this study was to investigate combinations of two synthetic oestrone analogues and the glycolysis inhibitor 2-deoxyglucose for potential synergistic effects on breast cancer cells

36

using cell enumeration, mitochondrial membrane potential and cell cycle, in an *in vitro* setting. Cell apoptosis, necrosis and autophagy pathways were assessed to indicate the mechanism of cytotoxicity.

1.22   Research objectives

1) To determine the cytotoxicity of oestrogen analogue combinations with 2-deoxyglucose on the breast cancer MCF-7 cell line and non-tumorigenic MCF-12A cell line.

2) To investigate the mechanistic properties of the synergistic combinations with regards to:
   - the involvement of the mitochondria using mitochondrial membrane potential
   - the potential induction of autophagy
   - cell cycle phase arrest
   - mode of cell death

37

Chapter 2: Materials & Methods

2.1. **Cell culture**

Ethical approval for the use of commercially available cell lines was obtained prior to initiation of the study from the Faculty of Health Science Student Research Ethics Committee of the University of Pretoria (230/2014).

2.1.1 Maintenance of cell cultures

The breast adenocarcinoma (MCF-7) (HTB-22) and non-tumorigenic spontaneously immortalised breast tissue (MCF-12A) (CRL-10782) cell lines were obtained from the American Type Culture Collection (ATCC). MCF-7 (human breast adenocarcinoma) cells were cultured in Dulbecco's Modified Eagle Medium (DMEM) supplemented with 10% foetal calf serum (FCS). For initial cell attachment and drug exposure experiments media was supplemented with 2% FCS for the duration of the experiment (5% CO_2, 37ºC). The MCF-12A (immortalised human non-tumorigenic breast epithelial cells) cell line was maintained and grown in a 1:1 mixture of DMEM and Ham's-F12 medium (1:1) supplemented with 10% FCS. For drug exposure experiments media was supplemented with only 2% FCS (5% CO_2, 37ºC). . Cells lines were cultured in the Department of Pharmacology tissue culture facility according to ATCC guidelines for the specific cell lines in tissue culture flasks supplemented with the appropriate media containing 10% FCS and sub-cultured three times a week.

All experiments and preparations were carried out utilizing aseptic techniques. Sample preparation was carried out in a laminar flow cabinet, all sterile solutions were filter-sterilized using a 0.22 µm pore size filter and all glassware, microfuge tubes, medium boats and non-sterile equipment were autoclaved for 30 minutes at 121°C.

2.1.2 Cell lines

The effects of the synergistic combinations of novel oestrone analogues and 2-deoxyglucose were investigated on the following cell lines:

Cell lines were selected in accordance with the subtypes of breast cancer. These subtypes include: luminal A, luminal B, HER2 positive, normal and basal; each of which have different diagnostic and treatment responses (Holliday and Speirs, 2011).

38

Table 2.1: The cell lines showing the various growth media and cell concentrations

Cell line	Tissue of origin	ATCC Number	Medium	Growth Characteristic	Doubling time (h)
MCF-7	Human mammary gland/breast adenocarcinoma	HTB-22	DMEM	Adherent	29
MCF-12A	Human breast epithelial tissue	CRL-10782	DMEM :Ham's -F12 (1:1)	Adherent	19

The most prevalent subtype being luminal A, accounts for approximately 75.3 % of breast cancer tumours in Caucasians, 59.4 % in African Americans and 71.4 % in Asian populations (Kwan *et al.*, 2009). This subtype of breast cancer is oestrogen or progesterone receptor positive and HER2-negative and is represented by the MCF-7 human breast carcinoma cell line (Kwan *et al.*, 2009, Petersen *et al.*, 1992). It is therefore favourable to test this cell line since the oestrogen receptors expressed by the MCF-7 cell line is a therapeutic target that is responsive to hormone therapy (Holliday and Speirs, 2011). The basal subtype of breast cancer is represented by the spontaneously immortalized cell line, MCF-12A (Kwan *et al.*, 2009, Subik *et al.*, 2010). This subtype is oestrogen-, progesterone- and HER2 receptor-normal (Kwan *et al.*, 2009). The above-mentioned cell lines therefore represent two different subtypes of breast tissues, as well as expressing different receptor profiles which can provide valuable information on the response that each type of breast cancer will have towards treatment with the experimental compounds.

2.1.3 Preparation of cells for experimental procedures

The non-tumorigenic and cancerous cell lines were cultured and maintained in culture flasks in a humidified incubator (Binder C150, USA) until approximately 80% confluence at 37°C and 5% CO_2.

The medium was discarded from the flask, the cells washed with sterile phosphate buffered saline (PBS) and 2-5 ml of trypsin/versene solution was added. The cells were then incubated for 5-10 minutes (37°C) until the cells rounded and appeared to detach from the plastic surface. All interior surfaces of the culture flask were wetted with the trypsin solution prior to decanting

39

the solution. The trypsin/versene solution (containing the cells) was then transferred to a sterile 15 ml tube. Media supplemented with 10% FCS was used to rinse the flask as well as to deactivate the trypsin/versene solution and then also added to the 15 ml tube. The cell suspension was centrifuged at 200 x *g* for 6 minutes, the supernatant discarded and the cell pellet re-suspended in 1 ml of the appropriate complete media.

An aliquot of the cell suspension (20 µl, prepared as above) was re-suspended in 180 µl of trypan blue in microfuge tubes and mixed well. At least 20 µl of this suspension was placed onto a haemocytometer and the cells counted using a Reichert Jung Micro Star microscope (40 x magnification).using trypan blue exclusion to determine the percentage of viable cells as well as to assess the integrity of the membrane.

Dilutions were then made in the appropriate media to give the cell concentrations required for the stock suspensions required for each specific assay to be performed.

Different cell concentrations specific to each assay were used. Cells were seeded at a cell density of 6.25×10^4 cells/ml in 96-well plates. Experiments conducted in 6-well plates were seeded at a density of 5×10^4 and cells were seeded at a density of 4×10^5 in 75 cm^2 flasks.

2.1.4   Cell culture reagents

I.   *Dulbecco's Minimum Essential Medium (DMEM)*

DMEM as well as all chemicals required for supplementation were obtained from Sigma Aldrich (St. Louis, USA). A mass of 67.35 g DMEM powder was dissolved in 5 litres of autoclaved double de-ionized pyrogen-free water. The double de-ionized water was produced by the Elga PureLab Ultra water unit in the Department of Pharmacology. The pH of the media was adjusted prior to filtration with 18.5 g NaHCO$_3$ after which appropriate quantities of 1N HCL or 1N NaOH were added if necessary to obtain a final pH of 7.4. A Sartorius vacuum flask filter system with a Sartorius glass-fibre pre-filter and a 0.2 µm cellulose acetate filter was used to filter the medium under vacuum. The medium was then forced through 0.2 µm filters via a Heidolph peristaltic pump. Media was dispensed into sterile 500 ml flasks A volume of 5 ml penicillin/streptomycin was added to 500 ml of the cell culture medium. Medium was stored at 4°C and directly prior to use was supplemented with 10% FCS for plating and attachment of cells or 2% FCS for drug exposure and the remainder of the assay.

40

II. DMEM/Kaighn's modified Ham's F12 (1:1) mixture for MCF-12A cell line

DMEM, Kaighn's modified Ham's F12 as well as all necessary supplements were supplied by Sigma Aldrich (St. Louis, USA). A mass of 11.1 g of powdered DMEM/Ham's F12 media was dissolved in 1 litre of autoclaved double de-ionized pyrogen free water. The de-ionized water was produced from the Elga PureLab Ultra water unit in the Department of Pharmacology. $NaHCO_3$ (2.5 g) was added prior to filtration to adjust the pH after which appropriate quantities of 1N HCL or 1N NaOH were added if necessary to obtain a final pH of 7.4. A Sartorius vacuum flask filter system with a Sartorius glass-fibre pre-filter and a 0.2 µm cellulose acetate filter was used to filter the medium under vacuum. The medium was then forced through 0.2 µm filters via a Heidolph peristaltic pump. A volume of 5 ml penicillin/streptomycin was added to 500 ml of the cell culture medium and stored at 4°C.

A 1:1 mixture of DMEM and Kaighn's modified Ham's F12 medium was prepared according to ATCC guidelines and further fortified to 100 ng/ml cholera toxin, 20 ng/ml epidermal growth factor, 0.01 mg/ml insulin and 500 ng/ml hydrocortisone. Prior to use, the medium was supplemented with 10% FCS for plating and attachment of cells or 2% FCS for exposure and the assay.

III. Dimethyl sulfoxide (DMSO)

100% DMSO was purchased from Merck (Longmeadow, Modderfontein), kept under sterile conditions and stored at room temperature and used undiluted.

IV. Foetal Calf serum (FCS)

Foetal calf serum was purchased from Biochrom Ltd. (Cambridge, UK). FCS was heat inactivated for 45 minutes at 56°C, centrifuged to remove the precipitate and stored at 4°C and decanted when necessary. FCS was used to supplement all cell culture medium. A FCS concentration of 10% was used for cell growth and attachment, a concentration of 2% for experimental compounds exposure to the cells.

V. Insulin

Insulin was purchased from Sigma Aldrich (St. Louis, USA) and 5 mg was dissolved into 500 ml of a 1:1 DMEM/Kaighn's modified Ham's F12 mixture (see above) media and stored at 4°C.

41

VI.   *Penicillin/streptomycin*

Penicillin/streptomycin solution was obtained from Life Technologies (Johannesburg, RSA) and stored at 4°C. A volume of 5 ml penicillin/streptomycin was added to 500 ml of the cell culture medium.

VII.   *Phosphate buffered saline (PBS)*

Phosphate buffered saline powder was purchased from BD Bioscience (Woodmead, RSA) and 9.23 g was dissolved in one liter of distilled water and stored at 4ºC as per protocol. For sterile conditions, the solution was autoclaved.

VIII.   *Trypan blue*

Trypan blue was obtained from Merck (Longmeadow, Modderfontein). A mass of 20 mg was dissolved in 10 ml of PBS to a final concentration of 0.2%. The solution was then filtered, covered in foil and stored at room temperature.

IX.   *Trypsin/versene solution*

A trypsin/ versene solution was obtained from Highveld Biologicals (Sandringham, South Africa). The solution consists of 0.25% trypsin, 0.1 % EDTA in calcium and magnesium free phosphate buffered saline stored at 4°C and used as purchased.

2.2 Experimental compounds

Two *in silico*-designed oestrone analogues (ESE-15-ol and ESE-16) were synthesised by iThemba Pharmaceuticals (Pty) Ltd (Modderfontein, Gauteng). 2-ethyl-3-O-sulphamonyl-estra-1,3,5(10),15-tetraen-17-ol (ESE-15-ol), 2-ethyl-3-O-sulphamoyl-estra-1,3,5(10),16-tetraene (ESE-16) and the glycolysis inhibitor, 2-deoxyglucose (2-DG) were used for cytotoxicity screening both in isolation and in combination.

42
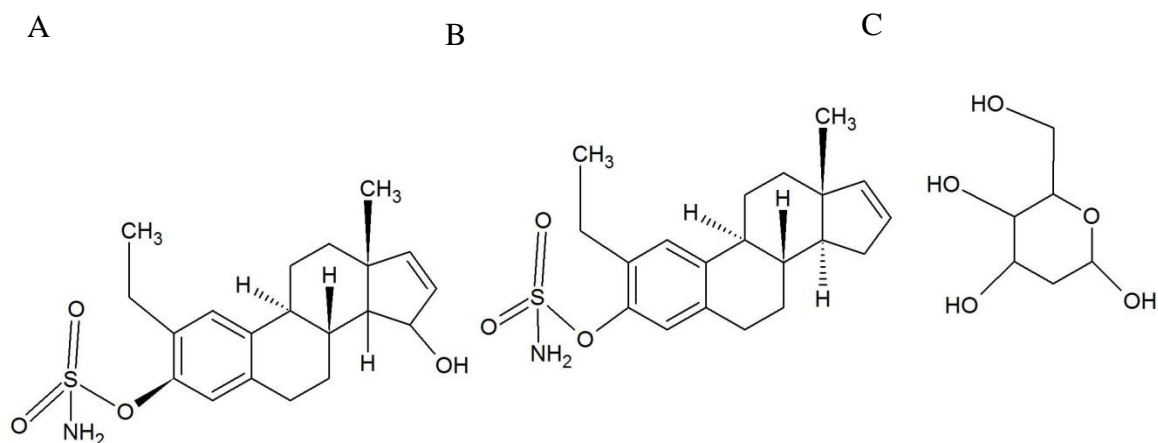
Figure 2.1: The chemical structures of ESE-15-ol (A), ESE-16 (B) and 2-DG (C) generated from Chemsketch 12(Freeware) (www.acdlabs.com).

2.2.1 Preparation of experimental compounds

I. *2-ethyl-3-O-sulphamonyl-estra-1,3,5(10),15-tetraen-17-ol (ESE-15-ol)*

Molecular weight: 359.16 g/mol

A 25 µM stock solution was prepared by diluting 2 µl of 1 mM (3,59 mg in 10 ml DMSO) ESE-15-ol in 78 µl DMSO. The stock solution was stored at -80°C in 2 µl aliquots after which the appropriate cell culture medium containing 2% FCS was added on day of exposure. The final in-well DMSO concentration was 0.07%.

II. *2-ethyl-3-O-sulphamoyl-estra-1,3,5(10)16-tetraene (ESE-16)*

Molecular weight: 361.50 g/mol

A 10 mM stock solution was prepared by dissolving 3.6 mg in 1 ml of DMSO. A volume of 10 µl of this stock solution was then diluted in 390 µl of DMSO to a final stock concentration of 250 µM and stored in 2 µl aliquots. Prior to exposure the appropriate media containing 2% FCS was added to each aliquot. The final in well DMSO concentration was 0.05%.

III. *2-Deoxyglucose (2-DG)*

Molecular weight: 164.16 g/mol

A 0.93 M stock solution was prepared by dissolving 1 g in 6.5 ml of HBSS. The stock solution was stored in 6 µl aliquots at -80°C. Prior to exposure the appropriate medium containing 2% FCS was added to each aliquot. The final in well HBSS concentration was 0.29%.

43

IV. *Vehicle treated control*

A vehicle treated control was prepared by dissolving 2 µl of DMSO in the appropriate medium and added to 15 µl of HBSS in the appropriate medium.

2.3 Experimental procedures

2.3.1 Cell viability assays

2.3.1.1 Aim

The aim of this study was to determine the cytotoxicity of the synergistic combinations (obtained from a previous study) on the breast cancer cell line (MCF-7) and non-tumorigenic cell line (MCF-12A) following 72 hours exposure and utilizing the sulforhodamine B cell enumeration assay (SRB).

2.3.1.2 Preparation of cells for sulforhodamine assay

Cells were counted and prepared as stated above. Approximately 80 µl of cell suspension was plated into each well of a sterile 96 well plate to give 5.12×10^3 cells per well, (80 µl/well of a $6,25 \times 10^4$ cells/ml suspension) and the plate incubated at 37°C, 5% CO_2 for 24 hours in order to allow for cell attachment. Cells were exposed to the experimental compounds ESE-15-ol and ESE-16 at a concentration range of 3.125-400 nM and 2-deoxyglucose at a concentration range of 0.40-50 mM. The compounds were then tested in combination with 2-DG at a concentration of 17.5 nM (ESE-15-ol), 134 nM (ESE-16) and 2.7 mM (2-DG). Cells were incubated for a further 72 hours at 37 °C, 5% CO_2.

2.3.1.3 SRB assay

The SRB assay is a colorimetric assay used to determine the cell number that would indicate the extent of proliferation or cytotoxicity resulting from treatment with a specific test compound (Voigt, 2005). Sulforhodamine B is a dye that under acidic conditions binds to and stains basic protein within the cell (Henriksson *et al.*, 2006).

After 72 hours incubation in the presence of the individual or combinations of experimental compounds, the SRB assay was performed as previously described. The T0 plate was removed prior to exposure of the experimental compounds (at 24 hours) and the SRB assay performed. Trichloroacetic acid (TCA) (10%, 80 µl) was added to the cell culture plates to fix the cells after which the plates were stored overnight at 4°C, gently washed four times with flowing water and allowed to dry. A volume of 100 µl SRB solution (0.57% in 1% acetic acid) was added and plates incubated at room temperature for 30 minutes. Plates were then washed four

44

times with 100 µl of a 1% acetic acid solution to remove any excess dye and the plate again allowed to dry. A volume of 200 µl of Tris buffer (10 mM, pH 10.5) was added and the plates placed on a shaker for approximately 1 hour to dissolve the dye. The absorbance was measured at 560 nm with a reference wavelength of 630 nm using an ELX800 UV universal microplate reader (Bio-Tek Instruments Inc., Vermont, USA). Data obtained was used to determine the concentration of the experimental compounds which cause 50% growth inhibition (GI_{50}).

The GI_{50} is calculated using the following formula (Grever *et al.*, 1992):

$$\textbf{Growth inhibitory effect} = [(\textbf{T} - \textbf{T}_0)/(\textbf{C} - \textbf{T}_0)] \textbf{ x 100}$$

Where:

T represents the absorbance values at the test concentration after an incubation period of 72 hours and removal of background noise

T$_0$ represents the absorbance values at time zero after the removal of background noise

C represents the absorbance values of the drug-free vehicle control after 72 hours after removal of background noise

From this assay, results are presented as the mean ± standard error of the mean (SEM) using Graph Pad Prism 5.0 (GraphPad Software, San Diego California USA, www.graphpad.com). The concentrations of the experimental compounds for the remaining assays were determined according to the GI_{50} concentrations obtained.

2.3.1.4 Cell viability statistics

A minimum of three independent experiments were performed with internal triplicates. Cell viability was calculated and represented as the percentage of the untreated control and reported as the mean ± the standard error of the mean (SEM). Non-linear regression and column statistics were conducted in order to determine the mean, standard error of the mean and the GI_{50} of the compounds utilized in isolation prior to combination therapy. The non-parametric Kruskal-Wallis test was conducted for the compounds tested at the concentration obtained from previous synergistic experiments. The Dunnett's post-hoc test was used to compare the significant differences between each compound tested. GraphPad Prism 5.0 (GraphPad Software, San Diego California USA, www.graphpad.com) and Microsoft Excel 2007 (Roselle, IL) were used to determine and represent statistical and graphical evaluations.

45

2.3.1.5 Reagents

I.   Acetic acid

100% Acetic acid was purchased from Saarchem Pty Ltd. (Krugersdorp, RSA). A volume of 10 ml was dissolved in 990 ml of distilled water to obtain a final concentration of 1% and stored at room temperature.

II.   Tris Hydroxymethylaminomethane (Tris buffer)

Tris buffer was purchased from Research Organics Inc. (Cleveland, Ohio). Tris buffer (120 mg) was dissolved in 100 ml of distilled water to obtain a final concentration of 10 mM. The pH was adjusted with sodium hydroxide to 10.5 and stored at room temperature.

III.   Sulforhodamine B (SRB)

SRB was purchased from Sigma Aldrich (St. Louis, USA) and 57 mg was dissolved in 100 ml of 1% acetic acid to a final concentration of 0.057%. The container was covered in foil and stored at 4°C.

IV.   Tricholoroacetic acid (TCA)

TCA was supplied by Merck Pty Ltd (Longmeadow, Modderfontein) and 90 g was dissolved in 300 ml of distilled water to obtain a concentration of 30% and stored at 4°C.

2.3.2   Apoptosis/necrosis

2.3.2.1 Aim

The aim of this study was to evaluate the possible mechanism of cell death induced by the experimental compounds ESE-15-ol, ESE-16 and 2-DG in isolation and in combination using the MCF-7 and MCF-12A cell lines following 72 hours exposure.

2.3.2.2 Preparation of cells for apoptosis/necrosis

MCF-7 and MCF-12A cells were counted (described in Section 2.1.3) and seeded in 6-well plates in the appropriate medium containing 10% FCS at 5 x 10^4 cells per ml (1.2 ml/well) and incubated at 37°C, 5% CO_2 for 24 hours to allow for cell attachment. The media was removed and changed to the same media containing 2% FCS. The cells were exposed to the experimental compounds ESE-15-ol, ESE-16 and 2-DG or the drug combinations at the above mentioned concentrations both in isolation and in combination for 72 hours. Staurosporine at 10μM (24 h) was used as a positive control for apoptosis and the cells incubated in accordance with the optimal concentration from previous apoptotic studies (Blackmore *et al.*, 2014).

46

2.3.2.3 Apoptosis/necrosis assay

Annexin-V FITC staining was used to detect the presence of apoptotic cells by measuring the flip of phosphatidylserine from the inner to the outer plasma membrane, which is reported to occur at early stages of apoptosis (Sawai and Domae, 2011, Span *et al.*, 2002). Loss of membrane integrity enables propidium iodide (PI) to access and fluorescently stain the DNA, which was used to detect the presence of necrotic cells and late apoptosis (Hurrell and Outhoff, 2013, Sawai and Domae, 2011, Span *et al.*, 2002).

After 72 hours exposure of the experimental compounds, the media was removed into 15 ml sterile tubes, the wells washed with sterile PBS and the cells trypsinized as mentioned above (Section 2.1.3). The trypsin solution was removed, the wells washed with sterile PBS containing 1% FCS and transferred into the 15 ml tubes containing the removed media and centrifuged at 200 x *g* for 5 minutes. The necrosis control was removed in the same manner and 200 µl of sterile PBS was added along with 800 µl of 100% ethanol and incubated at 4ºC for 10 minutes. The supernatant was discarded for the remaining samples and PBS containing 1% FCS was added and again centrifuged at 200 x *g* for 5 minutes.

The supernatant was discarded, the cells were re-suspended in 950 µl of binding buffer and transferred into flow cytometry tubes. Annexin V-FITC (2 µl) was added and mixed well before incubating the samples in the dark at room temperature for 10 minutes. A volume of 2 µl Propidium iodide (PI) (40 µg/ml) was added to the samples containing Annexin V-FITC and the samples immediately analysed.

The fluorescence of Annexin V-FITC and propidium iodide was measured with a fluorescent monitoring FC500 flow cytometer (Beckman Coulter, South Africa (Pty) Ltd) at a wavelength of 525 nm (FL1, AnnexinV-FITC) and >575 nm (FL3, PI) where 10 000 events were counted per sample. The data was plotted as scattergrams with the fluorescence signal of Annexin V against that of propidium iodide and the data gated into four quadrants based on the negative and positive control samples. During development of the initial protocol, colour compensation was accounted for.

The lower left quadrant detected viable cells with minimal propidium iodide and annexinV-FITC staining, the upper left quadrant detected the early apoptotic cells with minimal propidium iodide staining and high FITC staining, the upper right quadrant represented cells in late apoptosis shown by high propidium iodide and FITC staining and the remaining quadrant the necrotic cells with maximal propidium iodide staining. The initial protocol gating

47

was set according to unstained cells (using scattered light) in order to eliminate clusters as well as the untreated control to include 98% viability. The axes were representative of a log scale of Annexin V-FITC on the vertical axis and PI on the horizontal axis.

2.3.2.4 Statistics

Data was analysed using GraphPad Prism 5.0 (GraphPad Software, San Diego California USA) where the percentage of cells in the viable, early and late apoptosis as well as the necrosis quadrants were represented in bar graphs. Kruskal-Wallis was used in order to identify the statistical significance between treatment groups relative to the untreated control. Column statistics was performed to calculate the mean and the standard error of the mean for each quadrant of each treatment group.

2.3.2.5 Reagents

I.   Annexin-V FITC

Annexin-V FITC was purchased from BD Biosciences (Saint Jose, CA), stored at 4°C and used undiluted.

II.   Binding buffer

All the chemicals contained in binding buffer were purchased from Sigma Aldrich (St. Louis, USA). The buffer was stored at 4°C. The following reagents were dissolved in sequence in 100 ml of distilled water: Hepes (238 mg), sodium chloride (876 mg), potassium chloride (37.3 mg), calcium chloride (26.5 mg), magnesium chloride (9.5 mg). The pH was adjusted to 7.4.

III.   Ethanol

Ethanol (96%) was supplied by Skychem (Alberton, RSA) and stored in the freezer to keep it cold for fixation of the cells. Ethanol was used undiluted.

IV.   Propidium iodide (PI)

PI was purchased from Sigma Aldrich (St. Louis, USA). A mass of 2 mg was dissolved in 50 ml PBS (40 µg/ml), covered in foil and stored at 4°C.

48

2.3.3 Polarization optical differential interference contrast (PlasDIC) and light microscopy

2.3.3.1 Aim

The aim of this study was to assess the morphological changes of MCF-7 and MCF-12A cells when exposed to the experimental compounds for 72 hours in support of the results obtained from apoptosis/necrosis studies on the MCF-7 and MCF-12A cell lines.

2.3.3.2 Preparation of cells for PlasDIC and light microscopy

MCF-7 and MCF-12A cells were counted (Section 2.1.5) and seeded in 6-well plates in the appropriate medium containing 10% FCS at 5×10^4 cells per ml (1.2 ml/well) and incubated at 37°C, 5% CO_2 for 24 hours to allow for cell attachment. The media was removed and changed to the same media containing only 2% FCS. The cells were exposed to the experimental compounds ESE-15-ol, ESE-16 and 2-DG at the different concentrations mentioned above both in isolation and in combination for 72 hours.

2.3.3.3 PlasDIC and light microscopy

PlasDIC produces images of the cell with reduced contrast when the sample is illuminated with a lesser degree of coherence. It utilizes Köhler-type illumination with destructive interference (Esslinger and Gross, 2015). PlasDIC is useful in cellular studies as it reveals many intracellular structures that cannot normally be seen using light microscopy without specific staining. It is specifically utilized to study living cells and often to examine cellular division.

After 72 hours incubation in the presence of the drugs or drug combinations, plates were imaged under a ZeissAxiovert 40 CFL microscope (Carl Zeiss AG, Oberkochen, Baden-Württemberg, Germany) at a magnification of 400x. The appropriate lenses were changed for PlasDIC and light microscopy. Images captured on a digital camera were examined for morphological changes relative to the control.

2.3.4   Cell cycle

2.3.4.1 Aim

The aim of this part of the study was to determine the effect of the experimental compounds on cell cycle progression on the MCF-7 and MCF-12A cell lines after 72 hours.

2.3.4.2 Preparation of cells for cell cycle

MCF-7 and MCF-12A cells were seeded in 75 cm^2 flasks at a cell concentration of 4×10^5 cells/flask (10 ml/flask) and incubated at 37°C, 5% CO_2 for 24 hours to allow for cell attachment. The media was then removed and serum-free DMEM media added to allow for

49

cell synchronization. After 48 hours, cells were trypsinized, washed with PBS supplemented with 1% FCS, counted and plated into sterile 6-well plates at a concentration of $5x10^4$ (1.2 ml/well) and incubated for 24 hours. The cells were then exposed to the experimental compounds, ESE-15-ol (17.5 nM), ESE-16 (134 nM) and 2-DG (2.7 mM) and incubated for 72 hours at 37°C, 5% CO_2. Staurosporine (4 µM, 24 hours) was used as a positive control for the sub-G1 phase (Charlot *et al.*, 2004, Hurrell and Outhoff, 2013).

2.3.4.3 Cell cycle assay

To determine in which cell cycle phase the majority of cells were, the average DNA content was measured utilizing fluorescent dyes such as propidium iodide (PI) (Hirt, 2013). Propidium iodide binds nucleic acids upon entering a cell and on binding to the DNA exhibits intense fluorescence (Davey and Hexley, 2011). PI is excited by blue light at a wavelength of 488 nm and is capable of staining double-stranded nucleic acid including RNA which must be removed using RNAse (Darzynkiewicz *et al.*, 1980, Pozarowski and Darzynkiewicz, 2004). The determination of the effect that the experimental compounds have on the cell cycle, gave useful insight into their mechanisms of action. Cell cycle analysis was performed by amendment of the method described by Hurrell *et al* utilizing a standard flow cytometric protocol (Hurrell and za, 2013).

After 72 hours, the growth medium was removed, cells trypsinized and washed with sterile PBS containing 1% FCS and centrifuged for 5 minutes at 200 x *g*. The supernatant was discarded and 1 ml of sterile PBS containing 1% FCS was added and the tubes centrifuged. After discarding the supernatant, 100 µl of sterile PBS containing 1% FCS was added to each tube and 3 ml of ice cold 70% ethanol were added drop wise while gently vortex mixing. Samples were then placed in the fridge (4°C) for a minimum of 24 hours.

The tube for the G1 control (nutrient deprived cells) was removed at the first phase of trypsinization, centrifuged at 200 x *g* for 5 minutes and washed twice with sterile PBS and sterile PBS containing 1% FCS and ethanol was added then refrigerated. The control was added and incubated for the remaining 24 hours prior to ethanol fixation.

Samples were centrifuged, the supernatant discarded and 1 ml of 40 µg/ml PI solution containing RNAse (made up just prior to use), 0.1% Triton X-100 in PBS was added to each tube and incubated in a non-sterile incubator (37°C, 5% CO_2) for 40 minutes. The relative DNA content (fluorescence) was measured with a fluorescent monitoring FC500 flow cytometer

50

(Beckman Coulter, South Africa (Pty) Ltd) at a wavelength of 575 nm (FL3) where 10 000 events were counted.

2.3.4.4 Statistics

All data distributions were analysed using Multicycle version 3.0 deconvolution software for Windows (Phoenix Flow Systems, San Diego, CA, USA) whereby the relative quantity of DNA was represented in either the sub-G1, G1, S and G2/M phases. A Kruskal-Wallis with a Dunnett's post-hoc test was used to determine the statistical significance between the treatment groups relative to the control. Column statistics were performed to identify the mean and the standard error of the mean between each phase of the cell cycle as well as between treatment groups.

2.3.4.5 Reagents

I. Ethanol

Ethanol was supplied by Skychem (Alberton, RSA). A 70% ethanol was prepared by diluting 35 ml of 96% up to 50 ml of distilled water and was stored in the fridge at 4°C.

II. Propidium iodide (PI)

PI was purchased from Sigma Aldrich (St. Louis, USA). A mass of 2 mg (40 µg/ml) was dissolved in 50 ml of PBS (containing 0.1% Triton-X 100), covered in foil and stored in the fridge at 4ºC.

III. Ribonuclease A (RNAse)

RNAse powder was purchased from Sigma Aldrich (St. Louis, USA) and stored in the freezer at 0ºC. A mass of 100 µg/ml was dissolved in the PI/Triton-X 100 PBS solution prior to use.

IV. Staurosporine

Staurosporine aglycone was purchased from Sigma Aldrich (St. Louis, USA). The powder (5 mg) was dissolved in 5 ml of DMSO to obtain a stock solution of 3.2 mM after which 1 ml was removed and diluted with 500 µl of DMSO to a final stock concentration of 2.14 mM. Aliquots (30 µl) of the 2.14 mM stock were stored at -80°C. A volume of 2 µl of 2.14 mM was dissolved in 1068 µl of the appropriate media to give a final in-well concentration of 4 µM.

V. 0.1% Triton-X 100

Triton-X 100 was purchased from Sigma Aldrich (St. Louis, USA). A volume of 50 µl was dissolved in 50 ml of PI solution and stored at 4°C.

51

2.3.5 Mitochondrial membrane potential (ΔΨm)

2.3.5.1 Aim

The aim of this part of the study was to determine the possible involvement and effect on the mitochondria in the initiation of cell death by the test compound combinations on both the MCF-7 and MCF-12A cell lines.

2.3.5.2 Preparation of cells for MMP

MCF-7 and MCF-12A cells were seeded in sterile translucent white 96-well plates for fluorescent assays at a concentration of 6.25×10^4 cells per ml (80 µl/well) in the appropriate media (2% FCS) and allowed to attach for 24 hours. Cell were exposed to the experimental compounds ESE-15-ol (17.5 nM), ESE-16 (134 nM) and 2-DG (2.7 mM) for 24 and 48 hours. Tamoxifen (14 µM, 24 hours) was used as a positive control for membrane depolarization (Nigam *et al.*, 2008).

2.3.5.3 Mitochondrial membrane potential (ΔΨm) assay

Mitochondrial membrane potential is evaluated through the staining of cells with a cationic fluorescent dye that changes emission wavelength based on concentration and pH of the environment. The assessment of changes in the ratio of fluorescence intensity provides an indication of the accumulation of the dye within the mitochondria (Garner *et al.*, 1997). The cationic dye utilized is liphophilic and equilibrates across the mitochondrial membrane in a Nernstian manner and accumulate in the matrix of the membrane inversely proportional to the membrane potential (Perry *et al.*, 2011). More dye will accumulate in a hyperpolarized membranes and vice versa for depolarization of the mitochondrial membrane. JC-1 (5,5',6,6'-tetrachloro-1,1',3,3'-tetraethylbenzimidazolylcarbocyanine iodide) is a commonly used lipophilic, ratiometric, cationic dye used to assess mitochondrial membrane potential (Galluzzi *et al.*, 2007, Perry *et al.*, 2011).

The JC-1 Mitochondrial Membrane Potential protocol, adapted from Nuydens *et al.* (Nuydens *et al.*, 1999) by van Tonder *et al* (Nuydens *et al.*, 1999; Van Tonder *et al.*, 2014) for use in a 96 well format, was used and samples analysed using a FluoStar Optima fluorescence plate reader (Bio-Tek Instruments Inc., Vermont, USA) (Nuydens *et al.*, 1999, Van Tonder *et al.*, 2014).

After 24 and 48 hours, the supernatant was aspirated and 80 µl of JC-1 staining solution at a concentration of 10 µM in HBSS was added to the wells and incubated at 37°C, 5% CO_2 for 2

52

hours. Post-incubation, the JC-1 solution was removed and 100 µl of HBSS was added to each well, aspirated, a second volume of 100 µl HBSS added to each well and the plates analysed. The fluorescence for the monomeric form was measured at a λ_{ex} (excitation wavelength) of 485 nm and λ_{em} (emission wavelength) of 535 nm and for the J-aggregate form at a λ_{ex} of 560 nm and a λ_{em} of 595 nm. Internal triplicates were plated and averaged for the untreated (no test compound) and positive control (Tamoxifen 14 µM). Results were interpreted as a ratio of the aggregates to the monomeric form as a percentage of the control. The following formula was used:

$$\text{MMP (\%)} = ((\frac{Rs}{Rc})/\text{average aggregate/monomer ratio of controls}) \times 100$$

Where:
Rs represents the fluorescence of the aggregates
Rc represents the fluorescence of the monomers

2.3.5.4 Statistics

A minimum of three independent experiments were performed with internal triplicate. MMP was calculated as a percentage of the ratio of aggregates to monomers in relation to the untreated control. A one-way ANOVA was conducted for the compounds alone and in combination to determine statistical significance in comparison to the untreated control. The Dunnett's post-hoc test was used to compare the significant differences between each compound tested relative to the untreated control. Microsoft Excel 2007 (Roselle, IL) was used to determine ratios and percentages. Graphical and statistical evaluations were statistically analysed in GraphPad Prism 5.00 (GraphPad Software, San Diego California USA, www.graphpad.com).

2.3.5.5 Reagents

I. Hank's balanced salt solution (HBSS)

Phenol red dye free HBSS was supplied by Highveld Biologicals (Sandringham, South Africa), stored at 4°C and used as purchased.

II. 5,5',6,6'-tetrachloro-1,1',3,3'-tetraethylbenzimidazolecarbocyanine iodide (JC-1)

JC-1 was purchased from Sigma Aldrich (St. Louis, USA). A mass of 5 mg was dissolved in 5 ml DMSO to a stock concentration of 1.5 mM and stored in 53 µl aliquots at -80°C. A volume

53

of 7897 µl of HBSS was added to the 53 µl aliquot. This was used for the staining procedure where a final in-well concentration of 10µM was obtained.

III.   Tamoxifen

Tamoxifen citrate was obtained from Sigma Aldrich (St. Louis, USA) and made up to a stock solution of 30 mM by dissolving 16.90 mg in 1 ml of DMSO. The stock solution was stored in 2 µl aliquots at -80°C. The 30 mM stock (33 µl) was then diluted to a 1 mM stock by dilution in 1 ml DMSO. Aliquots (24 µl) of the 1 mM stock were stored at -80°C. Prior to exposure, 1142 µl of the appropriate media supplemented with 2% FCS was added to the 1 mM stock for a final in-well concentration of 20 µM.

2.3.6   Transmission electron microscopy (TEM)

2.3.6.1 Aim

The aim of this part of the study was to identify sub-cellular morphological changes and confirm the formation of multi-membrane autophagosomes to confirm the induction of autophagy on the MCF-7 cell line after 24 hours.

2.3.6.2 Preparation of cells for TEM

MCF-7 cells were counted (Section 2.1.5) and seeded in 25 cm^2 sterile culture flasks in the appropriate medium containing 10% FCS at 2 x 10^5 cells per well (10 ml/well) and incubated at 37°C, 5% CO_2 for 24 hours to allow for cell attachment. The media was then changed to DMEM containing only 2% FCS. The cells were then exposed to ESE- 15-ol (17.5 nM), ESE-16 (134 nM) and 2-DG (2.7 mM) both in isolation and in combination for 24 hours. Tamoxifen was used as a positive control for autophagy and was incubated in the plate at 10 µM for 24 hours.(Codogno and Meijer, 2005)

2.3.6.3 TEM assay

Transmission electron microscopy was used in order to visualize the intracellular morphology of the autophagic compartments. Several characteristics aid in the identification of autophagosomes and structures indicative of autophagy. The autophagosome consists of a double membrane vacuole containing undegraded cytoplasm and/or organelles. The cytoplasm of autophagosomes contains cytoplasmic components such as rough endoplasmic reticulum (ER), mitochondria or ribosomes. Autophagosomes often lie in-between two segments of

54

rough endoplasmic reticulum and the nuclear components show partial chromatin condensation (Barth *et al.*, 2010).

After 24 hours of culture in the presence of the drugs alone or in combination, the samples were trypsinised as previously described, centrifuged at 200 x *g* for 5 minutes, the supernatant discarded and the pellet re-suspended in 1 ml of the fixing solution (composition shown below in Section 2.3.6.4) and incubated at room temperature for 1 hour. The samples were then centrifuged at 600 x *g* for 5 minutes, the supernatant discarded and rinsed 3 times for 10 minutes each in 0.075 M phosphate buffer. Samples were fixed in 0.5% osmium tetraoxide in a fume hood for 1 hour, centrifuged (600 x *g*, 5 minutes) and washed 3 times in distilled water. Dehydration was then performed in sequentially higher concentrations of ethanol (30%, 50%, 70%, 90%, 100%, 100%, 100%) for 10 minutes per concentration and then incubated at room temperature with agitation overnight. Samples were centrifuged and infiltration with embedding resin was performed by adding 100% ethanol to 100% Quetol in a 1:1 ratio. Samples were then incubated for 1 hour. Samples were centrifuged at 600 x g for 5 minutes and pure Quetol was added and incubated at room temperature for 4 hours. Samples were then polymerized at 60°C for 39 hours. Ultra-thin sections (2 µm) were cut using a microtome and placed on grids. The sections were contrasted for 10 minutes in 5% aqueous uranyl acetate and rinsed in water. Reynolds' lead citrate was added for 2 minutes to contrast samples and rinsed in water. Samples were then imaged using the JEM 2100P Dual TEM 200 kB (Jeol, MA, USA) at a magnification of 8000x for whole cells and 25 000x for internal organelles. All sample preparation and microscopy work was performed at the Microscopy Unit at the University of Pretoria.

2.3.6.4 Reagents

I.   **Ethanol Absolute**

Ethanol was purchased from Merck (Pty) Ltd. (Longmeadow, Modderfontein) and was used undiluted for the 100% ethanol requirements. It was then diluted to a 90, 70, 50 and 30% v/v solutions in distilled water.

II.   **Fixing solution**

Formaldehyde and phosphate buffered saline were purchased from Merck (Pty), Ltd (Longmeadow, Modderfontein). Glutaraldehyde was purchased from Agar Scientific Ltd (Stansted Essex, UK) and double distilled water was supplied by the Microscopy Department at the University of Pretoria

55

The following dilution was prepared in a 1:1:3:5 ratio:

- 25% Formaldehyde
- 25% Glutaraldehyde
- Double distilled water
- 0.15 M Phosphate buffered saline

All chemicals were mixed just prior to use.

III. Osmium tetraoxide

Osmium tetraoxide solution EM grade was purchased from SPI supplies (West Chester, USA) and used undiluted.

IV. Quetol

Quetol embedding resin was made up of the following components to a final mass of 15 g:

- TAAB 812 Resin was purchased from TAAB laboratories (Berkshire, UK). A mass of 7.85 g was weighed out in a plastic beaker.
- Nadic Methyl Anhydride (NMA) was purchased from SPI Chem (West Chester, USA). NMA (5.3 g) was added to the solution.
- Dodecenyl Succinic Anhydride (DDSA) was purchased from SPI Chem (West Chester, USA). DDSA (2.05 g) was weighed out into the above mixture.
- Benzyldimethylamine (BDMA) was purchased from Agar Scientific Ltd (Stansted Essex, UK). BDMA (0.152 g) was weighed out and added to the mixture.

All chemicals were well mixed just prior to use.

V. Reynolds' lead citrate

Reynolds' lead citrate consists of the following components:

- Lead nitrate was obtained Agar Scientific (Stansted Essex, UK) and 1.33g was weighed out.
- Trisodium citrate was obtained from Agar Scientific (Stansted Essex, UK) and 1.76 g was weighed out.
- Double distilled water was obtained from the Microscopy Department at the University of Pretoria. A volume of 300 ml of freshly boiled double distilled water was measured out.

56

The suspension was then vigorously shaken for 1 minute and left to stand for 30 minutes, shaking intermittently to ensure complete conversion of lead nitrate to lead citrate. A volume of 8 ml of sodium hydroxide (0.18%) was then added and made up to 50 ml.

VI.   Uranyl acetate

Uranyl acetate was purchased from Merck (Pty) Ltd (Longmeadow, Modderfontein). A 5% solution was made up by dissolving 5 g of uranyl acetate in 100 ml of double distilled water.

2.3.7 Western Blots

2.3.7.1 Aim

The aim of this part of the study was to investigate the induction of autophagy by monitoring the autophagic marker, microtubule-associated protein 1 light chain 3 alpha (LC3) using the drug treated MCF-7 cell line after 24 hours treatment.

2.3.7.2 Preparation of cells for western blot

MCF-7 cells were counted (described in Section 2.1.5) and seeded in 6-well plates in the appropriate medium containing 10% FCS at 2×10^5 cells per ml (1.2 ml/well) and incubated at 37°C, 5% CO_2 for 24 to allow for cell attachment. The media was then changed to DMEM containing 2% FCS. The cells were subsequently exposed to ESE- 15-ol (17.5 nM), ESE-16 (134 nM) and 2-DG (2.7 mM) both in isolation and in combination for 24 hours. Tamoxifen was used as a positive control for autophagy and the cells were incubated at a concentration of 10 µM for 24 hours (Codogno and Meijer, 2005).

2.3.7.3 Western blotting

Western blotting is a qualitative and relative quantitative analytical approach that initially utilizes gel electrophoresis to separate and identify proteins of interest according to their molecular masses. Cells are lysed with Laemmli sample loading buffer containing 2% SDS in order to release the protein from the treated cells in order to be loaded onto an electrophoresis gel. When a voltage is applied, the negatively charged proteins travel through the gel towards the positive electrode. After protein separation, transfer of the proteins to a membrane is done by rapid semidry electrophoretic transfer. Blocking of the membrane with milk protein solution ensures that there is no non-specific binding of the anti-LC3 antibody being probed onto the membrane (Mahmood and Yang, 2012).

Post-incubation of experimental compounds, the media was collected and centrifuged for 5 minutes at 200 x *g*. The supernatant was discarded and the pelleted cells kept for further use.

57

Wells were washed once with sterile PBS and then lysed with 150 µl Laemmli buffer supplemented with β-mercaptoethanol, warmed to 90°C and. Cells were removed via agitation with a scraper and transferred to microfuge tubes along with the floating cells recovered from the media. The cell lysates were then boiled for 5 minutes at 100°C, centrifuged at 14 000 x *g* for 10 minutes and stored at -80°C.

The Precision Plus molecular weight protein standard (10 µl) as well as the protein samples (20 µl) were loaded onto a Mini-Protean TGX StainFree pre-cast gel (4-20%) and separated for 15 minutes at 60 V after which the voltage was then increased to 120 V till the samples reached the bottom of the gel. The proteins were then transferred using the semidry technique onto a PVDF membrane at 2.5 A for 7 minutes. Midi format 0.2 µm PVDF membranes were then blocked in 2% milk powder solution in PBS-T (PBS with 0.2% Tween20) for 30 minutes. The membranes were then washed twice with PBS-T and incubated with the primary anti-LC3 antibody (rabbit polyclonal reared) in PBS-T supplemented with 2% BSA at 4°C with slow agitation overnight. Following incubation, membranes were washed three times with PBS-T, incubated with anti-β-actin antibody and diluted in PBS-T with 2% BSA at 4°C for 40 minutes. Membranes were then washed three times with PBS-T and incubated with the secondary antibodies anti-mouse and anti-rabbit conjugated to HRP (secondary antibodies to anti-LC3 and anti-β-actin) diluted in PBS-T with 2% BSA at 4°C for 1 hour. Membranes were then washed three times for 5 minutes each with PBS-T at room temperature. Bands were then visualized with freshly prepared ECL substrate and imaged using the ChemiDoc MP imaging system (Bio-Rad, Johannesburg, RSA).

2.3.7.4 Statistics

Images obtained were analysed using Bio-Rad ImageLab software 5.2.1 (Bio-Rad, Johannesburg, RSA, www.biorad.co.za) and normalization volume values plotted using Graph Pad prism 5.0 (GraphPad Software, San Diego California USA, www.graphpad.com). A Kruskal-Wallis with a Dunnett's *post-hoc* test was performed to identify the statistical significance between the treatment groups relative to the untreated control.

2.3.7.5 Reagents

I. Anti-β-actin antibody

Anti-β-actin antibody (2.7 mg/ml) (mouse monoclonal IgG1 reared – Abcam, Cambridge, USA). was purchased from Biocom Biotech (Centurion, RSA). Anti-β-actin antibody (1 µl) was diluted in 5 ml PBS-T (phosphate buffered saline with 0.2% Tween 20) prior to use and stored at 4°C.

II. Bovine serum albumin (BSA)

BSA was purchased from ChemCruz (Santa Cruz Biotechnology Inc., Texas, USA). BSA (100 mg) was dissolved prior to use in 5 ml of PBS-T (phosphate buffered saline with 0.2% Tween 20) and stored at 4°C.

III. Laemmli Buffer

Laemmli buffer was purchased from Bio-Rad (Johannesburg, RSA), stored at room temperature and used undiluted.

IV. β-Mercaptoethanol

β-mercaptoethanol was purchased from Merck (Pty), Ltd (Longmeadow, Modderfontein). A volume of 50 µl of β-mercaptoethanol was diluted in 950 µl of Laemlli buffer prior to use.

V. Milk powder

Fat free milk powder was purchased from Parmalat (Midrand, RSA). A mass of 100 mg was dissolved in 5 ml of PBS-T prior to use.

VI. pAb anti-LC3-FITC antibody

The anti-LC3 (rabbit polyclonal reared) conjugated FITC primary antibody (Novus Biologicals Southpark, USA) was purchased from Novus Biologicals (Southpark, USA). A volume of 1 µl was diluted in 5 ml of PBS-T (phosphate buffered saline with 0.2% Tween 20) prior to use and stored at 4°C.

VII. Phosphate buffered saline with 0.2% Tween 20 (PBS-T)

Powdered phosphate buffered saline was purchased from BD Bioscience (USA) and 9.23 g was dissolved in one litre of distilled water and stored at 4°C. Tween 20 was purchased from Sigma Aldrich (St. Louis, USA). Tween 20 (2 ml) was diluted in 1 liter of PBS and stored at room temperature (PBS-T).

59

VIII.   Running Buffer

All chemicals contained in running buffer were obtained from Sigma Aldrich (St. Louis, USA).

Running buffer was made up to a 10x buffer which was diluted to a 1x upon use. Constituents (10x) consist of:

104.63 g 3-(N-morpholino)propanesulfonic acid (MOPS)

60.57 g Tris buffer

10 g Sodium dodecyl sulphate (SDS)

2.92 g ethylenediaminetetraacetic acid *(*EDTA)

Above chemicals were diluted in 1 litre of distilled water and stored in the fridge at 4 ºC.

For the electrophoresis the buffer was diluted 10x with deionised water and used to fill the tank.

IX.   Secondary antibodies anti-mouse and anti-rabbit conjugated to HRP

The secondary antibodies anti-mouse and anti-rabbit conjugated to HRP (PKL) were purchased from Biocom Biotech (Centurion, RSA). A volume of 0.5 µl of anti-mouse and 1 µl of anti-rabbit were diluted in 5 ml of PBS-T containing 100 mg BSA prior to use and stored at 4°C.

X.   Tamoxifen

Tamoxifen citrate was obtained from Sigma Aldrich (St. Louis, USA) and made up to a stock solution of 30 mM by dissolving 16.90 mg in 1 ml of DMSO. The stock solution was stored in 2 µl aliquots at -80°C. The 30 mM stock (33 µl) was then diluted to a 1 mM stock by dilution in 1 ml DMSO. 20 µl aliquots of the 1 mM stock were stored at -80°C. Prior to exposure, 380 µl of DMEM supplemented with 2% FCS was added to the 1 mM stock for a final in-well concentration of 10 µM.

XI.   ECL substrate

ECL substrate was purchased from Bio-Rad Laboratories (Johannesburg, RSA). The luminol enhancer (750 µl) and the hydrogen peroxide (750 µl) were stored in the fridge at 4ºC and combined just prior to use.

60

Chapter 3 Results and Discussion

The experimental compounds ESE-15-ol, ESE-16 and 2-DG were tested in an *in vitro* setting, alone and in combinations, on the MCF-7 breast adenocarcinoma and MCF-12A non-tumorigenic cell lines. Various experiments were performed in order to identify the effect of the compounds with respect to cytotoxicity, mitochondrial membrane potential as well as to determine the possible mode of cell death initiated. The possible mode of cell death assays were focused on apoptosis and autophagy. Microscopic studies were employed to observe morphological changes in these cells after exposure to the experimental compounds.

3.1 Cell enumeration

3.1.1 Concentrations that inhibit cell growth by 50% (GI_{50}) on cancer and normal cell line

The colorimetric SRB assay was used in order to determine the effect of different concentrations of each of the experimental compounds in isolation and combination to find the concentrations and combinations of compounds that inhibited of cell growth by 50% in comparison to the untreated controls.

This was also used as verification of results reported in the literature (not conducted in this study). Results from this study are presented below in Table 3.1.

Table 3.1 GI_{50} concentrations represented as the mean concentration of the three experimental compounds after 72 hours in the MCF-7 and MCF-12A cell lines.

Cell line	ESE-15-ol (nM)	ESE-16 (nM)	2-DG (mM)
MCF-7	34.1 ± 1.1	20.6 ± 1.3	1.3 ± 1.2
MCF-12A	141.0 ± 1.3	140.1 ± 1.1	1.7 ± 1.1

Results are reported as the mean concentration $\pm$ standard error of the mean (SEM). n = 9

The MCF-7 and MCF-12A cell lines showed at least 100 000 times a greater sensitivity to the oestrone analogues than for 2-DG. ESE-15-ol appeared to inhibit the growth of the breast adenocarcinoma cells to a greater extent than the non-tumorigenic MCF-12A cell line: a GI_{50} value of 34.1 nM was observed on the MCF-7 cell line compared to 141.0 nM on the MCF-12A cell line. The glycolysis inhibitor, 2-DG was less effective against both cell lines in comparison to the oestrone analogues. GI_{50} concentrations of 1.3 mM and 1.7 mM were calculated for 2-DG after 72 hours on the MCF-7 breast adenocarcinoma and MCF-12A non-tumorigenic cell lines, respectively.

61

It was observed that the tested cell lines were more sensitive to ESE-16 where a GI_{50} value of 20.6 nM was calculated for the MCF-7 cell line and appeared to inhibit the growth of the cancer cells to a greater extent than the non-tumorigenic MCF-12A cells with a calculated GI_{50} of 140.1 nM. The results observed in Table 3.1 are in contrast to previous studies where van Tonder reported GI_{50} values of approximately 2 fold greater than those reported in the present study. Differences observed in the GI_{50} values of previously studies to the present study could be attributed to a number of parameters. These include but are not limited to the degree in which the cells were stressed, shifts in the pH of the media, different cell batches with different number of passages as well as changes of seasons which have been noted to affect the growth and susceptibility of the cells. During incubation, levels of carbon dioxide might have varied between studies which in turn would affect how stressed the cells were. Differences could also be attributed to lag times in the initial 24 hour incubation of the cells. Following 24 hours, the treatments administered had a response relative to the initial starting conditions which could possibly have a lag time. This accounts for increased variability between different studies conducted. The dose response curves of ESE-15-ol, ESE-16 and 2-DG for the MCF-7 and MCF-12A cell line are shown in Figures 3.1 and 3.2

From the results shown in Figure 3.1, cell numbers decreased in a typical dose-dependent manner for both the MCF-7 and MCF-12A cell lines. The effect of ESE-15-ol on cell viability on the MCF-7 cell line (Figure 3.1) was less pronounced than the effect of ESE-16. Cell viability decreased rapidly above 20 nM exposure for both ESE-15-ol and ESE-16. After exposure to these experimental compounds (ESE-15-ol and ESE-16) at a concentration of 100 nM a shift from an inhibitory effect on cellular growth to the initiation of cellular death was noted as negative percentages of cell number.

Literature has reported cytotoxicity of ESE-15-ol on the MCF-7 cell line with an IC_{50} value of 55 ± 2.73 nM after 48 hours exposure (Stander *et al.*, 2012). A lower concentration (34.1 ± 1.1 nM) of ESE-15-ol in the present study was reported and the increased sensitivity observed, could possibly be a result of the longer incubation period of 72 hours. It was observed that 2-DG had a significantly lower cytotoxic effect on the MCF-7 cell line than each of the oestrone analogues alone and post exposure cell numbers remained high relative to the oestrogen analogues.

Previous studies on the SNO oesophageal carcinoma cell line, have shown that the experimental compound, ESE-16, inhibited cellular proliferation at a concentration range of

62

0.18-0.22 µM in the (WolmaransMqoco *et al.*, 2014). In contrast to this, cell enumeration results conducted on the MCF-7 cell line in the present study presented a GI_{50} of 20.6 nM, which is considerably lower than observed in previous studies. The increased susceptibility of MCF-7 cells to treatment with ESE-16 could be attributed to the characteristics of this cell line. MCF-7 cells are capable of processing oestradiol through the use of oestrogen receptors in the cytoplasm (www.atcc.org, 2014). Due to the fact that these compounds are oestrone analogues, it is possible that this attribute aids in lower treatment doses in order to inhibit cell growth (www.atcc.org, 2014). The results obtained in the present study depict increased sensitivity of the cells to ESE-15-ol and ESE-16 than previously obtained. This could be attributed to the lower FCS concentration used in the present study. The cells were incubated and treated in 2% FCS which could result in increased sensitivity of the cells to the experimental compounds due to decreased growth factors. The decrease in growth factors results in starvation of the cells which results in stress of the cell and increased sensitivity to the experimental compounds. The 2% FCS could also increase sensitivity of the cells due to decreased binding by steroid binding proteins in the media.

A GI_{50} concentration of 50 nM after treatment with ESE-15-ol on the MCF-12A in the present study cells parallels results obtained in previous studies (Stander *et al.*, 2012). Comparable results to treatment with ESE-15-ol were noted after treatment with ESE-16. Data in the present study indicates that the MCF-12A cell line was less susceptible to both the experimental compounds ESE-15-ol and ESE-16, with a less pronounced decrease in cell viability in comparison to that seen in the MCF-7 cell line. A shift from a growth inhibitory effect to cell death, was observed after treatment with the two highest concentrations (25 and 50 mM) of 2-DG in the MCF-12A cell line. The experimental compounds were observed to be toxic to the cells irrespective of varying culture conditions to previous studies.

3.1.2 Combination therapy
The synergistic combinations of ESE-15-ol, ESE-16 and 2-DG were assessed based on the Chou and Talalay method which merges the mass-action law principle with the mathematical induction and deduction principles for the effects of the interaction of multiple drugs (Chou, 2006). GI_{50} values for individual compounds were obtained after 72 hours exposure. The experimental compounds were then tested in combination using a checkerboard approach using GI_{50} values previously determined by van Tonder and combined in ratios (¼, ½, 1, 2 and 4 GI_{50} concentrations). The data was then converted to the fraction of cells that were affected and CalcuSYN software used to calculate the combination indexes (CI).

63

Combination indexes of less than one indicated synergism, an additive effect if the combination index was approximately equal to one and an antagonistic effect with a CI greater than one. From the wide range of concentrations tested for each of the experimental compounds, the most effective combination where the compounds showed synergism were selected for the remainder of the assays. The concentrations of the synergistic combinations used in this study were previously determined by van Tonder (Tonder, 2016). Previously, van Tonder reported (Table 2.6) that 16.75 nM of ESE-16 is the most promising synergistic concentration in combination with 2.7 mM 2-DG. The lowest combination index was obtained after treatment with ESE-16 at 134 nM in combination with 10.76 mM 2-DG. Due to this, 134 nM ESE-16 was selected for the present study. A concentration of 10.76 mM is an extremely toxic competitive inhibitor to glucose. Treatment at such a high concentration of 2-DG would induce severe cell stress and induce hypoxia into the experimental procedure. The glucose concentration present in most media is approximately 5 mM. Due to this, approximately half of this concentration i.e 2.7 mM 2-DG was selected for this study. This provides an effective concentration for using 2-DG in combination with ESE-16 and ESE-15-ol to observe the effective mechanisms of cell death counter to purely starving the cells with high concentrations of 2-DG. The experimental compounds were therefore tested at the following concentrations: 17.5 nM (ESE-15-ol), 134 nM (ESE-16) and 2.7 mM (2-DG). The effects of the compounds in isolation and in combination on cell viability are represented below in Figure 3.2.

64

MCF-7

Log concentration of ESE-15-ol (nM)

Log concentration of ESE-16 (nM)

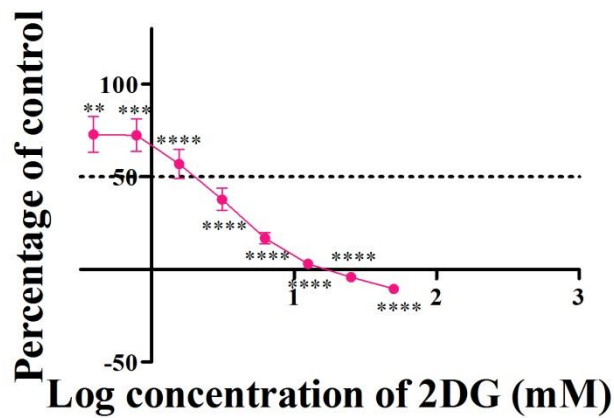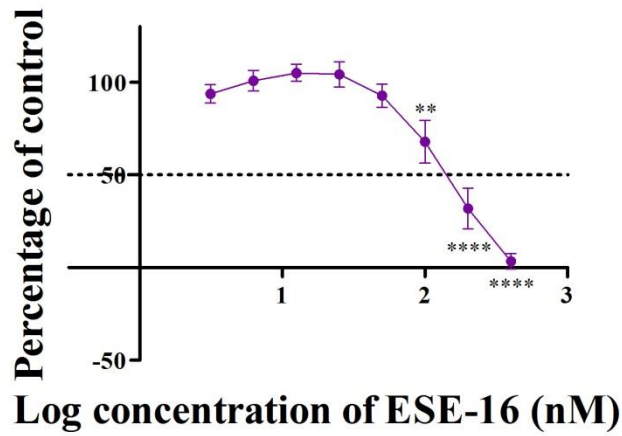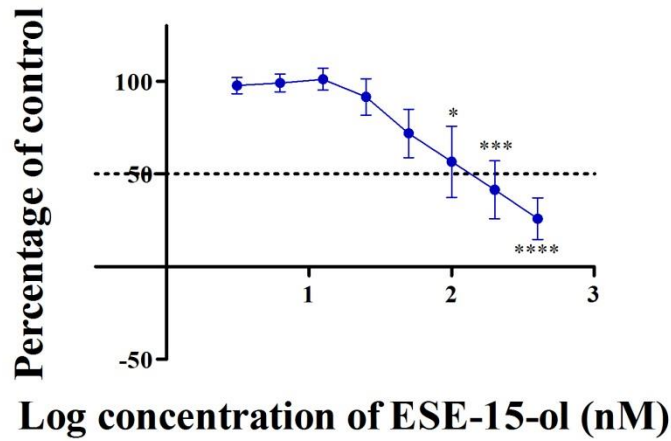Log concentration of 2DG (mM)

65
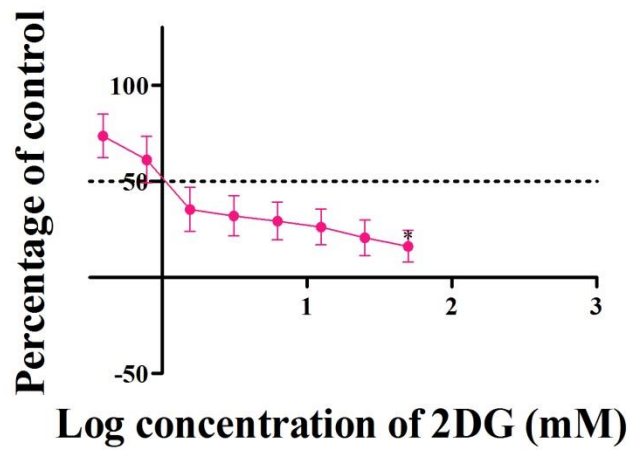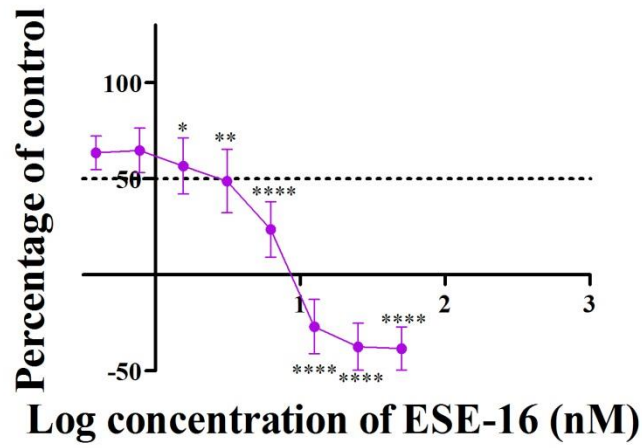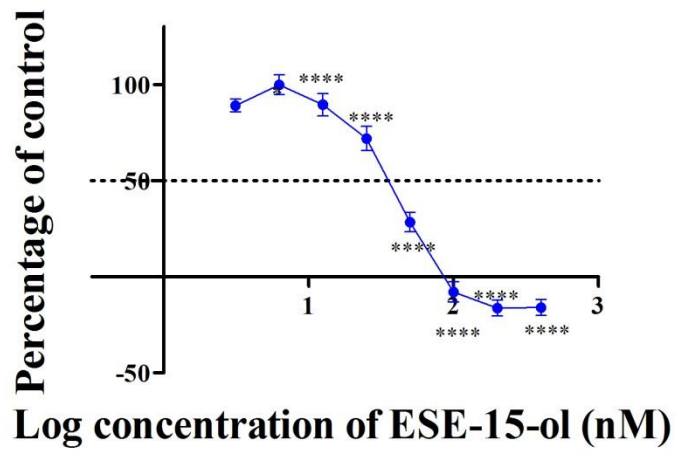
Figure 3.1 The effect of ESE-15-ol, ESE-16 and 2-DG on the growth of the MCF- and MCF-12A cell lines after 72 hours exposure. Note the change in concentration for the 2DG. Line graphs show the average results obtained from 3 independent experiments. n=9. *p<0.05, **p<0.01, ***p<0.001, ****p<0.0001.

66

From the results illustrated in Figure 3.2 as expected, ESE-16 (134. nM) had a greater effect on both cell lines due to exposure to the cells at a higher concentration than ESE-15-ol (17.5 nM). A greater decline in cell number was noted in the MCF-7 cell line after treatment with the experimental compounds ESE-15-ol (17.5 nM) and 2-DG (2.7 mM) alone and in combination in comparison to that of the non-tumorigenic MCF-12A cell line. These findings suggest that the experimental compounds appeared to have some selectivity to the MCF-7 breast cancer cell line. Treatment with ESE-16 alone and in combination with 2-DG were observed to result in a greater decrease in cell number in MCF-12A treated cells in comparison to MCF-7 cells.

The effects observed in the present study for the compounds ESE-15-ol, ESE-16 and 2-DG alone and in combination were not exclusive to the MCF-7 cell line and also elicited cytotoxic effects on the non-tumorigenic MCF-12A cell line.

Treatment with ESE-16 resulted in cell death in the MCF-12A cells compared to what appears as a growth inhibition in the MCF-7 cell line. The combined treatment of ESE-16 and 2-DG not only exhibited a greater effect than each of these compounds alone, it also proved to be more cytotoxic than the combination of ESE-15-ol and 2-DG. This cytotoxic effect was observed in both the MCF-7 and MCF-12A cell lines. The experimental compound ESE-16 elicited a greater effect on the non-tumorigenic cell line. The combination of ESE-16 with 2-DG however had a greater effect on the MCF-7 cell line than the MCF-12A cell line.
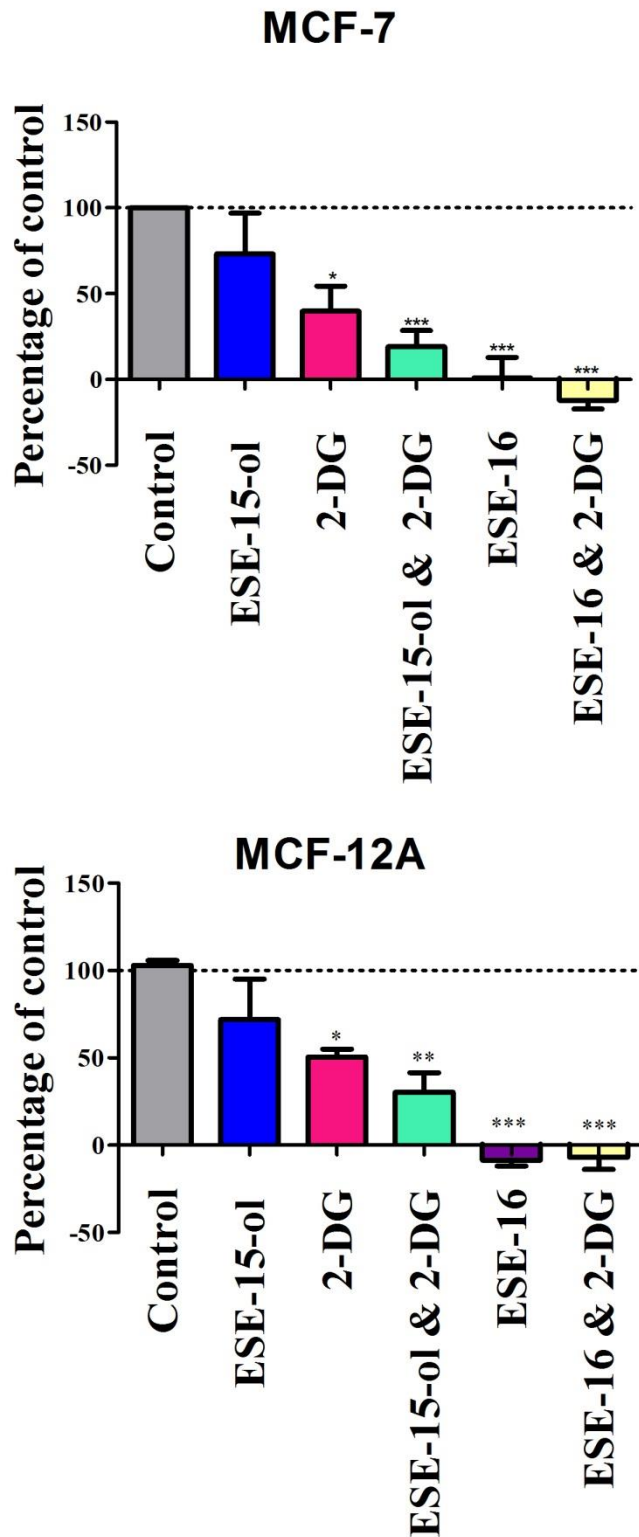
67

Figure 3.2 The effect of ESE-15-ol, ESE-16 and 2-DG alone and in combination on the growth of the MCF-7 and MCF-12A cell lines after 72 hours exposure. Bar graphs show cell viability of the combined results obtained from 7 independent experiments. n=7, *$p<0.05$, **$p<0.01$, ***$p<0.001$.

68

3.1.3 Discussion

ESE-15-ol and ESE-16 are analogues of 2-ME. These compounds have an addition of a sulphamate group at position 3 of the oestradiol backbone. Similarly as previously mentioned, the compound (8R, 13S,14S,17S)-2-Ethyl-13-methyl-7,8,9,11,12,13,14,15,16,17-decahydro-6H-cyclopenta[a]-phenanthrene-3,17-diyl bis(sulfamate) (EMBS) is derived from 2-ME (Visagie *et al.*, 2014) and falls into the same family of the oestrone analogues tested in this study. This suggests that results obtained in the present study after treatment with ESE-16 and ESE-15-ol could parallel results obtained in previous studies after treatment with EMBS. Due to limited literature available on the oestrone analogues used in the present study, observing the effects of similar compounds could assist in a broader understanding of the mechanism of ESE-15-ol and ESE-16.

The combination of ESE-15-ol and ESE-16 was reported to result in a dose-dependent decrease in cell viability of MCF-7 cells, indicative of anti-cancer activity. This confirms results obtained in previous studies after treatment with EMBS (Bubert *et al.*, 2007, Visagie *et al.*, 2014). ESE-15-ol in the present study resulted in approximately a 30% decrease in cell viability in both MCF-7 and MCF-12A cell lines. The 30% decrease in cell viability resulted from a lower concentration of the oestrone analogue than that used in previous studies. Previously, a 40% growth inhibition was reported after treatment of EMBS at 0.4 µM (Visagie *et al.*, 2014). As previously mentioned, this could be attributed to the lower concentration (2%) of FCS used in the present study resulting in increased sensitivity of the cells to the experimental compounds. The present study was reported after a 72 hour incubation in contrast to previous studies on EMBS where incubation occurred over a 24 hour period.

The lower GI_{50} values for ESE-15-ol and ESE-16 observed in the present study compared to the 400 nM GI_{50} for EMBS could be due to the above mentioned differences in methods carried out.

The cytotoxicity observed on the MCF-7 cell line in the present study parallels results previously obtained after treatment with the structurally similar compound 2-ethyl-3-O-sulphamoyl-estra-1,3,5(10),15-tetraen-17-one estrone (ESE-15-one) (Stander *et al.*, 2011). A IC_{50} concentration of 130 nM was reported for ESE-15-one in combination with DCA on the MCF-7 cell line after 24 hours exposure. The cytotoxic effect present in the present study parallels the results previously obtained however, the inhibitory concentrations of the oestrone analogues cannot be directly compared due to different assay conditions used.

69

As previously mentioned, ESE-15-ol and ESE-16 used in the present study, are derived from the same parent compound (2-ME) as the oestrone analogues EMBS and ESE-15-one used in previous studies (StanderStander *et al.*, 2011, Visagie *et al.*, 2014). From the results obtained in the present study as well as from published data, it can be observed that the oestrone analogues function effectively in a nanomolar range. This could be beneficial in future studies in order to obtain a therapeutic effect with a decreased side effect profile that is often observed by compounds treated in the micromolar range.

In contrast to previous results, treatment with ESE-15-ol showed 50% growth inhibition of MCF-7 cells at a concentration of 34.1 nM (Table 3.1). Data indicates that ESE-15-ol effectively inhibits cell growth of MCF-7 breast cancer cells to a greater extent than non-tumorigenic MCF-12A cells. A GI_{50} value of 55 nM after 48 hours exposure was previously reported for ESE-15-ol using MCF-7 cells. After treatment with 50 nM of ESE-15-ol, MCF-12A cells were shown to be minimally affected (Stander *et al.*, 2012). The results obtained in the present study support previous studies with a reported growth inhibition at 141.0 nM in the MCF-12A non-tumorigenic cell line and 34.1 nM in MCF-7 breast cancer cells. This implies possible cytotoxic selectivity of ESE-15-ol to cancerous cells. Future prospectives for this compound could aim at conducting experiments to indicate whether ESE-15-ol is capable of inhibiting cell growth at lower concentrations if the treatment period is extended. Cancer cells proliferate rapidly and by introducing dosing cycles, the normal cells are capable of recovering in-between treatment regimens. There are several factors that influence the chemotherapeutic dose administration cycle. Some of these factors include the type of cancer, the stage progression, the compound administered as well as the toxicity associated with that compound and the time necessary to recover from such toxicities. The administration cycle of chemotherapeutic agents varies according to the compound being administered. The correct administration cycle is determined through cell assays, animal models and often clinical trials prior to marketing. Although the administration cycle is dose dependent, according to Chemocare, chemotherapy is generally administered weekly, bi-weekly or monthly. A cycle usually consists of two bi-weekly administrations per month however the optimal number of cycles depends on the cancer status (Stockler *et al.*, 2003). Doses may be administered for a certain number of consecutive days followed by a withdrawal period to allow recovery of affected healthy tissue (www.cancer.org, 2015).

The administration of chemotherapeutic agents often induces liver toxicity. Due to this, many chemotherapy agents doses are lowered and dosing intervals increased (Santini *et al.*, 2002).

70

Administration of chemotherapeutic agents has been linked to changes in the liver including the appearance, defects in liver cell regeneration as well as poor parenchymal haemostasis. Studies have observed that chemotherapy results in lesions in the vascularity of the liver (Aloia *et al.*, 2006). Karoui *et al* reported in 2006 that preoperative chemotherapy resulted in the atrophy of hepatocytes and possible necrosis of the liver cells (Karoui *et al.*, 2006). Following the administration of chemotherapeutic drugs renal toxicity has been observed. The toxicity displayed was reported to be dose dependent as well as having a cumulative effect (Akilesh *et al.*, 2014, Bokemeyer *et al.*, 1996). Chemotherapeutic agents are administered in cycles in order to try and delay this cumulative effect. When a chemotherapeutic agent is administered repeatedly, the compound accumulation in the body is often what triggers renal toxicity (Akilesh *et al.*, 2014). Previously conducted phase II studies on 2-ME (1000 mg/day) reported grade 2 and 3 abnormalities in liver function, however the liver function returned to normal following cessation of 2-ME (Lakhani *et al.*, 2003).

Lower concentrations over an extended time period are beneficial in that there is the potential to decrease adverse side effects with the dose being administered less frequently. This could possibly aid in less liver and kidney toxicity with possible improvements in the compounds biological half-life.

Previous studies have shown that the experimental compound, ESE-16, inhibited cellular proliferation in a concentration range of 0.18-0.22 µM using the SNO oesophageal cancer carcinoma cell line. When exposed to MCF-7 cells, previous studies reported a GI_{50} of 20.6 nM. (Wolmarans *et al.*, 2014). After a 24 hour treatment of HeLa cervical adenocarcinoma cells with ESE-16, an inhibitory concentration (IC_{50}) value of 500 nM was obtained (Theron *et al.*, 2013). The IC_{50} refers to the concentration at which the cellular proliferation was reduced by half (Ibrahim *et al.*, 2014). Previous studies reported that ESE-16 was more potent on adenocarcinoma cells than the parent compound 2-ME which decreased cell numbers by 70% after addition of 1 µM 2-ME for 72 hours. A direct comparison cannot be drawn unless ESE-16 and 2-ME are tested on adenocarcinoma cells for the same time period of either 24 or 72 hours.

Further studies showed that MCF-7 cell growth decreased by 54.41% after addition of 100 nM ESE-16 for 24 hours (VisagieTheron *et al.*, 2013). The results obtained in the present study prove favourable to previous studies as a lower concentration of ESE-16 (20.6 nM) was required to inhibit cell proliferation with an increased treatment period. Due to an extended

71

exposure time, the compound was capable of eliciting its effects on the cells at a lower concentration in contrast to a higher dose that is needed due to a shorter period of exposure. This indicates that by increasing the exposure time; the concentration of test compound necessary to elicit an anti-proliferative effect is lowered. A compound is only fully eliminated from the body after 7 to 8 half-lives (Doweiko, 2011).

In the present study, ESE-16 was reported to have a greater effect on the MCF-7 cell line than ESE-15-ol however the concentrations of these compounds differ and are not directly comparable. Previous studies were reported to elicit similar effects (Visagie et al., 2013).

Data has reported that a concentration of 20 mM was usually used in order to target cancer cells through glycolytic inhibition (Wu et al., 2009). In the present study it was possible to target the MCF-7 cancer cells at a lower concentration of 1 mM of 2-DG although it has been shown in previous studies that a concentration of 1 mM (5% FCS) 2-DG has minimal effects on MCF-7 breast cancer cells after an incubation period of 5 days (Kaplan et al., 1990). This however could be due to different assay conditions and the use of tetrazolium in contrast to SRB. In contrast to this, treatment with 2-DG at a concentration of 1 mM (10% fetal bovine serum) for 72 hours has previously shown strong anti-proliferative effects on the prostate cancer cell line LNCaP, with cell numbers decreasing by approximately 70% (Sahra et al., 2010). The differences observed between the 2-DG having minimal effect and having a significant effect are attributed to different assay conditions however the FCS concentrations vary between the studies. This could further support the hypothesis made that the concentration of FCS used could account for the differences in the results obtained in the present study.

Differences in the effects elicited in previous studies after treatment with 1 mM 2-DG could also possibly be attributed to the higher glucose concentrations available to the cells (11 mM). 2-DG acts competitively with glucose transporters and due to the decrease in glucose at the tested concentration the effect elicited would be minimal. More cells are capable of surviving when exposed to high glucose concentrations (Kaplan et al., 1990). Previous studies that found little effect after treatment with 1 mM were exposed for 5 days (120 hours) in contrast to the 72 hours in this study.

In this study it was reported that 1 mM of 2-DG significantly reduced the growth of MCF-7 cells and this effect was further amplified when 2-DG was treated in combination with the oestrone analogues. The cytotoxic effect was increased at 5 mM 2-DG in previous studies and cell numbers decreased by 80% after 24 hour treatment with 20 mM 2-DG (Cheng et al., 2012).

72

Growth inhibition (50%) was observed in MCF-7 breast cancer cells treated with a concentration of 3.5 mM 2-DG for 5 days (Kaplan *et al.*, 1990). This is in contrast to the results obtained in the present study (Figure 3.1) where a concentration of 1.3 mM resulted in 50% growth inhibition. Differences in the results obtained could be attributed to different cell enumeration assays that were performed as well as to the increased sensitivity of the cells due to the lower (2%) FCS concentration. Serum deprivation is a technique used to synchronise cell cycle which ascertains to cell proliferation inhibition. Previous studies utilized the 2,3-bis[2-methoxy-4-nitro-5-sulfophenyl]-2H-tetrazolium-5-carboxanilide inner salt (XTT) assay where cells were incubated for 72 hours (Sahra *et al.*, 2010) and the micro-culture tetrazolium assay using a 5 day incubation (Kaplan *et al.*, 1990) to determine cell numbers. The SRB assay used in this study has been optimized for adherent cells in 96-well plates in order to screen compounds for toxicity (Vichai and Kirtikara, 2006). It has also previously been noted that the XTT and MTT assays are not linear with cell numbers when the cells are plated at high densities and the cell lines tested differ in the ability to reduce the dye. It has also been observed that these assays have high intra- and inter-assay variability. The SRB assay has been deemed to have increased sensitivity and reproducibility as well as increased linearity (Keepers *et al.*, 1991).

Previously conducted clinical studies have pointed to the fact that 2-DG alone will not result in significantly favourable decreased levels of cell proliferation (Landau *et al.*, 1958). The experimental compounds ESE-15-ol, ESE-16 and 2-DG in combination have been shown to be effective at inhibiting MCF-7 cell growth at relatively lower concentrations in contrast to previously conducted experiments. To further reduce the concentrations required to elicit an effective response, combination therapy has been widely used.

It was proposed by Maschek *et al.* that 2-DG should be combined with anti-mitotic compounds as the anti-mitotic compounds will target rapidly dividing tumour cells while 2-DG will target the slower proliferating cells at the inner core of the tumour (Maschek *et al.*, 2004). The cells located in the inner core are more reliant on glycolysis and an anti-glycolytic agent will best target them (Tagg *et al.*, 2008). A phase I clinical trial assessing the safety, pharmacokinetics and maximum tolerated dose of 2-DG in combination with docetaxel was successful and a phase II study is underway for the use of this combination in solid tumours (Raez *et al.*, 2013). The combination of 2-DG with metformin amplified the anti-proliferative effect supporting that 2-DG elicits an improved anti-proliferative effect when used in combination (Sahra *et al.*, 2010). Data presented by Tagg *et al.* has reported that the combination of the 2-ME derived

73

oestrone analogues with 2-DG is an effective way to potently target breast and prostate cancers (Tagg *et al.*, 2008). These studies show that combination therapy is an effective way to target advanced solid tumours.

The effective treatment of solid tumours may be improved by the combination of anti-angiogenic agents and microtubule disrupters with a glycolysis inhibitor. It is hypothesized that the inhibition of angiogenesis should result in sustained hypoxic conditions and increased dependence of the tumour on aerobic glycolysis. This in turn will make the tumour more susceptible to 2-DG treatment. This theory was validated by the combination of 2-Methoxyoestradiol-3,17-O,O-bis-sulphamate (STX140), a derivative of 2-ME and an available disrupter of microtubules, with the glycolysis inhibitor 2-DG. Studies performed after 72 hours utilizing Alamar blue via fluorescence analysis on MCF-7 breast cancer cells showed that STX140 (500 nM) inhibited cellular proliferation by 48% (Maschek *et al.*, 2004) and 2-DG (8 mM) by 50%. In the LNCaP androgen-sensitive human prostate adenocarcinoma cell line, a greater decrease in cell proliferation was noted after treatment using the combinations of STX140 and 2-DG. *In vivo* studies performed on MCF-7 xenograft models showed the tumour to decrease by 1.7 times that of the untreated control when treated with STX140. Treatment with 2-DG in combination with STX140 resulted in 3.5 times decrease in the size of the tumour (Maschek *et al.*, 2004).

The combination of ESE-15-ol and ESE-16 with 2-DG proved to be effective as the tumour cells reliant on glycolysis were targeted through glycolytic inhibition. Results shown in Figure 3.2 showed that the combination of ESE-15-ol and 2-DG was more effective at inhibiting the growth of MCF-7 breast cancer cells than the compounds alone. This was also noted after treatment with ESE-16. The experimental compounds ESE-15-ol, ESE-16 and 2-DG therefore showed synergism when targeting the MCF-7 breast cancer cell line. From cell viability results obtained it appears that the MCF-7 cell line is more susceptible to treatment than the MCF-12A non-tumorigenic cell line, however selectivity of the compounds are not exclusive to the MCF-7 cell line.

3.2 Apoptosis/necrosis

A flow cytometric method was used to assess whether cells had entered apoptosis after shorter incubation times in the presence of the synergistic combinations of the oestrone analogues and 2-DG which were shown to exhibit cytotoxic effects. The technique involved the staining of treated cells with FITC conjugated Annexin-V and propidium iodide following a well-

74

established flow cytometric protocol. Annexin-V FITC was used to identify cells in early apoptosis via the phosphatidylserine flip from the inner to the outer membrane (Van Engeland *et al.*, 1998). Propidium iodide enters a cell only when the membrane integrity is compromised and stains cellular DNA (Nicoletti *et al.*, 1991). Necrotic cells were detected by the increase in PI fluorescence.

The results shown in Figure 3.4 and 3.5 displays the induction of cell death by apoptosis and necrosis after treatment with the experimental compounds. The known apoptotic inducer staurosporine was used as a positive control (Chipuk, 2014), and showed a decrease in cell viability (14.4% cell death) with increased apoptosis which served as an indication that the assay functioned correctly.

Treatment with ESE-15-ol alone had an effect on the MCF-7 cells relative to the untreated control (Table 3.2, Figure 3.3). Following treatment with 2-DG, necrosis (±10%) was apparent however only 1.9% apoptosis was noted. The combined treatment of ESE-15-ol and 2-DG had a marked effect on the cells with ± 21% necrosis and a slight increase in apoptosis (3.9%) compared to the untreated control.

The experimental compound ESE-16 showed greater toxicity to the breast cancer cells (MCF-7) than ESE-15-ol which was expected due to the higher concentration of ESE-16 used. This was observed by the larger percentage of necrotic and early phase apoptotic cells in ESE-16-treated groups. Data indicates an 18% greater decrease in cell viability in ESE-16-treated cells in comparison to cells treated with ESE-15-ol. The most pronounced effect in cell viability was observed with the combined treatment of ESE-16 and 2-DG where cell viability decreased approximately 50% relative to the untreated control with an increase in both early apoptosis and necrosis. From the results obtained, it appeared that the compounds in combination elicited a greater effect on the initiation of apoptosis than noted in this study for the apoptosis control.

MCF-12A-treated cells (ESE-15-ol, ESE-16 and 2-DG alone and in combination) demonstrated similar lack of apoptosis to that obtained in the MCF-7 cell line (Figure 3.4). ESE-15-ol showed an insignificant difference in apoptosis relative to the untreated control with approximately 92% of cells remaining viable. Treatment with 2-DG resulted in a greater apoptotic shift. The shift displayed in the MCF-12A non-tumorigenic cells was marked by an increase in cells undergoing apoptosis with 15.84% apoptotic compared to 2-DG-treated cells in the MCF-7 cell line. In contrast to results obtained for the breast adenocarcinoma cell line,

75

the combination of ESE-15-ol and 2-DG had less of an effect on the non-tumorigenic MCF-12A cells.

Treatment with ESE-15-ol and 2-DG resulted in 83% of cells that remained viable in contrast to that of 77% viability after treatment with 2-DG. Similar to results obtained in the MCF-7 cells, ESE-16 showed greater toxicity than ESE-15-ol and resulted in the initiation of early and late phase apoptosis as well as a significantly high percentage (46%) of necrosis. The combined treatment of ESE-16 and 2-DG increased early apoptosis by 18% in comparison to treatment of ESE-16 alone. Treatment of ESE-16 with 2-DG was observed to favour necrosis as a mechanism of cell death. This parallels the cytotoxicity results obtained in the present study where cell viability was significantly reduced and cell death was favoured. Due to the low percentage of FCS used in the present study, the cells may have been starved of growth nutrients and the effect elicited was amplified. Combining the treatment of ESE-16 and 2-DG with stressed, nutrient deprived cells may be the cause for the high percentages of necrosis observed.
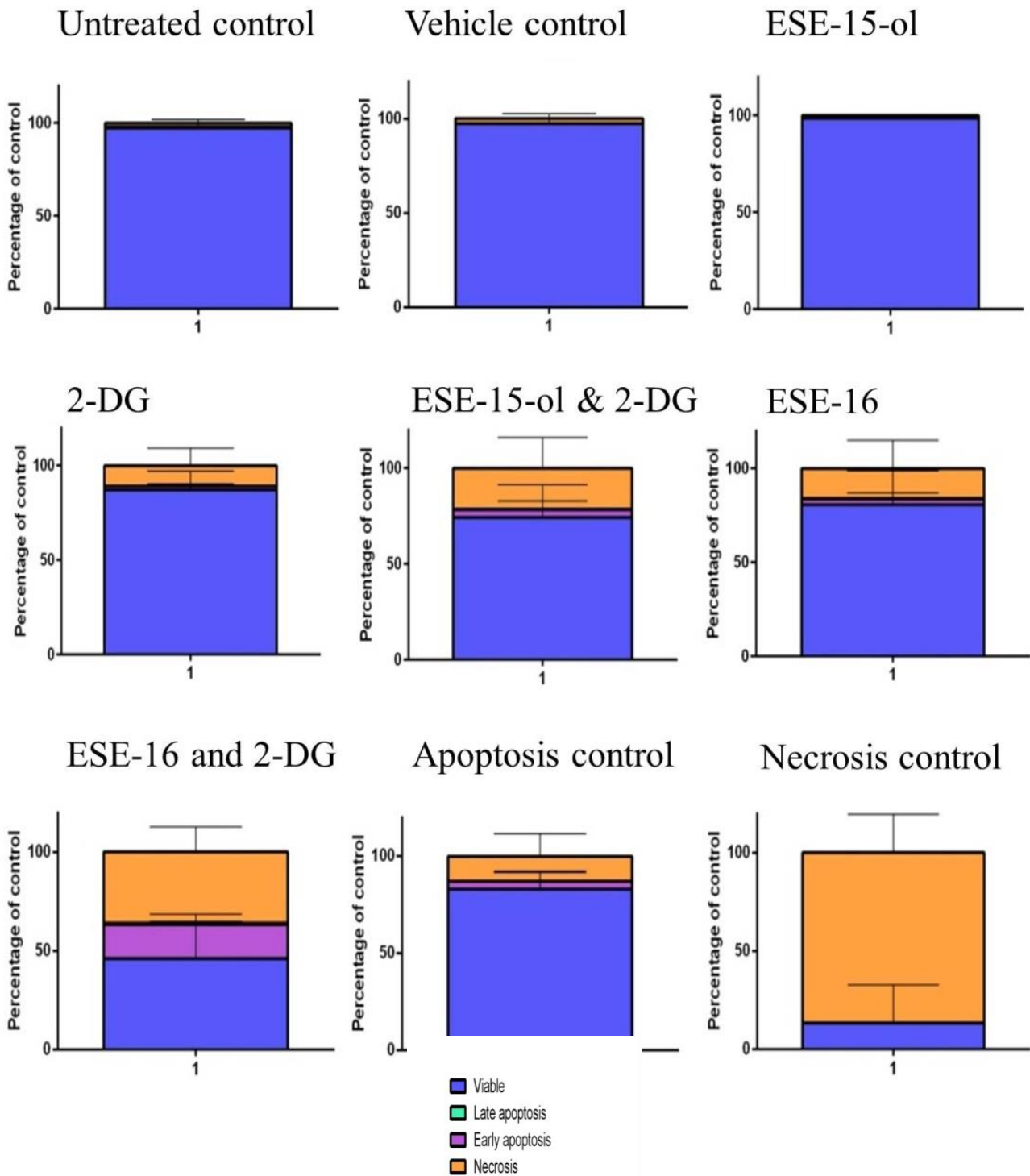
Figure 3.3 The effect on cell viability on the MCF-7 breast cancer cell line after treatment with the experimental compounds alone and in combination. Graphs are representative of the percentage of viable, early and late apoptotic and necrotic cells after 72 hours. Staurosporine (10 µM, 24 h) was used as a positive control for apoptosis. Pure ethanol (100%) was used as a necrosis control. Scatterplots represent one of three independent experiments with Annexin V-FITC on the vertical axis and PI on the horizontal axis. Bar graphs show the combined results obtained from 3 independent experiments. n=3
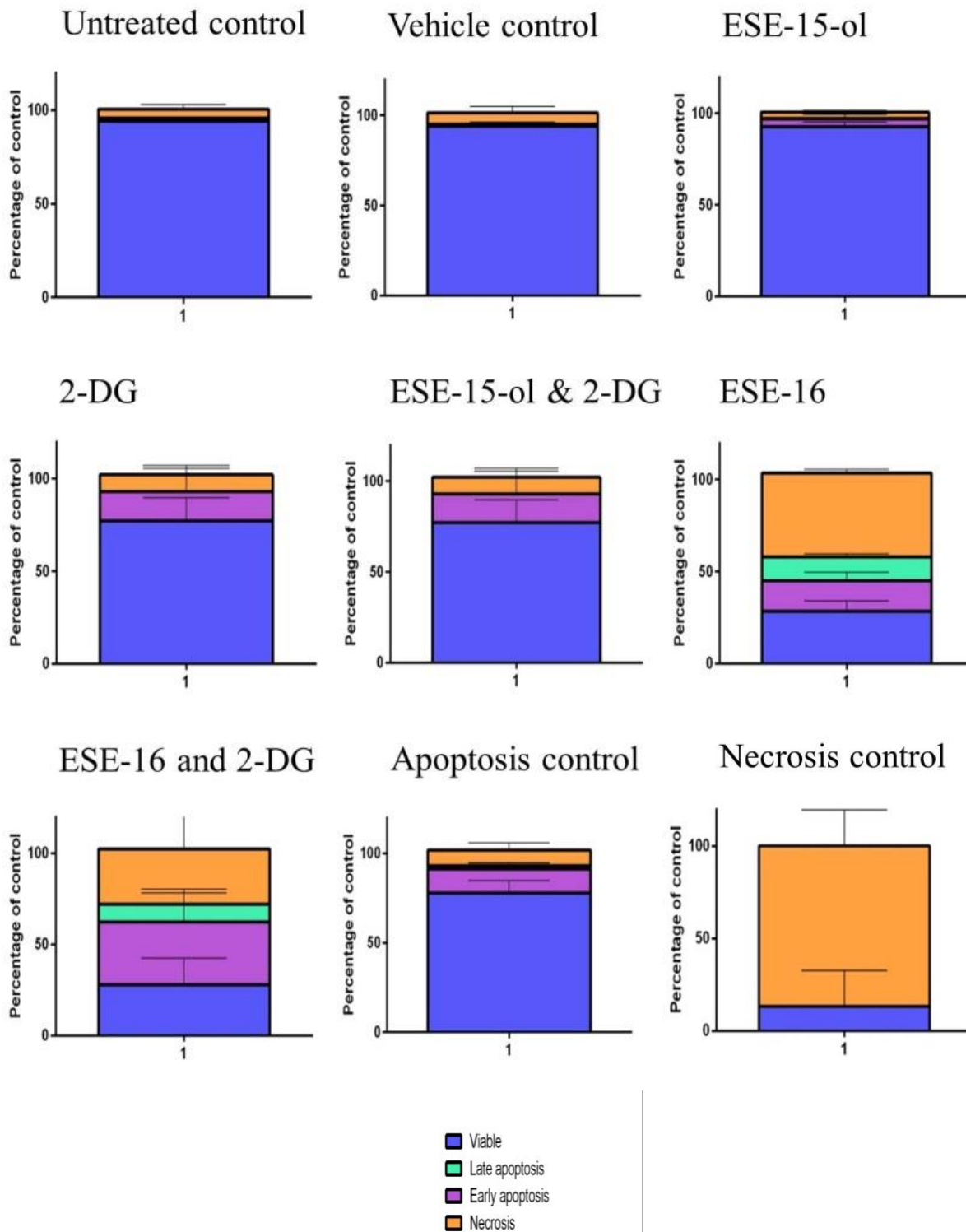
Figure 3.4 The effect on cell viability on the MCF-12A non-tumorigenic cell line after treatment with the experimental compounds alone and in combination. Graphs are representative of the percentage of viable, early and late apoptotic and necrotic cells after 72 hours. Staurosporine (10 µM, 24 h) was used as a positive control for apoptosis. Pure ethanol (100%) was used as a necrosis control. Scatterplots represent one of three independent experiments with Annexin V-FITC on the vertical axis and PI on the horizontal axis. Bar graphs show the combined results obtained from 3 independent experiments. n=3

Table 3.2 The type of cell death induced on the MCF-7 breast cancer cell after treatment with the experimental compounds alone and in combination after 72 hours.

	Viable cells	Early apoptosis	Late apoptosis	Necrosis
Untreated control	97.3 ± 1.4	0.2 ± 0.1	0.0 ± 0.0	2.6 ± 1.4
Vehicle control	97.2 ± 1.4	0.6 ± 0.4	0.0 ± 0.0	2.2 ± 1.1
ESE-15-ol	98.4 ± 0.3	0.2 ± 0.0	0.0 ± 0.0	1.4 ± 0.4
2-DG	87.1 ± 5.9	1.9 ± 0.7	0.0 ± 0.0	10.9 ± 5.4
ESE-15-ol & 2-DG	74.4 ± 9.9	4.1 ± 2.7	0.4 ± 0.3	21.2 ± 9.2
ESE-16	80.8 ± 10.3	3.1 ± 1.7	0.1 ± 0.1	15.9 ± 8.6
ESE-16 & 2-DG	45.9 ± 10.8 **	17.5 ± 3.0	0.8 ± 0.4	35.8 ± 7.3 *
Necrosis control	13.3 ± 11.3 ***	0.0 ± 0.0	0.0 ± 0.0	86.7 ± 11.3 ***
Apoptosis control	82.9 ± 5.0	4.2 ± 3.1	0.0 ± 0.0	12.9 ± 6.7

The mean percentage of cells $\pm$ SEM is reported for each phase. n=3. *$p<0.05$, **$p<0.01$, ***$p<0.001$. Apoptosis control: Staurosporine (10 µM); necrosis control: 100% ethanol

Table 3.3 The type of cell death induced on the MCF-12A non-tumorigenic cell after treatment with the experimental compounds alone and in combination after 72 hours.

	Viable cells	Early apoptosis	Late apoptosis	Necrosis
Untreated control	94.3 ± 1.2	1.33 ± 0.1	0.1 ± 0.1	4.9 ± 1.4
Vehicle control	94.0 ± 1.4	1.10 ± 0.1	0.1 ± 0.0	6.2 ± 2.1
ESE-15-ol	92.7 ± 1.4	4.33 ± 1.4	0.3 ± 0.2	$3.3 \pm 0,5$
2-DG	77.2 ± 7.2	15.83 ± 7.2	0.1 ± 0.1	9.0 ± 2.9
ESE-15-ol & 2-DG	83.0 ± 7.1	13.43 ± 7.8	0.2 ± 0.0	4.3 ± 0.8
ESE-16	28.5 ± 3.2 ***	16.63 ± 2.6	12.9 ± 0.9 *	45.7 ± 1.0 **
ESE-16 & 2-DG	27.87 ± 8.4 ***	34.67 ± 9.2 **	9.6 ± 4.8	30.3 ± 12.2
Necrosis control	0.3 ± 0.2	0.07 ± 0.1	0.4 ± 0.3	99.3 ± 0.5 ***
Apoptosis control	77.7 ± 4.2	13.60 ± 2.1	1.7 ± 0.9	8.9 ± 2.3

The mean percentage of cells $\pm$ SEM is reported for each phase. n=3. *$p<0.05$, **$p<0.01$, ***$p<0.001$. Apoptosis control: Staurosporine (10µM); necrosis control: 100% ethanol

3.2.1 Discussion

Data from the present study presented in Figures 3.3 and 3.4 shows amongst others the effect of ESE-15-ol on MCF-7 and MCF-12A cells. The results obtained in the present study differ from those obtained in previous studies. This could be attributed to different concentrations tested where the 17.5 nm ESE-15-ol used in the present study was insufficient on its own to elicit any pro-apoptotic effects. Previous studies showed the effect of ESE-15-ol (18 µM) on HeLa cells after 24 hours using flow cytometric analysis of Annexin V-FITC and PI. It was reported that early apoptosis increased to 41.17% with an increase in necrotic cells to 18.51% (Kumar *et al.*, 2015).

Previous studies observed the effect of the experimental compound ESE-15-ol after 24 hours on MDA-MB-231 oestrogen receptor negative breast cancer cells via flow cytometric analysis of the phosphorylation of Bcl-2 at Serine 70 (Ser 70) using a FlowCellect Bcl-2 Activation Dual Detection Kit (Stander *et al.*, 2012). Results showed that the expression of Bcl-2 in ESE-15-ol-treated cells was similar to that of the untreated control (Stander *et al.*, 2012). Phosphorylated Bcl-2 was observed to increase by 40% after treatment of ESE-15-ol relative to the vehicle control.

It has been noted that Bcl-2 plays an important role in the regulation of the mitochondrial membrane potential and has been linked to the initiation of apoptosis via the mitochondria (Letai and Kutuk, 2008). Phosphorylation of Bcl-2 at Ser 70 alone, has an anti-apoptotic effect however phosphorylation at multiple residues (Trp 69, Ser 70, Ser 87) has been associated with a G_2/M block in both MDA-MB-231 and MCF-7 cells. This block in cell cycle progression results in the initiation of apoptosis (Letai and Kutuk, 2008). In the previous study it was concluded that ESE-15-ol is capable of abolishing Bcl-2 phosphorylation homeostasis in a manner that stimulates the intrinsic apoptosis pathway. The pro-apoptotic effect is considered to occur through the dephosphorylation of Bcl-2 at Ser 70 (Stander *et al.*, 2012).

Treatment of ESE-15-ol (72 hours) did not result in the initiation of apoptosis (1.2%) with 98.4% of cells remaining viable (Table 3.2). There may be a possibility that phosphorylation of Bcl-2 occurred or the concentration of ESE-15-ol used in the present study was not great enough to abolish the Bcl-2 phosphorylation. This could possibly explain the anti-apoptotic results observed in the present study. As previously mentioned, the decreased percentage of

80

FCS could also be responsible for the results obtained due to possible mitochondrial membrane damage from the decrease in available nutrients.

ESE-15-ol has previously been shown to elicit apoptotic effects and the insignificant increase noted in the present study differs from previous studies. As mentioned above this could be attributed to the low concentration tested in the present study where ESE-15-ol alone was insufficient at eliciting a pro-apoptotic effect. The MCF-12A non-tumorigenic cell line showed an increase of 12.1% in apoptosis marked by a 1.6% decrease in cell viability (Table 3.3). A greater percentage (83%) of viable MCF-12A cells were reported in comparison to MCF-7 cells after treatment with ESE-15-ol and 2-DG.

Data in the present study showed that the combination of ESE-15-ol with 2-DG elicited a greater effect on MCF-7 breast cancer cells than ESE-15-ol in isolation (Figure 3.3). Combination therapy of ESE-15-ol with 2-DG was shown to decrease cell viability by 22.9% in MCF-7 cells and only by 11.3% in MCF-12A cells (Table 3.3). Results obtained in the present study (Figure 3.3, Table 3.2) showed that treatment of MCF-7 cells with 2-DG resulted in a decrease in viability with a negligible shift (1.7%) in apoptosis marked by an 8.3% increase in necrotic cells. At the dose of 2-DG (1 mM) tested in the present study, it is likely that little anti-cancer effect would be apparent in comparison to the recommended doses of 5 mM over a short time period especially if administered intravenously.

A high concentration of 2-DG for a short time period is not a practical application for chemotherapeutic treatments (D'Amato, 2008). By increasing the time period between treatments, compliance is increased as well as practicality as patients can receive treatment while maintaining a relatively normal life in contrast to staying at a hospital for more frequent administration (Conte and Guarneri, 2004).

Human monocytic leukemia U937 cells were exposed to $10\,\mu M$ etoposide in combination with 10 mM of 2-DG and the initiation of apoptosis was observed through flow cytometric using PI. Data reported that treatment of etoposide for 3 to 4 hours induced apoptosis however due to the absence of an apoptotic marker, no conclusions on the initiation of apoptosis can be drawn. Treatment of 10 mM 2-DG alone had little effect on the induction of apoptosis. It has been reported that 2-DG displays a dose-dependent effect that is dependent on the compound that with which it is combined *in vitro* (Haga *et al.*, 1998).

81

In the present study, treatment with ESE-16 resulted in a decrease of 65.8% cell viability in MCF-12A treated cells which supports previous findings where a 66% decrease in cell viability was observed after treatment with the oestrone analogue EMBS (0.4 µM, 24 hours). In the present study, the 16.5% decrease in cell viability in the MCF-7 cell line after treatment with ESE-16 contrasted previous studies which reported a 66% decrease in cell viability with an 22.22% increase in apoptotic cells (22.22%) and necrotic 12.25%) cells (Visagie *et al.*, 2015).

Previous studies utilizing Annexin V-FITC staining and flow cytometry to detect the presence of apoptosis in MCF-7, MDA-MB-231 and MCF-12A cell lines following ESE-16-exposure (200 nM) for 6, 12, 18, 24 and 48 hours reported an increase in apoptosis observed in MCF-7 and MDA-MB-231 cells through amplified phosphatidylserine (PS) externalization from the inner to the outer membrane. The increased effect observed was reported to have peaked 6 hours after addition of ESE-16. In contrast to this, the highest percentage of apoptotic cells was reported after 48 hour treatment of 200 nM ESE-16. After 24 and 48 hours, translocation of PS to the outer membrane was statistically amplified in MCF-7 and MDA-MB-231 breast cancer cells in comparison to MCF-12A non-tumorigenic cells. This data revealed that ESE-16 triggers apoptosis in cancer and non-tumorigenic cell lines however the response is greater in breast cancer cells (Stander *et al.*, 2013). In contrast to this, the present study did not observe a significant increase in apoptosis after treatment with ESE-16 in MCF-7 cells. The results in the present study may have been affected by the increased (72 hours) incubation time where by it is a possibility that the susceptible cells had died through the apoptotic pathway and only the resistant cells which still survived were represented in the results. Due to the 2% FCS concentration used, a greater amount of cells would have been susceptible to this possible mechanism.

Treatment with ESE-16 on MCF-12A cells in the present study, resulted in an increase in apoptosis by 29.53%, which parallels results previously obtained. Previous studies observed the initiation of apoptosis after 48 hours exposure of ESE-16 (Stander *et al.*, 2013). The combination of ESE-16 and 2-DG initiated apoptosis in the MCF-7 cell line as observed by the 51.4% decrease in cell viability and 18.1% increase in apoptosis relative to the untreated control (Table 3.2). MCF-12A cells treated with ESE-16 and 2-DG showed greater sensitivity with a greater decrease in viability (66.43%) and increase in apoptosis (42.84%) relative to the MCF-7 cell line (Table 3.3).

82

The compounds elicited a greater effect in combination than in isolation however at the concentrations tested, the experimental compounds were not selective for the MCF-7 cell line. The results obtained in the present study were not as pronounced as expected as well as previously reported however, the enhancement of the experimental compounds in combination was observed. From this, it can be hypothesized that the combination of oestrone analogues with other compounds such as 2-DG elicit a greater effect than the compounds alone however, further studies need to be performed to confirm this.

From the results obtained in the present study, conclusions on the mechanisms induced following exposure of the compounds cannot be deduced. As previously mentioned in Section 1.16 this could possibly be due to the integrated cell death mechanisms induced in contrast to a single mechanism. The experimental conditions in the present study vary from previous studies and it is possible that the cells are entering a quiescent state therefore no apoptosis is being elicited. For these reasons, these combinations warrant further mechanistic studies in order to ascertain the correct parameters required to optimise the initiation of the apoptotic pathway as a mechanism of cell death.

3.3 PlasDIC and light microscopy

PlasDIC and light microscopy were used to examine and identify morphological changes of MCF-7 and MCF-12A cells after exposure to ESE-15-ol, ESE-16 and 2-DG alone and in combination. All images were taken at a magnification of 40x.

Light and plasDIC microscopy photomicrographs (Figure 3.5) show the changes in morphology of MCF-7 breast cancer cells after treatment with the experimental compounds ESE-15-ol, ESE-16 and 2-DG alone and in combination. Light microscopy images revealed that after treatment with ESE-15-ol morphological changes in the MCF-7 cells were apparent relative to the untreated control. 2-DG-treated cells displayed a decreased cell density, membrane blebbing as well as rounding of cells. It was also evident that there was an increase in structures resembling vacuoles. The combination of ESE-15-ol and 2-DG further decreased cell density with increased rounding of cells and vacuole formation.

These morphological alterations were more evident after treatment with ESE-16. Combination treatment with ESE-16 and 2-DG resulted in a decrease in cell density, membrane blebbing, rounding of cells and several cells were morphologically similar to those in a metaphase block

83

as described in previous studies. Cells in metaphase display structurally complex clusters that are dispersed throughout the cytoplasm (Robbins and Gonatas, 1964). Cells in a metaphase block are identified by a dark cell image that is illuminated on the external surface by a bright 'halo' (Robbins and Gonatas, 1964). Although a nuclear dye which was not used in the present study is required to confirm phase arrest, from the above mentioned characteristics it can be hypothesised that there is a possibility of a metaphase arrest. (Figure 3.5, ESE-16 in combination with 2-DG)

PlasDIC and light microscopy images presented similar morphological changes in the MCF-7 cells treated with ESE-15-ol. The plasma membranes of ESE-15-ol and 2-DG treated MCF-7 cells differed morphologically compared to the untreated control. A further decrease in cellular density was observed in MCF-7 cells exposed to ESE-15-ol in combination with 2-DG. Treatment with ESE-16 displayed greater toxicity to the cells than ESE-15-ol as cell density was severely compromised, membrane blebbing more extensive and apoptotic body formation was increased. The combined treatment of ESE-16 and 2-DG on the MCF-7 breast carcinoma cell line showed similar morphological changes to that observed in ESE-16-treated cells. PlasDIC and light microscopy images show that ESE-16 and 2-DG further decreased cell density in comparison to the combination of ESE-15-ol with 2-DG.

Similar morphological changes were observed after treatment of the MCF-12A non-tumorigenic cells with the experimental compounds. Data presented in Figure 3.6 showed that treatment with the experimental compound ESE-15-ol had a morphological effect relative to the untreated control. A decrease in cell density was seen accompanied by membrane blebbing on some of the cells plasma membranes. Treatment with 2-DG resulted in increased blebbing and a decrease in cell density relative to the untreated control, however it was less pronounced in the MCF-12A than in the MCF-7 cells. The combined treatment of ESE-15-ol with 2-DG resulted in less morphological changes including changes in cell density and the formation of apoptotic bodies in the MCF-12A cell line in comparison to that of the MCF-7 cell line. Slight changes in cell density were observed after treatment with ESE-15-ol and 2-DG in MCF-12A cells; however the cells appeared to be morphologically similar to that of the untreated control.
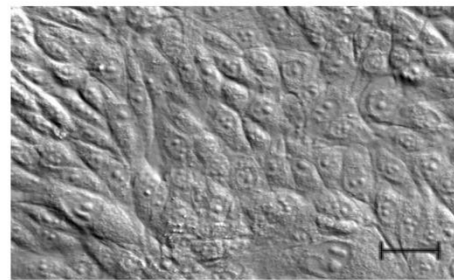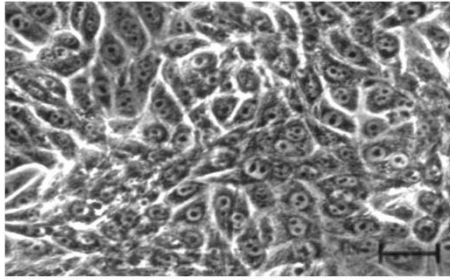
ESE-16 elicited a greater effect than ESE-15-ol on the MCF-12A cell line and the cellular density was significantly decreased with a loss in membrane integrity. After treatment with ESE-16 in combination with 2-DG an increase in cell remnants were visible. A greater effect on morphology of the MCF-12A cell line than on the MCF-7 cells by the combination of ESE-

84

16 and 2-DG was confirmed by both PlasDIC and light microscopy. Images obtained from PlasDIC microscopy showed the rounding of cells was more apparent after treatment with ESE-16 than after treatment with ESE-15-ol. The combined treatment of ESE-15-ol with 2-DG had the same effect on the morphology of the untreated control in the MCF-12A cell line with a less pronounced effect in comparison to treatment on the MCF-7 cell line. In contrast to this, ESE-16 and 2-DG had a greater detrimental effect on the MCF-12A cells in comparison to the MCF-7 cell line.
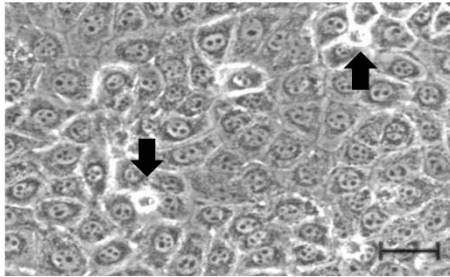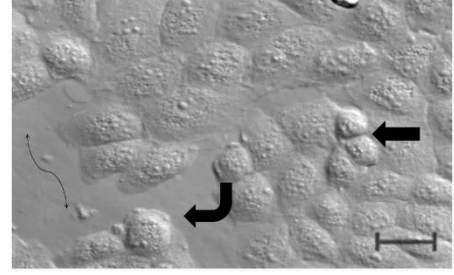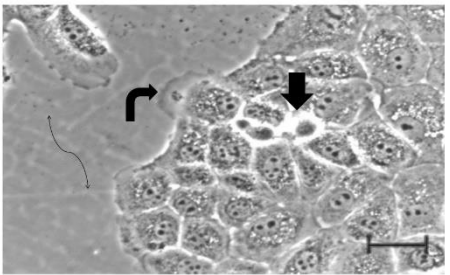
85

Light microscopy   **PlasDIC**

Untreated control

Vehicle control

ESE-15-ol

2-DG

Figure 3.5 Morphological changes of MCF-7 breast cancer cells obtained with light and PlasDIC microscopy after 72 h. Images are representative of one of six independent experiments. Scale bars in the images represent 100 µm.

Light microscopy   **PlasDIC**

Untreated control
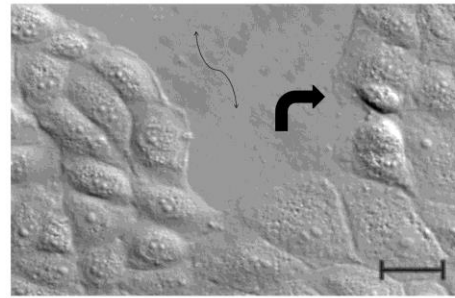
Vehicle control

ESE-15-ol

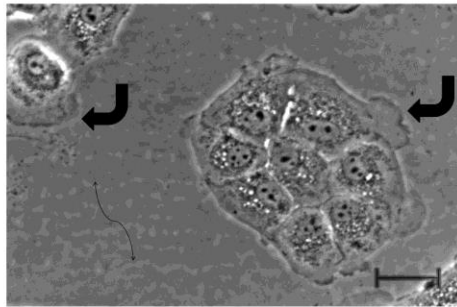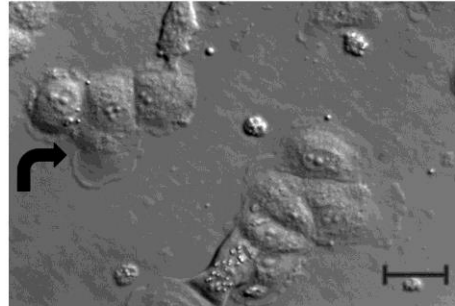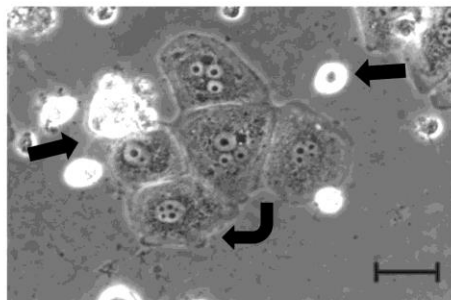2-DG

88
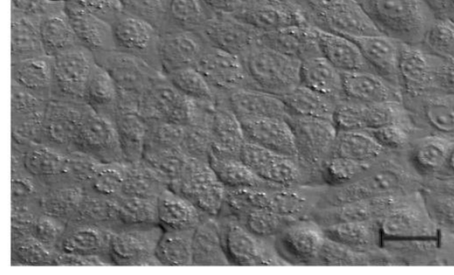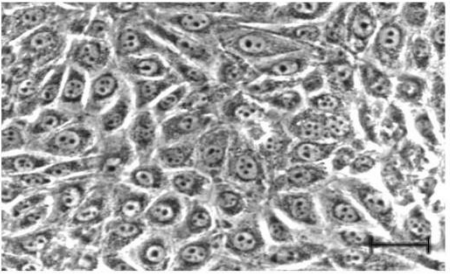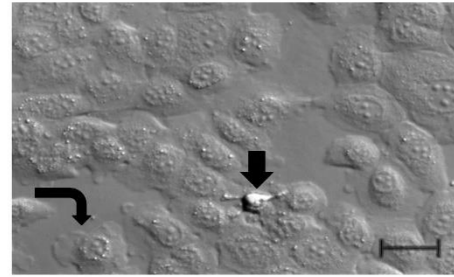
Light microscopy   **PlasDIC**
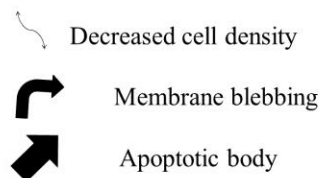
ESE-15-ol & 2-DG

ESE-16

ESE-16 & 2-DG

Decreased cell density

Membrane blebbing

Apoptotic body
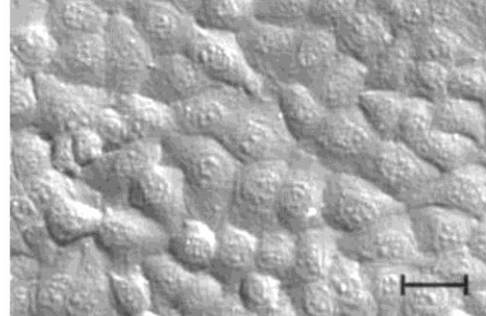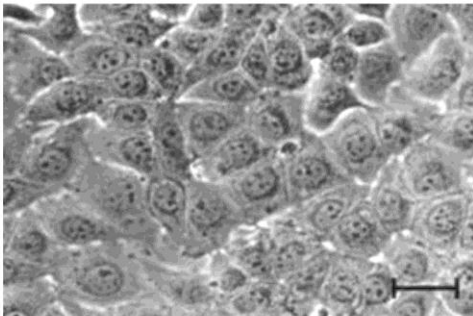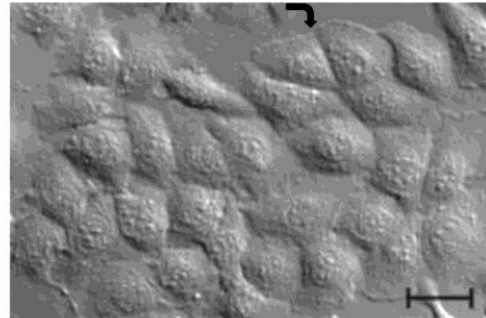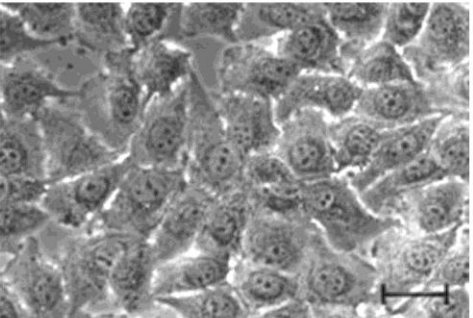
Figure 3.6 Morphological changes of MCF-12A non-tumorigenic cells obtained with light and PlasDIC microscopy after 72 h exposure to experimental compounds. Images are representative of one of four independent experiments. Scale bars in the images represent 100 µm.

89

3.3.1 Discussion

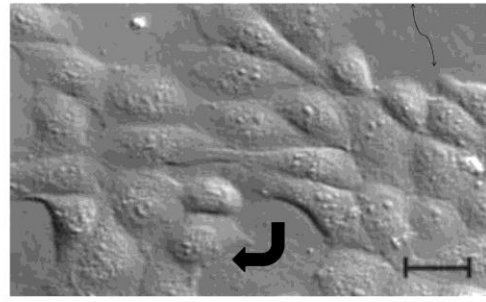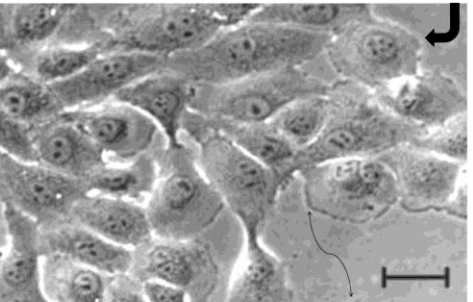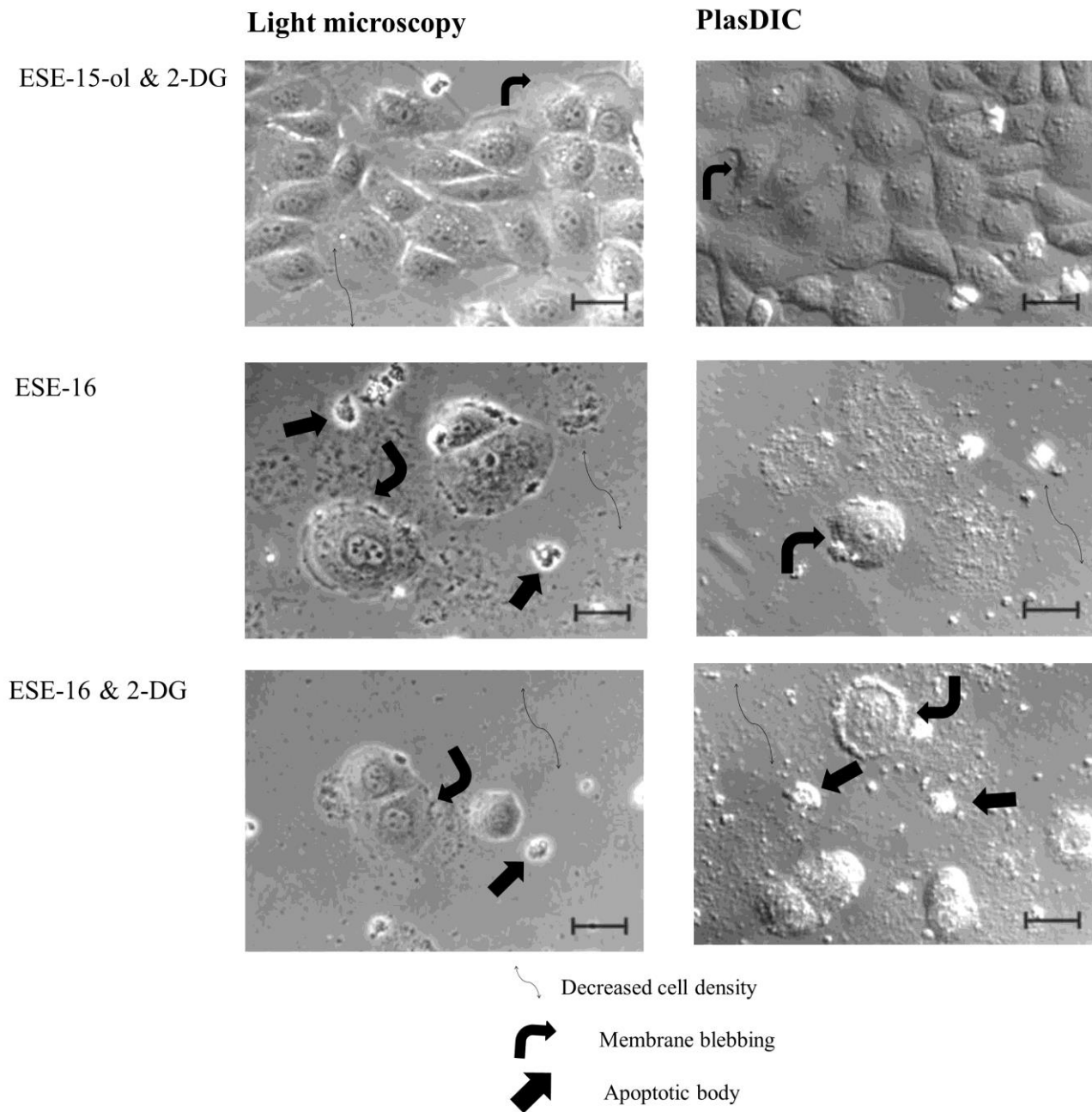From the above results obtained, treatment with ESE-15-ol in MCF-7 cells displayed morphological changes including apoptotic bodies, a slight decrease in cell density as well as what appears to be cells blocked in mitosis. These morphological characteristics of MCF-7 cells were more evident after treatment with ESE-16 (Figure 3.5). Treatment of ESE-15-ol on MCF-12A cells was observed to have little effect relative to the untreated control however treatment with ESE-16 resulted in lower cell density, rounding up of cells, apoptotic bodies being observed and cell debris evident. These results confirmed results previously obtained after treatment with EMBS (0.4 µM, 24 h) on MCF-7, MDA-MB-231 and MCF-12A cells where by typical characteristics of apoptosis were observed in all three cell lines. The morphological changes observed in the present study including the formation of apoptotic bodies, decreased cell density and cells that were observed to be blocked in metaphase confirmed results previously obtained. The MCF-7 and MDA-MB-231 treated cells were observed to have displayed greater effects after treatment with EMBS than the MCF-12A cell line (Visagie *et al.*, 2014).

The morphological changes in the present study after treatment with ESE-15-ol (Figure 3.5) were further confirmed in previous studies after treatment with the 2-ME analogue, ESE-15-one. The combined treatment of ESE-15-ol and 2-DG (Figure 3.5 and 3.6) resulted in greater morphological changes in MCF-7 cells than the non-tumorigeic MCF-12A cells. This was previously observed after treatment with ESE-15-one in combination with DCA (Stander *et al.*, 2015).

The morphology of ESE-16 treated MCF-7 cells after 72 hours in the present study (Figure 3.5) resulted in an overall decrease in cell viability relative to the untreated control with the presence of apoptotic bodies and blebbing on the membrane. These results parallel the morphological traits described in previous studies after treatment of SNO cells with ESE-16 (0.18 µM) for 24 hours (Wolmarans *et al.*, 2014, Wolmarans *et al.*, 2014). The increase of 'halo' effect cells in the present study confirm results previously obtained, where treatment with ESE-16 resulted in an increase of cells in a metaphase block which was apparent by the increased number of cells in the mitotic phase (Wolmarans *et al.*, 2014). This qualitative observation confirmed previous quantitative data where mitotic indices were determined (Van Zijl *et al.*, 2008).

90

Previously, it was reported that cells in the metaphase stage of mitosis significantly increased from 1.5% to 46% after treatment with ESE-16. (Wolmarans *et al.*, 2014). The increase in apoptotic body formation as well as the presence of cell debris observed in the present study, again confirms results previously obtained after treatment of ESE-16 (0.5 µM, 24 h) on HeLa cells. Cell shrinkage and the rounding of cells was previously described, indicative of a metaphase block (Theron *et al.*, 2013).

The present study showed that the oestrone analogues ESE-15-ol and ESE-16 affected cellular morphology in both the MCF-7 and the MCF-12A cell lines although with a less pronounced effect, confirming results from previous studies where the same and structurally similar compounds were tested. The combination treatment of ESE-15-ol and 2-DG elicited a greater effect on MCF-7 cells than ESE-15-ol alone with MCF-12A cells being less susceptible to these changes. Treatment with ESE-16 alone and in combination was observed to have a greater effect than ESE-15-ol on cell density, membrane blebbing and the formation of apoptotic bodies in both MCF-7 and MCF-12A cells. These results further support the observed apoptotic effects of the experimental compounds obtained in the apoptosis/necrosis assays reported in Section 3.2.

3.4 Cell cycle

Cell cycle analysis was performed to evaluate at which phase of cell division the cells were arrested after 72 hours of treatment with the experimental compounds ESE-15-ol, ESE-16 and 2-DG alone and in combination using the MCF-7 breast adenocarcinoma and MCF-12A non-tumorigenic cell lines. Cell cycle arrest was determined using flow cytometric analysis after PI staining which binds to and quantifies DNA in a cell.

In Figure 3.7, it was observed that the experimental compounds elicited an effect on the cell cycle of MCF-7 cells. ESE-15-ol treatment had a slight effect on cell cycle progression with what appeared to be an accumulation of cells in the G1 phase. No statistically significant changes in percentage of cells in the four different phases were noted. The percentage of cells in the G0/G1 phase was similar to that of the untreated control, however it was seen that ESE-15-ol treatment resulted in a negligible decrease (3.4%) in the S phase following a slight G2 increase (1.9%).

Following treatment with 2-DG, the percentage of cells in the G1 phase decreased compared to the untreated control. This was marked by a slight increase (4.5%) in the percentage of cells

91

in the S phase as well as the G2 phase (4.5%). The combination of ESE-15-ol and 2-DG was observed to show a slight yet insignificant decrease in the G1 phase (74.6%) relative to the untreated control (81.5%). Cells in the S phase represented an insignificant 9% of the cell population which was similar to the 9.3% in the untreated control. The combined treatment (ESE-15-ol and 2-DG) showed a statistically significant increase in the percentage of cells in the G2 phase (13.1%) relative to the untreated control (5%).

A greater decrease in the percentage of cells (relative to the untreated control) in the G1 phase was noted after treatment with ESE-16. Although not statistical different, it was noted that ESE-16 increased the sub-G1 phase that represents apoptotic cells. A slight increase in the S phase was observed with the G2 phase (11.2%) increasing by 6.2% relative to the untreated control (5.0%). Data showed that the combination of ESE-16 and 2-DG resulted in a minor increase (0.5%) of the sub-G1 apoptotic phase relative to the untreated control, which is contradictory to apoptotic results obtained in the present study. Treatment with ESE-16 alone resulted in a greater increase in the sub-G1 phase (8.4%) in comparison to the combination of ESE-16 with 2-DG (3.1%). The G1 phase showed a slight decrease of 9.6% after treatment with ESE-16 and 2-DG, and the S phase a negligible increase (1.6%) in the percentage of cells present. An insignificant increase (6.8%) in the percentage of cells at the G2 phase was noted after treatment with ESE-16 and 2-DG relative to the untreated control.

The cells synchronised in G1 through nutrient deprivation and the apoptotic positive control treated with staurosporine (producing sub-G1) were included in order to ensure that the assay was functioning correctly. The results are summarised in Table 3.4 where it can be seen that 86.2% of cells were arrested in the G1 phase after nutrient deprivation (G1 control). This large proportion of cells arrested in G1 was also noted in the untreated, vehicle control and ESE-15-ol treated cells. Treatment with the experimental compounds all resulted in increased S phase accumulation. Apoptosis was initiated by treatment with 4 µM staurosporine and this was used as a sub-G1 control. This control showed a statistically significant increase of 40.7% of cells in the sub-G1 phase. The experimental compound ESE-16 was observed to have increased the percentage of cells in the sub-G1 phase (5.8%) however the combined treatment of ESE-16 with 2-DG was observed to have no effect on the initiation of apoptosis.

Figure 3.8 illustrates the effect of the experimental compounds after 72 hours using the MCF-12A non-tumorigenic cell line. The untreated and vehicle controls showed a normal distribution of cells in the various cell cycle phases, with the majority of cells in the G1 phase and the

remainder split between the S, G2 and M phases. Treatment with ESE-15-ol resulted in a slight increase (4.3%) in the G1 phase (75.1%) relative to the untreated control (70.8%). This was paralleled by a slight decrease in the percentage of cells in the S (0.9%) and G2 phase (3.3%) relative to the untreated control. Very little effect was noted after treatment with 2-DG where the percentage of cells in each phase were similar to the untreated control. Data indicated that a decrease (4.8%) in the G1 phase was observed after treatment of ESE-15-ol combined with 2-DG. This decrease was marked by a slight increase of 4.6% in the S phase. In contrast to results summarised in Figure 3.10, treatment with ESE-16 had little effect on the MCF-12A sub-G1 phase relative to that in the MCF-7 cell line. The percentage of cells present in each cell cycle phase after treatment with ESE-16 on the MCF-12A cell line was very similar to those obtained in the untreated control. The combination of ESE-16 with 2-DG showed a similar spread within the cell cycle to ESE-16 treatment alone. This combination showed a slight increase (3.5%) in the S phase and a slight decrease (3.9%) in the G2 phase relative to the untreated control. The experimental compounds were observed to have no effect on the sub-G1 phase as observed by the low percentages present within this phase.

The G1 control showed a marked increase in the percentage of cells present in the G1 phase (84.5%). A statistically significant increase in the percentage of cells arrested in the sub-G1 phase was noted after treatment with staurosporine, a positive sub-G1 inducing control. The MCF-12A cell line showed a statistically significant decrease in the percentage of cells present in the G2 phase when treated with staurosporine.

Figures 3.8 and 3.9 illustrate the typical cell cycle analysis following exposure to the experimental compounds showing the changes in the percentage of cells present at each of the four classical cell cycle phases. The MCF-12A non-tumorigenic cell line appeared to be less affected by the experimental compounds ESE-15-ol, ESE-16 and 2-DG alone and in combination in comparison to the MCF-7 cell line.

Figure 3.7 Cell cycle blockades after treatment with the experimental compounds on the MCF-7 cell line after 72 hours test compound exposure. Histograms represent one of three independent experiments. Bar graphs show the combined results obtained from 3 independent experiments. Staurosporine (4 µM) was used as a Sub-G1 control and nutrient deprivation (48 hours) as a G1 control
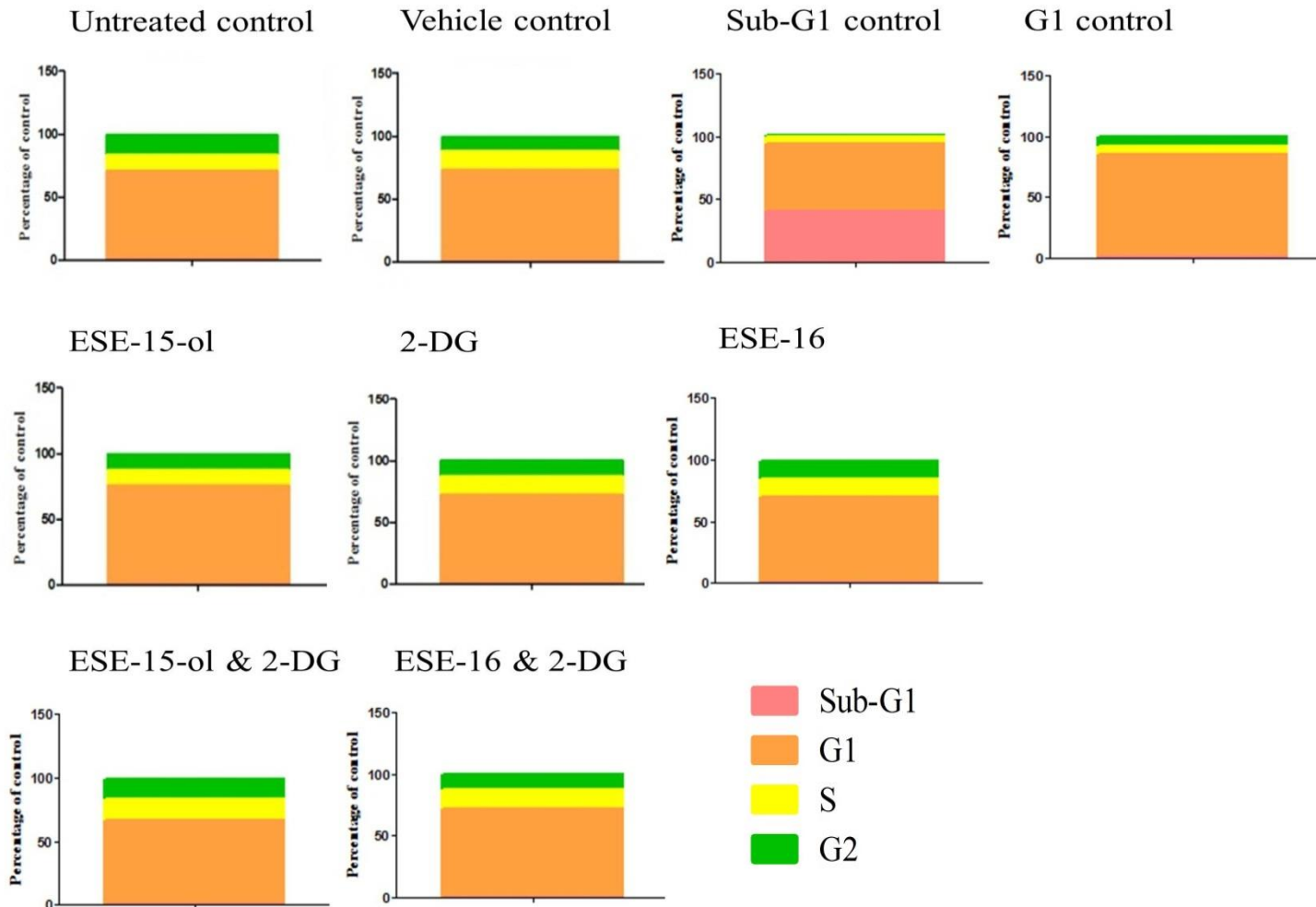
94

Figure 3.8 Cell cycle blockades after treatment with the experimental compounds on the MCF-12A cell line after 72 hours test compound exposure. Histograms represent one of three independent experiments. Bar graphs show the combined results obtained from 3 independent experiments. Staurosporine (4 µM) was used as a Sub-G1 control and nutrient deprivation (48 hours) as a G1 control
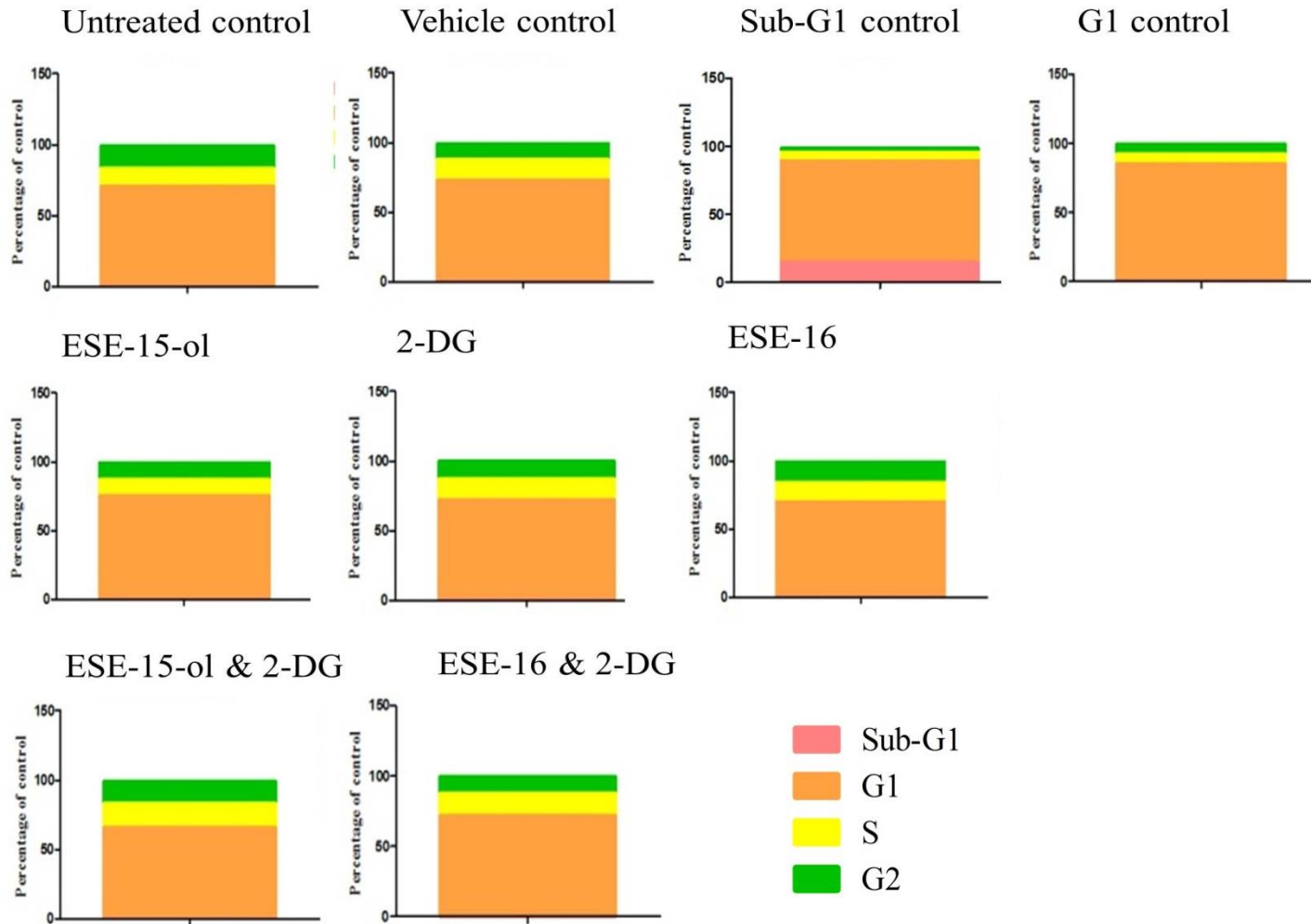
95

Table 3.4 The effect of different the treatments for 72 hours on cell cycle of MCF-7 breast cancer cells after treatment with the experimental compounds alone and in combination.

	Sub-G1	G1	S	G2
Untreated control	2.6 ±2.5	81.5 ± 3.7	9.3 ± 4.8	5.0 ± 1.0
Vehicle control	1.0 ± 0.5	83 9 ± 4.7	8.6 ± 4.9	5.3 ± 0.8
ESE-15-ol	0.8 ± 0.6	85.3 ± 3.3	5.9 ± 1.9	6.9 ± 1.7
2-DG	1.2 ± 0.7	73.6 ± 5.2	13.8 ± 5.1	9.5 ± 0.7
ESE-15-ol & 2-DG	1.0± 0.6	74.6 ± 2.9	9.0 ± 0.7	13.1 ± 2.7 *
ESE-16	8.4 ± 5.5	66.0 ± 3.5	11.5 ± 2.1	11.2 ± 0.4
ESE-16 & 2-DG	3.1 ± 1.8	71.9 ± 2.4	10.9 ± 1.8	11.8 ± 2.0
G1 control	3.3 ± 2.4	86.2 ± 1.8	5.1 ± 1.1	6.3 ± 0.8
Staurosporine	40.7 ± 12.8 ***	53.4 ± 14.0 *	5.6 ± 2.7	0.9 ± 0.4

The mean percentage of cells ± SEM is reported for each phase. n= 3. *p<0.05, ***p<0.001. G1 control: nutrient deprivation, Sub-G1 control: 4 µM staurosporine

Table 3.5 The effect of different the treatments for 72 hours on cell cycle of MCF-12A non-tumorigenic cells after treatment with the experimental compounds alone and in combination.

	Sub-G1	G1	S	G2
Untreated control	0.3 ± 0.3	70.8 ± 2.9	12.6 ± 0.5	15.6 ± 2.7
Vehicle control	0.2 ± 0.2	73.2 ± 1.2	14.4 ± 2.7	11.8 ± 1.5
ESE-15-ol	0.3 ± 0.3	75.1 ± 3.5	11.7 ± 3.6	12.3 ± 1.2
2-DG	0.2 ± 0.2	72.1 ± 8.0	15.1 ± 5.9	12.6 ± 2.5
ESE-15-ol & 2-DG	0.2 ± 0.2	66.0 ± 9.8	17.2 ± 4.9	16.1 ± 6.3
ESE-16	0.3 ± 0.3	70.0 ± 7.0	14.0 ± 4.2	15.3 ± 3.7
ESE-16 & 2-DG	0.1 ± 0.1	71.7 ± 9.4	16.1 ± 5.6	11.7 ± 4.3
G1 control	0.7 ± 0.7	84.5 ± 5.9	7.1 ± 1.8	7.5 ± 3.5
Staurosporine	28.2 ± 11.2 ***	66.3 ± 12.6	4.8 ± 0.7	0.2 ± 0.1 *

The mean percentage of cells ± SEM is reported for each phase. N = 3. *p<0.05, ***p<0.001. G1 control: nutrient deprivation, Sub-G1 control: 4 µM staurosporine

96

3.4.1 Discussion

In the present study, treatment with ESE-15-ol resulted in a decreased percentage of MCF-7 cells in the sub-G1 phase relative to the untreated control. The sub-G1 phase of MCF-12A cells were unaffected after treatment with ESE-15-ol relative to the untreated control. Previous findings reported that after 48 hours exposure the effect of ESE-15-ol (50 nM) on the non-tumorigenic MCF-12A cell line was less pronounced than on the MCF-7 and MDA-MB-231 cancerous cell lines. In contrast to results obtained in the present study, previous studies reported a 12.93% decrease in the percentage of non-tumorigenic MCF-12A cells present in the sub-G1 phase in contrast to the MDA-MB-231 cells. It has been previously reported that, an increase of 22.24% in the Sub-G1 phase was observed with ESE-15-ol on MCF-7 cells in comparison to the MCF-12A cell line after treatment (Stander *et al.*, 2012). Treatment with EMBS (0.4 µM, 24 h) in previous studies, resulted in a 36% increase in the sub-G1 phase in MCF-7 cells, 28% in MDA-MB-231 cells and 33% in MCF-12A cells (Visagie *et al.*, 2015).

Cell cycle analysis in the present study, was performed over a 72 hour treatment period which, from previous results, hypothesizes that the cells should have entered the sub-G1 status representing cells in apoptosis. A greater percentage of cells were observed in the G2 phase than in the sub-G1 phase which is expected in cells not under apoptosis. This is in contrast to the cell viability results obtained in the present study where the experimental compounds effectively killed the cells. Differences between the results obtained in the present study to previous studies could be accounted for by cell population variation.

The differences observed between the present study and previous studies may possibly be due to the variation in experimental design including different incubation periods, experimental concentrations and FCS concentrations. Treatment of ESE-15-ol in the present study (Table 3.4) resulted in a 3.8% increase in the G1 phase of MCF-7 cells. Although this is not a remarkable increase it does parallel previous studies which reported an increased G1 phase after treatment of ESE-15-ol (Stander *et al.*, 2012, van Vuuren *et al.*, 2015). As observed in Table 3.5, the G1 phase of MCF-12A cells increased by 4.2% relative to the untreated control

Treatment with ESE-15-ol was observed to have had little effect on the G2 phase relative to the untreated control with an increase of 1.9% in MCF-7 and 3.3% in MCF-12A cells. This is in contrast to previous studies which described ESE-15-ol as an inducer of a mitotic block after treatment with ESE-15-ol (Stander *et al.*, 2012). After 12 and 24 hours, it was previously

97

reported that ESE-15-ol results in an increased percentage of cells in G2/M (van Vuuren *et al.*, 2015), which was not observed in the present study. Previously, an increase of 50% in MCF-7 cells, 63% in MDA-MB-231 cells and 52% in MCF-12A cells were reported in the G2/M phase after treatment with EMBS (0.4 µM, 24 h) (Visagie *et al.*, 2015). The oestrone analogue ESE-15-one induced a G2/M block in MCF-7 and MCF-12A cell lines after 24 hours drug exposure (Stander *et al.*, 2015). These results suggest that oestrone analogues of 2-ME induce a G2/M block in cell cycle progression, however, this was not observed after treatment with ESE-15-ol alone in the present study.

Treatment with 2-DG (1 mM) (Table 3.4 and 3.5) resulted in a negligible sub-G1 decrease of 1.4% in MCF-7 cells and 0.1% in MCF-12A cells. These percentages are in contrast to previous results which reported an increase in the sub-G1 phase of osteosarcoma cells after treatment with 2-DG (3.6 mM) (Maher *et al.*, 2004). Previous studies observed the increased sub-G1 phases after treatment with 2-DG at higher concentrations of 3.5-5 mM on various cell lines (Zhang *et al.*, 2006). In the present study, 1 mM 2-DG was used and due to this the percentage of cells reported in the sub-G1 phase could be less than that previously reported. At a lower concentration, less cell death is expected to be apparent in comparison to previous studies that utilized higher concentrations of 2-DG. Previous studies have reported that 2-DG is capable of eliciting various effects on the cell cycle in a dose dependant manner. Previously, it was observed that 5 mM of 2-DG had little effect relative to the untreated control on HepG2 cells but induced a G2/M block on SKOV3 cells. The IGROV1-R10 and MSTO-211H cells responded to 2-DG (5 mM) treatment via an increase in the sub-G1 phase. This data implies that the effect on 2-DG varies amongst cell lines irrespective of the concentration remaining constant. It was previously hypothesised that the effect elicited by 2-DG was that the proliferation of cells was not arrested but reduced, cell proliferation stopped even when apoptosis was not detected, apoptosis was induced when strong arrest in cell cycle occurred and cells were observed to mostly undergo apoptosis (Zhang *et al.*, 2006).

Similar to previous studies conducted, the present study observed changes in the S/G2 phases of the cell cycle at a lower concentration of 1 mM 2-DG. Results reported in Table 3.4 that treatment with 2-DG on MCF-7 breast cancer cells resulted in an increase of 4.5% in cells in the S phase and in total a 9% increase in the S/G2 phase. A slighter lower increase was observed in the MCF-12A cell line with a total 5.5% increase in the S/G2 phase.

98

The combination of ESE-15-ol with 2-DG elicited a statistically significant arrest in the G2 phase which was not observed for ESE-15-ol alone. This was noticeable by an 8.1% increase in the percentage of MCF-7 cells relative to the untreated control, arrested in the G2 phase (Table 3.4). These results confirm previous studies where 2-DG (1.2 mM) in combination with rhodamine 123 (Rho123) after 72 hours induced a late S/G2 block in osteosarcoma cells marked by the transition to apoptosis (Maher *et al.*, 2004). Similar to previous studies, results obtained in the present study showed that MCF-12A cells are less susceptible to the combination of ESE-15-ol and 2-DG, resulting in only a 0.5% decrease in the percentage of cells in the G2 phase. Overall it was concluded that the combination of the oestrone analogue ESE-15-ol and 2-DG resulted in a M block. This observation, parallels morphological features and hypotheses described in Section 3.3.

Data in the present study (Table 3.4) observed an increase of 5.8% in the sub-G1 of ESE-16 treated cells using the MCF-7 cell line. Previous studies showed a larger sub-G1 increase of 27.38% relative to the untreated control after treatment with ESE-16 (0.5 µM, 24 h) on HeLa (cervical adenocarcinoma cells) cells (Theron *et al.*, 2013). It can be noted that the magnitude of the effect on cell cycle is dependent on the concentration of ESE-16. This was observed when comparing a previous study which resulted in a greater increase in the sub-G1 phase after treatment with ESE-16 at 0.5 µM in contrast to the previous study which treated with ESE-16 at 134 nM. The results obtained in the present study confirmed previous studies where a 6.28% increase in the sub-G1 phase relative to the untreated control was noted after treatment of ESE-16 (0.18 µM) on SNO cells (Wolmarans *et al.*, 2014). The percentage of cells in the G1 phase was reported to decrease by 23.41% marked by a 15.49% increase in the G2/M phase after treatment with ESE-16. The increase in the G2/M phase was attributed to ESE-16 eliciting a metaphase block (Wolmarans *et al.*, 2014).

Treatment with 2-DG in the present study resulted in a 6.2% increase in the G2 phase suggesting that ESE-16 elicited its effects through a G2/M block in the cell cycle. These results parallel previous studies which reported a statistically significant increase of 29.55% in the G2/M phase. ESE-16 has been reported to elicit its effect on spindle formation and described as a spindle poison resulting in a G2/M block (Theron *et al.*, 2013, van Vuuren *et al.*, 2015).

Treatment of MCF-12A cells with ESE-16 in the present study reported 70% viability in comparison to MCF-7 cells which reported 66% cell viability. The sub-G1 fraction of MCF-12A treated cells did not increase relative to the untreated control and the G1 fraction showed

99

results to be negligible (0.8% increase). The G2 fraction of ESE-16 treated cells did not increase relative to the untreated control. Previous studies suggest that the MCF-12A non-tumorigenic cell was less susceptible to ESE-16 than the MCF-7 cell line, however from the results obtained in the present study, this conclusion cannot be drawn.

The combination of ESE-16 with 2-DG in the present study was observed to elicit a greater G2/M block than ESE-16 alone. A 6.8% increase was noted in the G2 phase of MCF-7 cells following treatment with ESE-16 and 2-DG. Treatment of ESE-16 with 2-DG resulted in a 3.9% decrease in the G2/M phase relative to the untreated control of MCF-12A cells. From this it can be hypothesized that the combination of 2-DG with the oestrone analogues is a more effective cell cycle inhibitor than the compounds in isolation.

3.5 Mitochondrial membrane potential

Mitochondrial membrane potential was assessed through fluorescence ratio analysis of the cationic dye JC-1. The fluorescent ratio is expressed as the aggregate (red) to the monomer (green). This was performed in order to determine the effect and possible involvement of the mitochondria in the initiation of cell death induced by the combinations on the MCF-7 and MCF-12A cell lines. Mitochondrial involvement possibly leading to intrinsic apoptosis pathway activation was assessed through determination of whether an increase (hyperpolarization) or decrease (depolarization) in the mitochondrial membrane potential relative to the untreated control was initiated by the drug treatment.

Data indicates a significant depolarisation of the mitochondrial membrane potential after treatment with the known depolarising agent tamoxifen, indicating that the assay was sensitive enough and functioning correctly. Several incubation periods were tested to optimise this method and from results obtained as well as previous studies conducted, the incubation time chosen was 24 and 48 hours.

The results shown below (Figure 3.9) depict a time-dependent effect of the experimental compounds alone and in combination on both the MCF-7 and MCF-12A cell lines. Data reported that exposure of ESE-15-ol (24 hours) on the MCF-7 cells depolarised the mitochondrial membrane potential relative to the untreated control. 2-DG-treated cells showed an insignificant depolarisation of 3.6 %. Data indicates a statistically insignificant depolarisation in the combined treatment with ESE-15-ol and 2-DG and elicits a response very similar to that of 2-DG alone (24 h). It was observed that slight hyperpolarisation occurred after

100

treatment with ESE-16 on the MCF-7 cell line after 24 hours. However, a slight depolarisation in mitochondrial membrane potential was observed when treated with the combination of ESE-16 and 2-DG.

Similar results were observed for the MCF-12A non-tumorigenic cell line. ESE-15-ol-treated cells showed depolarisation (28% decrease) of the mitochondrial membrane potential compared to the untreated control cells. Treatment with 2-DG resulted in depolarisation relative to the untreated control with a greater effect on MCF-12A cells compared to the MCF-7 cell line. Similar results were observed with the treatment of ESE-15-ol and 2-DG where depolarisation was noted. After 24 hours ESE-16 exposure on the MCF-12A cell line showed a 6.5% depolarisation in contrast to a 8.4% hyperpolarisation in MCF-7-treated cells. Data showed a statistically significant mitochondrial membrane depolarisation after 24 hours exposure to the combined treatment of ESE-16 and 2-DG.

The experimental compounds were observed to elicit a similar effect to tamoxifen after a 48 hour incubation period. After 48 hour exposure, statistically significant changes in the mitochondrial membrane potential were observed (Figure 3.9). ESE-15-ol induced depolarisation of the mitochondrial membrane of MCF-7 breast cancer cells by 21.1% relative to the untreated control. Similar results were noted for treatment with 2-DG with a depolarisation of 19%. The combination of ESE-15-ol and 2-DG resulted in little increase in the percentage (17.3%) depolarisation of the membrane potential with no additive depolarisation effect evident. An 11% hyperpolarisation was seen after treatment with ESE-16 which showed a 18.4% depolarisation after treatment with a combination of ESE-16 with 2-DG.

Exposure of the compounds for 48 hours demonstrated greater effects on the MCF-12A non-tumorigenic cell line. Treatment with the experimental compounds elicited a 13.6% depolarisation in ESE-15-ol treated cells, 41.3% after treatment with ESE-16 and 28.6% after 2-DG treatment relative to the untreated control. However 2-DG alone had a greater effect on the mitochondrial membrane potential of MCF-12A cells than the combination of ESE-15-ol and 2-DG after 48 hours. The experimental compound ESE-16 (28.6%) elicited a significantly greater effect than ESE-15-ol (13.6%) however, the combination of ESE-16 with 2-DG (37.7% depolarisation) did not have a greater effect than the compounds alone. The combination of

101

ESE-15-ol or ESE-16 with 2-DG however, had no greater effect than the compounds in isolation.
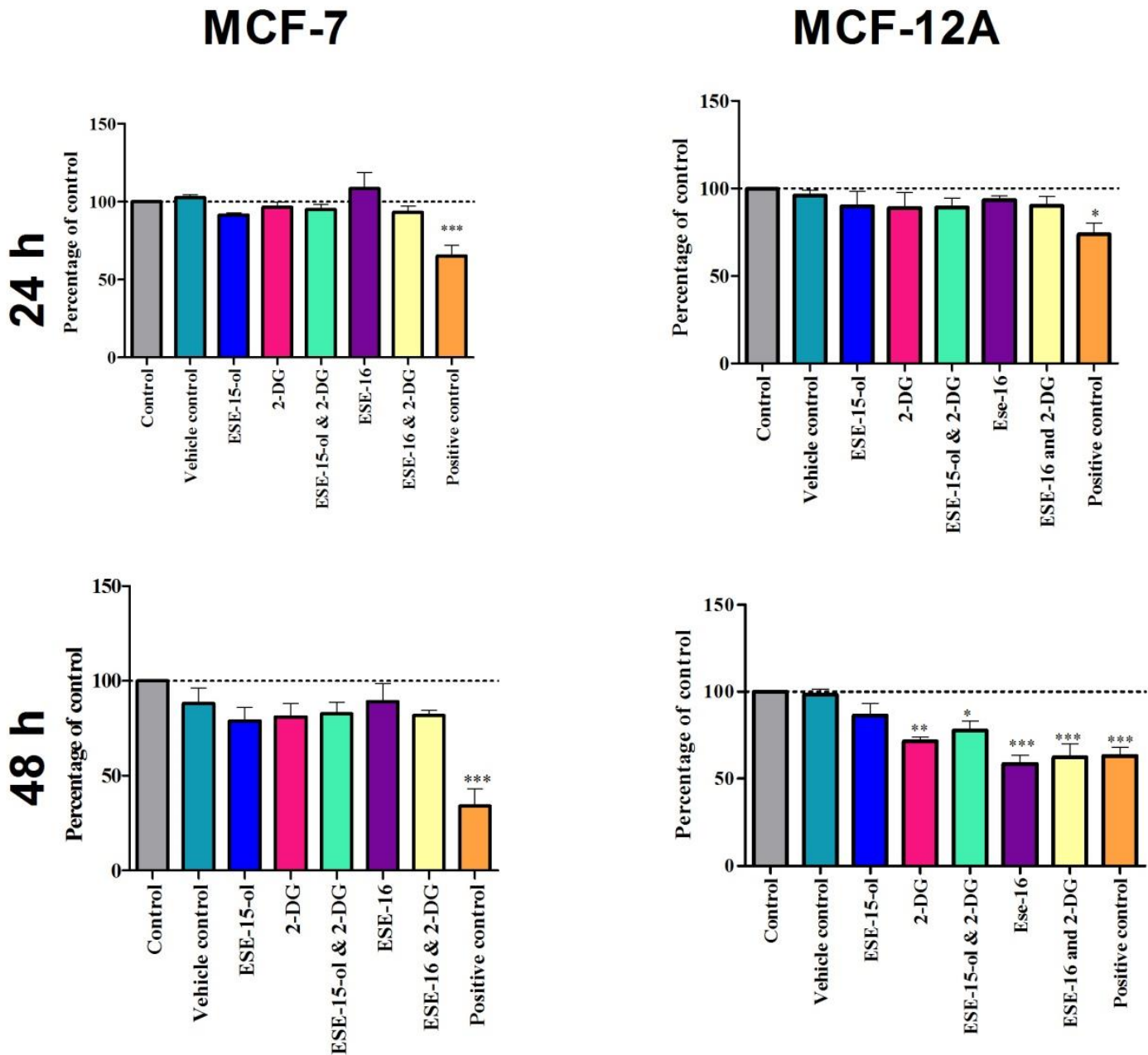
Figure 3.9 The effect of the experimental compounds ESE-15-ol, ESE-16 and 2-DG alone and in combination after 24 and 48 h on the mitochondrial membrane potential of MCF-7 breast adenocarcinoma cell line and MCF-12A non-tumorigenic cells. Tamoxifen (14 µM, 24 h) was used as a positive control for membrane depolarization. Bar graphs show the combined results obtained from 3 independent experiments.
n = 3, *p<0.05, **p<0.01, ***p<0.001.

102

3.5.1 Discussion

Mitochondrial membrane potential is evaluated through the loading of cells with a membrane permeable cationic fluorescent dye that accumulates in regions of high acidity. The high concentration of dye results in aggregation and a red shift in the excitation and emission wavelengths. Assessment of changes in the ratios at the different wavelengths indicated the degree of polarisation of the mitochondria which is measured as a comparison between untreated control cells and the equivalent experimental compound treated cells. (Garner *et al.*, 1997). The cationic dye utilized has high lipophilicity that allows easy equilibration across the mitochondrial membrane and accumulates in the intra-membrane space inversely proportional to the membrane potential. More dye will accumulate in a hyperpolarized membrane and vice versa for depolarization of the mitochondrial membrane (Perry *et al.*, 2011). JC-1 (5,5',6,6'-tetrachloro-1,1',3,3'-tetraethylbenzimidazolylcarbocyanine iodide) is the lipophilic, ratiometric, cationic dye used to assess this parameter (Galluzzi *et al.*, 2007, Perry *et al.*, 2011). If the membrane potential is reduced, the dye does not accumulate in the mitochondria and remains in the cytoplasm in the monomeric form, which emits green fluorescence.

Treatment in the present study treatment with ESE-15-ol for 24 hours showed only slight membrane depolarisation, however no statistical significance was observed. The observed effect in the present study parallels previous results reported, however the effect noted in the present study was less pronounced than that previously reported. The slight depolarisation of the mitochondrial membrane noted in the present study after treatment with ESE-15-ol contrasts previous studies which reported an extensive depolarisation after treatment with ESE-15-ol (50 nM, 24 h) on MCF-7 and HeLa cervical adenocarcinoma cells (Stander *et al.*, 2012) (Visagie *et al.*, 2013). It was previously reported that treatment with ESE-15-one (130 nM, 24 h) resulted in a 1.5-2.2 fold decrease in the mitochondrial membrane potential in MCF-7 cells relative to untreated control after analysis with the Mitocapture apoptosis kit (Stander *et al.*, 2015). Flow cytometric analysis of another 17-β oestradiol analogue, EMBS (500 nM, 24 h) reported a 26% decrease of the mitochondrial membrane potential in MCF-7 cells along with a decrease in the oestrogen receptor-negative tumorigenic metastatic MDA-MB-231 breast cancer cell line (Visagie *et al.*, 2015). Treatment with ESE-15-ol in the present study was observed to have similar effects to those previously reported however the less pronounced effect could be related to different experimental conditions. ESE-15-ol in the present study was tested at a lower concentration (17.5 nM) and in 2% FCS which as explained above, could

account for differences observed. The decrease in available nutrients for the cell and the 'cell starvation' mentioned above could affect the energy production of the cells which would have an impact on the mitochondria in the cell.

Data shown in Figure 3.5 reported that there was a 10.2% statistically insignificant depolarization of the membrane after 24 hours (MCF-12A). A greater depolarisation effect was however observed in the MCF-12A cell line in comparison to the MCF-7 cell line. Previously it was reported that treatment with ESE-15-one (130 nM, 24 h) did not influence the mitochondrial membrane depolarisation in MCF-12A treated (Stander *et al.*, 2015). Treatment of MCF-12A cells with ESE-15-ol for 48 hours resulted in paralleled results to treatment after 24 hours with a 10.2% depolarisation of the mitochondrial membrane potential relative to the untreated control. This could imply that ESE-15-ol has a limited effect on mitochondrial mechanisms, and involves more of extrinsic pathways than the dependence on cytochrome *c*. However, this limited effect could be greater if the concentration of ESE-15-ol was increased and could be tested in future studies.

The combined treatment of ESE-15-ol and 2-DG only showed a slight effect on the mitochondrial membrane potential relative to the untreated control after 24 (10.9% depolarisation) and 48 hours (17.3% depolarisation) in MCF-7 cells. ESE-15-ol in combination with 2-DG did not elicit a greater effect on membrane depolarisation than either of the compounds alone. Following 48 hours, a statistically significant depolarisation was observed after exposure to the combined treatment of ESE-15-ol and 2-DG on the non-tumorigenic MCF-12A cells. This would indicate a lack of selectivity of the experimental compounds for the cancer cells. From the results obtained, it was however observed that the combination of ESE-15-ol and 2-DG elicits a greater effect following a longer exposure period which could be beneficial in the future treatment of neoplasms.

The MCF-12A cell line was observed to show similar changes in mitochondrial membrane potential to that obtained using the MCF-7 cell line. The combination of ESE-15-ol with 2-DG did not result in increased depolarisation relative to the compounds alone. After 24 hours, the combined treatment of ESE-15-ol and 2-DG showed a slight depolarisation that only showed significance relative to the untreated control after 48 hours.

Mitochondrial membrane depolarisation has been linked to the induction of apoptosis via the intrinsic pathway (Kluck *et al.*, 1999). As mitochondrial membrane depolarisation was not evident when treating cells with ESE-15-ol in combination with 2-DG, it is possible that these

104

compounds do not necessarily elicit its effects via the mitochondria at the concentrations tested in the present study. Although depolarisation was observed, the mechanism of action could possibly involve the extrinsic pathway when treated at low concentrations (17.5 nM) in contrast to the intrinsic pathway that involves mitochondrial membrane depolarisation.

From the Warburg effect on cancer cells, a target for cancer treatment is glycolytic inhibition (Warburg, 1956). Previous studies have utilized compounds involved with inhibition of mitochondrial oxidative phosphorylation (OXPhos) in combination with glycolytic inhibitors (de Jong *et al.*, 1992). 2-DG has previously been used to target glycolysis in cancer cells (Chen *et al.*, 2007) where it was shown that at concentrations above 1 mM, cancer cells with mitochondrial respiratory defects, especially those in hypoxic environments, undergo ATP depletion resulting in cell death (Liu *et al.*, 2001). Intracellular ATP levels were observed to decrease 20 to 30% more in MCF-7 cells than the non-tumorigenic MCF-10A cell line when treated with 2-DG in combination with coenzyme-Q conjugated to an alkyl triphenylphosphonium cation (Mito-Q) (Cheng *et al.*, 2012). *In vivo* studies administering 16 mM 2-DG intravenously to female Sprague Dawley rats for a period of 1, 3 or 5 days showed both a dose and time dependent decrease (50%) in ATP levels that correlated to previously obtained cell viability results (Zhu *et al.*, 2005).

Results obtained in the present study after 48 hours (Figure 3.5) reported depolarisation of the mitochondrial membrane to a greater extent than that obtained after 24 hours exposure to 2-DG. In the present study, treatment of 2-DG (1 mM, 24 h) in MCF-7 cells resulted in a slight decrease of 3.6% in membrane potential relative to the untreated control (Figure 3.5). After 24 hours, the combination of 2-DG and the oestrone analogues resulted in a similar effect to that of 2-DG alone. This is in contrast to previous results obtained, where data reported that the combination of 2-DG with metformin resulted in an increased depolarization of the membrane in comparison to treatment with 2-DG alone. These findings supported the time-dependent decrease in intracellular ATP levels after treatment with 2-DG. ATP levels were significantly decreased by 70 % when cells were treated with 2-DG in combination with metformin (Cheong *et al.*, 2011). This confirms the enhanced effect of 2-DG when used in combination.

Following 48 hour treatment with 2-DG, a greater yet insignificant effect in membrane depolarisation of 19.1% was observed relative to 24 hour exposure. These results parallel previous results obtained where treatment of 2-DG (4 MM) on p-SK4 human gastric cancer cells resulted in depolarisation of the mitochondrial membrane relative to the untreated control

105

(Cheong *et al.*, 2011). These results are however not directly comparable as the data was obtained using the mitochondrial probe, Rhodamine 123 which differs from the method used in the current study. In the present study, 1 mM 2-DG was observed to cause membrane depolarisation after 48 hours exposure, however statistical significance of this was only noted in the MCF-12A cell line.

In the MCF-12A cell line, treatment with 2-DG alone and in combination with the oestrone analogues for 24 hours showed similar results to that obtained in the MCF-7 cell line. After 48 hours however treatment of the MCF-12A cell line with 2-DG resulted in statistically significant depolarisation of 28.6% of the mitochondrial membrane. The combination of 2-DG with ESE-15-ol or ESE-16 also showed significant mitochondrial membrane depolarised. In contrast to previous studies, the effect was not noticeably greater than 2-DG in isolation. From the results obtained it is possible that low concentrations of 2-DG may lack specificity towards the MCF-7 cell line, however when treated in combination the depolarisation effect is slightly amplified. The slight 3.6% depolarisation seen in the mitochondrial membrane potential could also suggest that cell death occurs via more than one pathway. The depolarisation could be linked to the induction of the intrinsic apoptotic pathway however the depletion of intracellular ATP levels has been linked to the induction of autophagy as a mechanism of cell death. This has been confirmed in studies conducted with the .treatment of 2-DG on prostate cancer cells where depolarisation occurred as well as the initiation of apoptosis (Ben Sahra *et al.*, 2010). From this it was hypothesized that the effects of 2-DG treatment may involve the autophagic pathway as a target in cellular death and homeostasis.

In the present study data collected after 24 hours exposure showed that in contrast to previous studies, treatment with ESE-16 resulted in hyperpolarisation in MCF-7 treated cells. Previously the use of the cationic JC-1 dye of the Mitocapture apoptosis kit via flow cytometric analysis reported that treatment with ESE-16 (200 nM, 6 to 48 h) resulted in depolarisation of the mitochondrial membrane in MCF- and MCF-12A cells. This effect was statistically significant after 18 hours in the MCF-7 and MCF-12A cell lines and became more pronounced in the MCF-7 cell line after 24 hours (Stander *et al.*, 2013). Flow cytometric analysis involves trypsinisation as well as the transferral of cells to tubes in which the cells can undergo stress and alterations (Cossarizza *et al.*, 1993). Flow cytometric analysis also involves the cells being fixed and no further changes in the cells can occur in contrast to fluorometry where cells are deprived from nutrients for the duration of the analysis.

106

The hyperpolarisation reported in the present study further contrasted previous studies which resulted in depolarisation of the membrane in SNO cells after treatment of ESE-16 (180 nM, 24 h) using the MitoTracker kit which utilizes a red MitoTracker JC-1 fluorescent dye (Wolmarans *et al.*, 2014). Mitochondrial membrane depolarisation was again previously observed after MCF-7 cells were treated with ESE-16 (180 nM, 24 h) where a two-fold increase in the number of cells showing depolarisation of the mitochondrial membrane was observed (Nkandeu *et al.*, 2013).

It was observed that after 48 hours, membrane potential depolarised but not significantly relative to the untreated control. Previous studies observed that the effect of ESE-16 on MCF-7 cells was more pronounced after 24 or 48 hours and this is similar to results from the present study with a greater depolarisation of the mitochondrial membrane after a 48 hour exposure time (Figure 3.9). In contrast to data previously presented, ESE-16 (134 nM) did not depolarise the mitochondrial membrane in MCF-7 cells to a greater extent than the positive control tamoxifen.

The results obtained also suggest the lack of selectivity of ESE-16-ol to the breast cancer MCF-7 cell line. It was noted that ESE-16 had a statistically significant depolarising effect on the MCF-12A cell line after 48 hours exposure. After 24 hours, ESE-16 significantly depolarised the mitochondrial membrane relative to the untreated control. Differences in data previously obtained and shown in Figure 3.9 could be attributed to the different experimental procedures that were carried out. Previous experiments examined membrane potential using the Mitocapture kit which makes use of a JC-1 cationic dye followed by flow cytometric analysis (www.biocat.com). The JC-1 Mitocapture dye accumulates in healthy cells producing a red fluorescence and in apoptotic cells remains in the cytoplasm produces a green fluorescence and can be detected within 30 minutes (www.biocat.com). In contrast to this, JC-1 in the present study was incubated for 2 hours which possibly could have affected the cells due to the longer period of nutrient deprivation. Data shown in Figure 3.9 is representative of fluorometric analysis with the dye JC-1. These two techniques could possible introduce variance into the results obtained due to the fact that fluorometric analysis occurs in the wells and the cells are not trypsinised or disrupted from their ideal culturing conditions (Roy and Hajnóczky, 2009).

As previously hypothesised for the combination of ESE-15-ol and 2-DG, the combined treatment of ESE-16 and 2-DG may not solely rely on mitochondrial mechanisms to elicit its anti-cancer effect. The depolarisation differences between the present and previous studies

107

could suggest that at the concentrations tested in this experiment, the compounds could elicit their effects via a pathway that is not reliant on the mitochondria and initiation of the intrinsic pathway. The observed hyperpolarisation in the present study could be attributed to the metabolic stress or altered metabolism that occurred. This could possibly indicate a stress response prior to depolarisation however further studies are required to further elucidate on this.

For this reason, autophagy as a mechanism of cell death was investigated. Previously, the studies performed above were analysed over a 72 hour incubation period in order to observe the overall effects elicited by the experimental compounds and whether or not cell death was induced

3.6 Transmission electron microscopy

Due to the cells decreasing in number when exposed for longer drug exposure times, autophagy studies were performed at 24 hours in order to observe the morphologic changes while the cells were are undergoing exposure related stress changes in contrast to the end effect elicited.

Transmission electron microscopy was used to examine ultrastructural changes of MCF-7 breast adenocarcinoma cells after 24 hours exposure to ESE-15-ol, ESE-16 and 2-DG alone and in combination. Cells were examined for changes in the cell size, membrane blebbing and integrity, vacuole formation, nuclear membrane integrity and cytoplasmic components. Whole cell digital photomicrographic images were taken at a magnification of 8000x, while intracellular structures were recorded at a magnification of 25 000x. This assay also served as a confirmation an appropriate time point at which western blot analysis was to be performed.

The untreated and vehicle control cells (DMSO and media, Chapter 2) displayed a more rounded and smoother plasma membrane with few extensions in comparison to the membranes of the cells exposed to the experimental compounds (Figure 3.10). The ultrastructure of untreated and vehicle control cells appeared relatively unaffected with "normal" nuclear and cytoplasmic components. The overall size of the cells was larger than the test compound treated cells with few signs of cellular distress such as membrane blebbing and nuclear condensation. The nuclei of untreated control cells showed indentation with two prominent nucleoli. Cytoplasmic components were abundantly present throughout the cytoplasm with little vacuole formation.

108

Treatment of MCF-7 cells with ESE-15-ol for 24 hours resulted in increased presence of microvilli on the plasma membrane, decreased cytoplasmic organelles and increased number of vacuoles (Figure 3.10). These vacuoles resembled autophagosomes containing engulfed material from the cell. Cell shrinkage was noted after treatment with 2-DG, with increased vacuole formation relative to the untreated control. A decrease in cytoplasmic organelles was also noted. The combination of ESE-15-ol with 2-DG further resulted in cellular shrinkage and distortion. Few cytoplasmic components were evident and increased vacuole formation resembled autolysosomes.

A known inducer of autophagy in MCF-7 cells, tamoxifen (Thorburn *et al.*, 2014), showed very similar ultrastructural changes to those observed in the treatment groups. These changes included increased microvilli from the membrane, disruption of the nucleus and nuclear membrane, and increased vacuole formation. The vacuoles of tamoxifen-treated cells showed engulfed material as seen in the experimental treatment groups. The double membrane vesicles resemble the structure of autophagosomes.

109

5 um

1 um

A

B

Untreated control
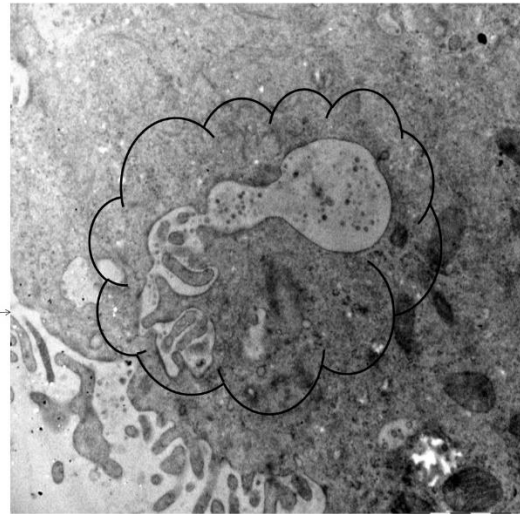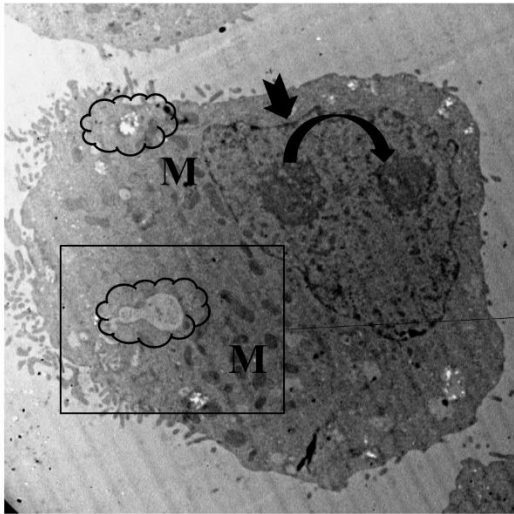
ESE-15-ol
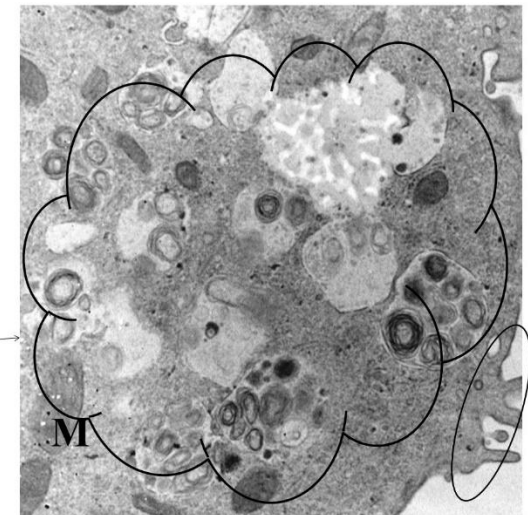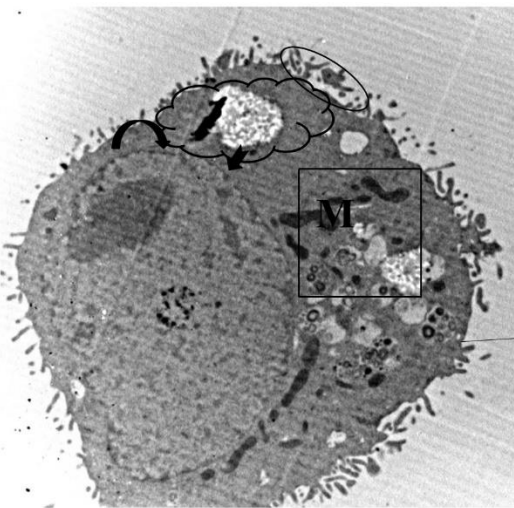
Vehicle control
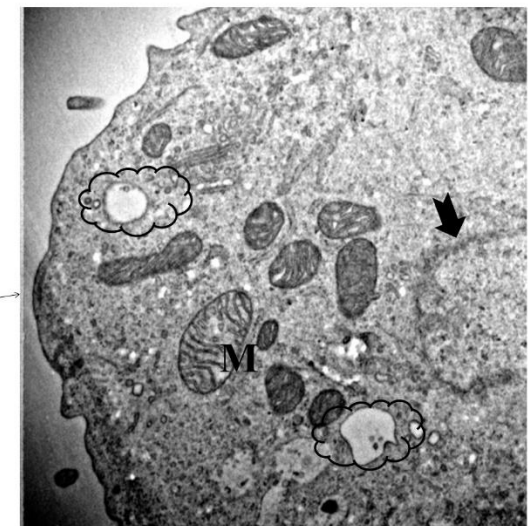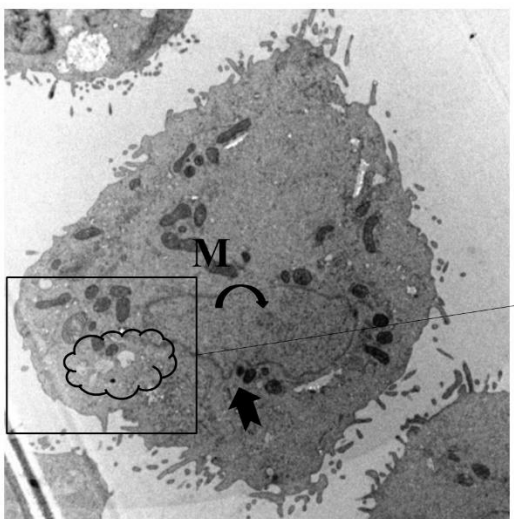
A

B

2-DG
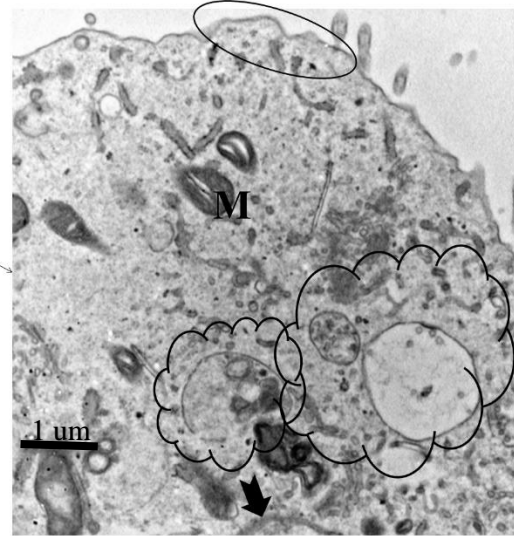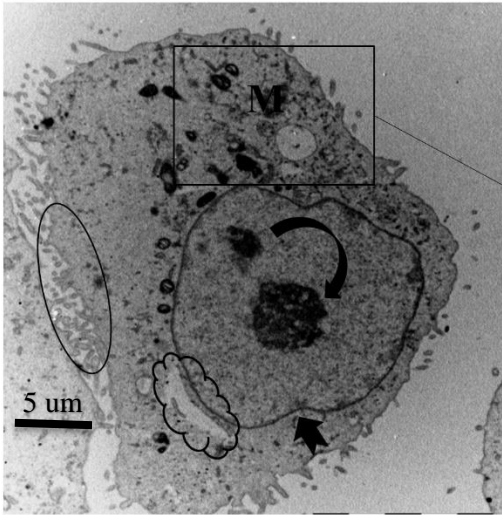
ESE-15-ol & 2-DG
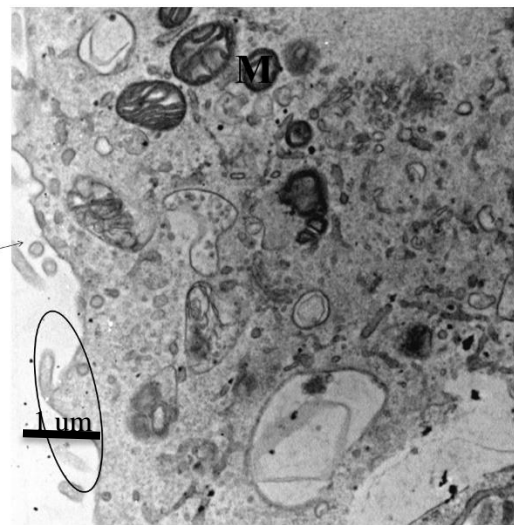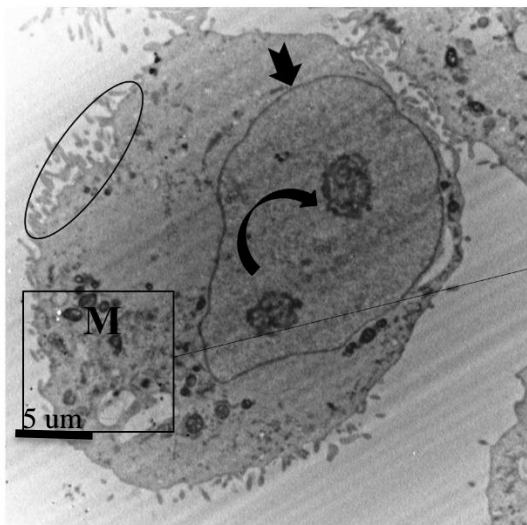
ESE-16
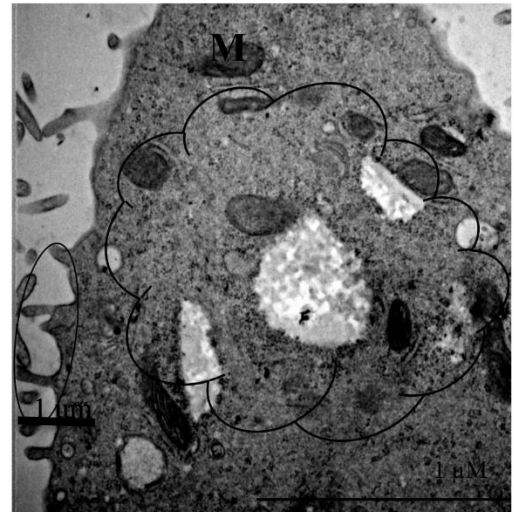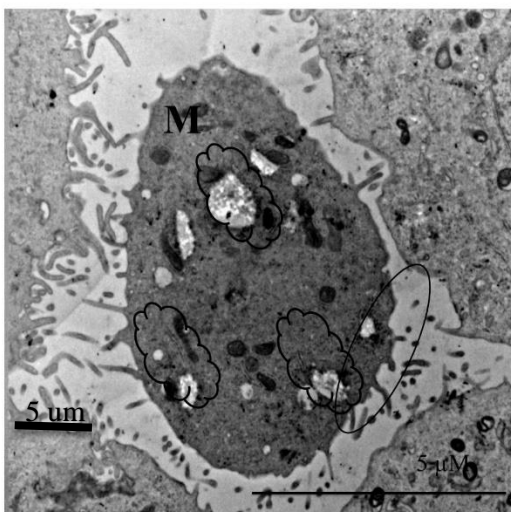
A   **B**

ESE-16 & 2-DG
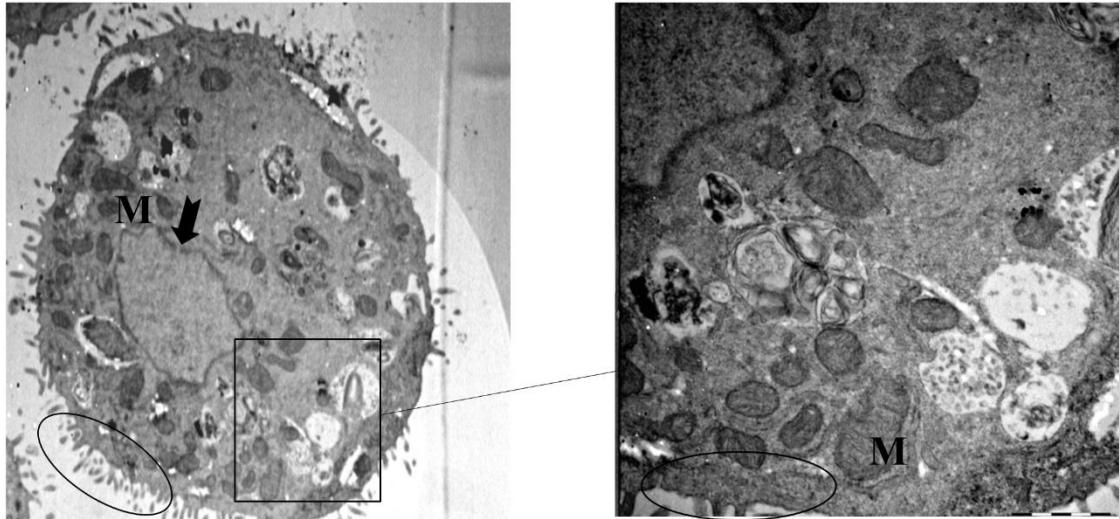
Positive control
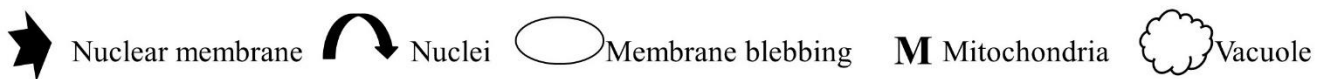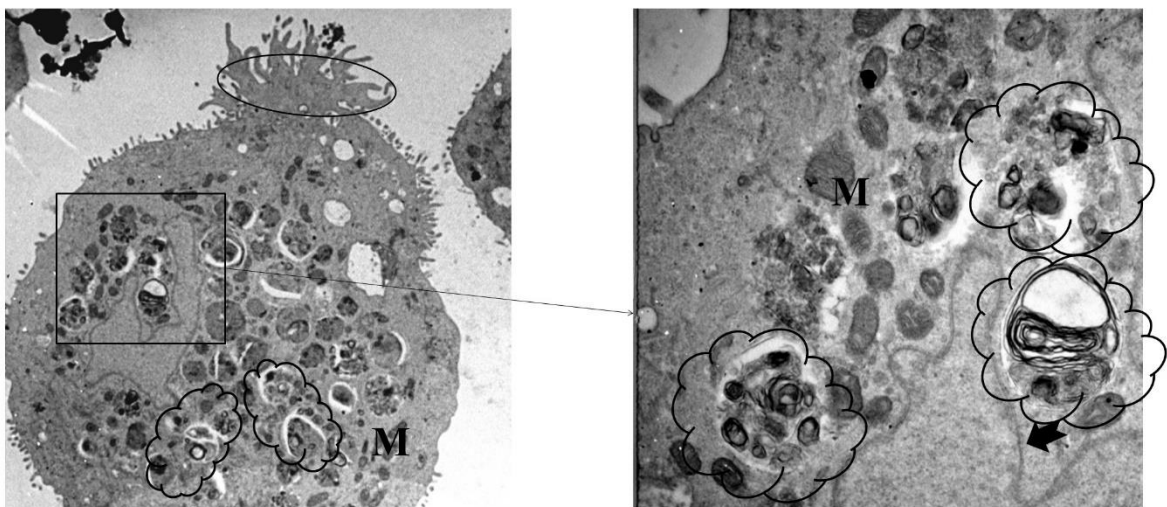
Figure 3.10 Ultrastructure of MCF-7 cells after 24hr exposure to the various treatments indicated. Mitochondrial cristae of 2-DG and 2-DG combination groups appear to show a trend of disruption. Column A shows whole cell images, column B shows ultrastructural detail of the cell in A. Subcellular structure is identified as shown in the legend at the bottom of the composite figure. Scale bars in lower magnification images represent 5 µm. Scale bars in higher magnification images represent 1µm.

Exposure of MCF-7 cells to ESE-16 for 24 hours resulted in increased microvilli from the plasma membrane as well as what appeared to be chromatin condensation. The cytoplasmic components were diminished and showed atypical shape and size with an increase in the number of vacuoles containing engulfed cytoplasmic components. The combined treatment of ESE-16 with 2-DG showed a greater effect on the cell morphology than when treated with the combination of ESE-15-ol with 2-DG. Cell shrinkage was noted, with extensive microvilli formation, a decrease in cytoplasmic organelles and hyper-condensation and fragmentation of the nucleus. The number of vacuoles was increased and typically displayed engulfed intracellular components. Vacuoles with double membranes and vesicles containing degraded components indicative of autophagosome formation were apparent.

More obvious intracellular morphological changes were observed for the combination treatments than the compounds in isolation. ESE-16 treatment had a more pronounced effect on the intracellular morphology than ESE-15-ol.

3.6.1 Discussion

In the present study, the untreated and vehicle treated controls of MCF-7 cells reported smooth plasma membranes with few protrusions from the cell membrane in comparison to the microvilli development seen in the treatment groups. The characteristics of the untreated cells were morphologically similar to previously reported observations. The ultrastructure of intracellular compartments of MCF-7 and MCF-12A cells were previously observed after treatment with 130 nM ESE-15-one alone and in combination with 7.5 mM DCA for 24 hours (Stander *et al.*, 2015). Data reported intact smooth cell membranes with little protrusions from the plasma membrane in untreated controls of both MCF-7 and MCF-12A cells.

From Figure 3.10 it was observed that the untreated control displayed morphological traits similar to those reported in literature. In Figure 3.10, the untreated as well as the vehicle control cells showed nuclear morphology with two nucleoli present which parallels data reported in previous studies. The nucleus of the untreated controls of previous studies displayed indentations with one or two nucleoli while increased numbers of mitochondria and endoplasmic reticulum were present in the cytoplasm (Stander *et al.*, 2015). Treatment with tamoxifen in the present study was reported to increase vacuole formation and resulted in distortion of the cells (Figure 3.10). This confirms results previously obtained where HeLa

113

cells treated with tamoxifen showed signs of cellular distress as well as characteristics of both apoptosis and autophagy (Theron *et al.*, 2013).

Data in the present study revealed increased vacuole formation resembling autophagosome formation as well as decreased cytoplasmic organelles after treatment with ESE-15-ol for 24 hours. These results parallel those previously reported after treatment with ESE-15-one. MCF-7 cells treated with ESE-15-one showed the formation of endosomes, autophagosomes and chromatids in metaphase (Stander *et al.*, 2015).

In the present study, ESE-15-ol and 2-DG treated cells were observed to result in cell shrinkage as well as increased vacuole formation indicative of autophagosome formation. The combined treatment of ESE-15-ol and 2-DG on MCF-7 cells showed similar morphological traits to that obtained in previous studies after the combined treatment of ESE-15-one and DCA where cell shape was distorted, marked by an increase in protrusions from the cell membrane. This combination was observed to increase vacuoles, apoptotic bodies and lysosomes and the chromatin within the nucleus displayed hyper-condensation marked by DNA fragmentation. The results obtained in the present study confirm those previously obtained and suggests that the oestrone analogues function more effectively in combination with glycolysis inhibitors with induction of ultrastructural morphological changes in the of MCF-7 cells.

In the present study, treatment with 2-DG alone displayed increased vacuole formation resembling autophagosomes similar to the effects previously reported in literature. Using TEM to assess 2-DG treatment at both 1 mM and 20 mM for 24 hours on LNCaP cells autophagy was observed to be induced. The combination of ESE-15-ol or ESE-16 with 2-DG in the present study confirms previous findings that report 2-DG to elicit a synergistic effect in combination treatments. The combination of 2-DG with metformin (5 mM) in previous studies was observed to inhibit autophagy and from this it was hypothesized that that this inhibition of autophagy could trigger apoptotic cell death in LNCaP cells (Sahra *et al.*, 2010). In contrast to previous studies using 2-DG in combination with metformin, the combination of 2-DG with the oestrone analogues ESE-15-ol or ESE-16 enhanced autophagy where increased vacuole formation, membrane protrusions and overall cell distortion was reported.

The results obtained in the present study (Figure 3.10) revealed similar ultrastructural changes after treatment with ESE-16 to that observed after treatment with the structurally similar EMBS. This similarity included increased vacuole formation relative to the untreated control. 114

Previous studies observed the effect of the oestrone analogue EMBS (0.4 µM) on the internal morphology of oestrogen receptor-positive breast adenocarcinoma MCF-7, oestrogen receptor-negative breast adenocarcinoma MDA-MB-231 and non-tumorigenic breast MCF-12A cells after 24 hours where the presence of apoptotic bodies, increased vacuole formation as well as cell debris in all three cell lines was reported (Visagie *et al.*, 2014, Visagie *et al.*, 2013).

Data reported in the present study was similar to that previously observed (Figure 3.10). The untreated and vehicle controls in the present study showed the morphological characteristics observed in previous studies such as the presence of cytoplasmic organelles with little vacuole formation. TEM has also been used to identify the presence of apoptosis and autophagy in HeLa cells after treatment with 0.5 µM ESE-16 for 24 hours (Theron *et al.*, 2013). Their data showed smooth cell membranes with few protrusions in untreated cells.

Data represented in Figure 3.10 supports the induction of autophagy reported in previous studies as ESE-16 treated cells displayed increase protrusions from the plasma membrane, chromatin condensation, as well as increased vacuole formation with engulfed material resembling what has previously been described as possible autophagosome formation. Treatment of HeLa cells with ESE-16 was previously reported to induce both apoptosis and autophagy. This was marked by increased vacuole formation, apoptotic bodies, hyper-condensation of the nucleus as well as increased protrusions from the plasma membrane (Theron *et al.*, 2013). These characteristics were further marked by an absent nuclear membrane and cell shrinkage.

Another study reported on treatment of SNO cells with a concentration of 0.2 µM ESE-16 for 24 hours with morphological analysis performed using TEM. The membrane of the nucleus was reported to have less definition than the untreated control, membrane blebbing was present on the cell membrane as well as the presence of apoptotic bodies was reported (Wolmarans *et al.*, 2014).

The effect of treatment with the combination of ESE-16 with 2-DG on MCF-7 cells on the ultracellular morphology was more pronounced in the present study than that reported in previous studies. Cellular protrusions from the membrane were more pronounced, membrane blebbing was increased as well as the presence of more vacuoles resembling autophagosomes were apparent.

115

The above mentioned morphological changes have been associated with autophagy, implying that the experimental compounds induced autophagy as a cellular response to the compounds. From this it can be speculated that the experimental compounds ESE-15-ol, ESE-16 in combination with 2-DG utilized autophagy as one of their cellular mechanisms to initiate cell death. This needed to be confirmed and the confirmation was performed by using western blotting to detect the presence of the autophagy marker LC3-II as described in the next section.

3.7 Western blot

The presence and relative quantification of LC3-II was determined using western blot analysis on MCF-7 cells after 24 hours exposure to ESE-15-ol, ESE-16 and 2-DG alone and in combination . Cellular proteins were harvested and separated by SDS gel electrophoresis followed by semi-dry transblotting onto PVDF membranes and western blotted in order to assay LC3-II.

The results are summarised in Figures 3.11 and 3.12 where the presence of the autophagic marker LC3-II after 24 hours treatment with the experimental compounds ESE-15-ol, ESE-16 and 2-DG alone or in combination are shown. Tamoxifen (10 µM, 18 h exposure), a known autophagic inducer (Kanzawa *et al.*, 2004, Stander *et al.*, 2015), was observed to display significantly higher levels of LC3-II than the untreated control (Figure 3.11). This served as an indication that the assay functioned correctly.

Treatment of MCF-7 cells with ESE-15-ol were observed to increase LC3-II levels relative to the untreated control (Figure 3.11) and a clearly visible band of LC3-II was observed on the membrane (Figure 3.12). LC3-II levels were also observed to increase relative to the untreated control after treatment with 2-DG. This increase however was slightly lower than that observed after treatment with ESE-15-ol. In Figure 3.12, LC3-II bands appeared to have relatively more intense bands after treatment with ESE-15-ol in combination with 2-DG compared to each of the compounds alone.

116
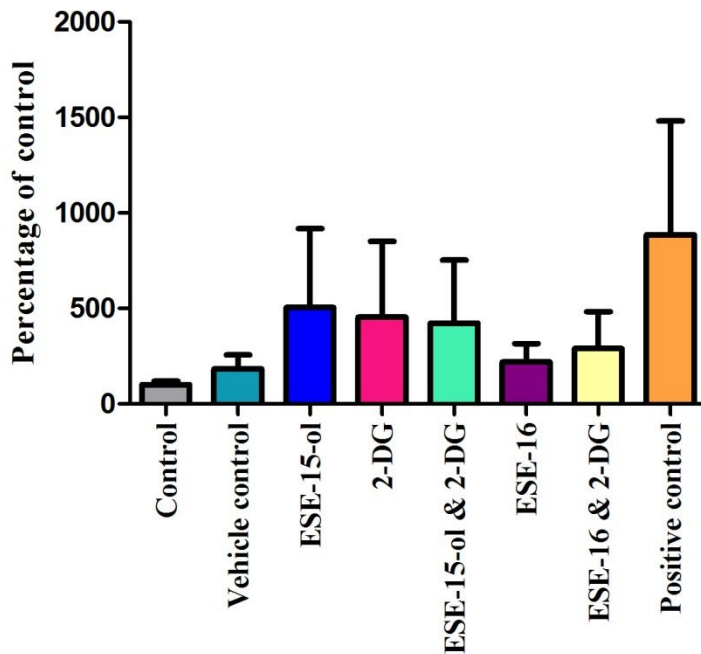
Figure 3.11 Quantification of induction of the autophagy marker LC3-II following treatment with ESE-15-ol, ESE-16 and 2-DG alone and in combination using the MCF-7 cell line. Tamoxifen was used as the positive control to induce autophagy (18 h, 10 µM). Bar graphs show the averaged results of 3 independent experiments. Statistical significance was not observed. n = 3

The relative increase in LC3-II expression after combination treatment with ESE-15-ol and 2-DG was more pronounced than that of either ESE-15-ol and 2-DG alone (Figure 3.12) however the average effect was not a statistically significant increase (Figure 3.11). Interestingly according to the combined results summarised in Figure 3.11, ESE-16 had less effect on the expression of LC3-II in comparison to ESE-15-ol. In Figure 3.12, treatment with ESE-16 was observed to show bands of hiigher intenisty in contrast than ESE-15-ol. The combination of ESE-16 and 2-DG increased LC3-II expression relative to the untreated control.

117
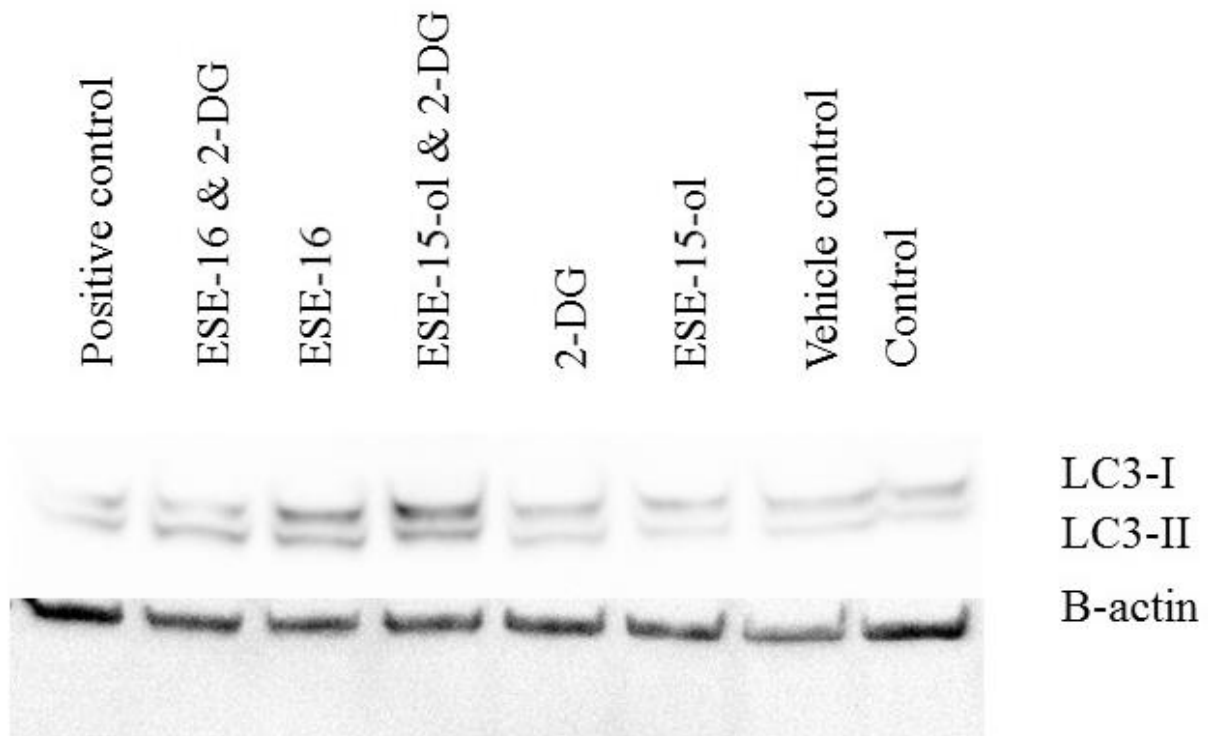
Figure 3.12 Western blot assessment of LC3-I and LC3-II levels in MCF-7 cells after 24 hours treatment with ESE-15-ol, ESE-16 and 2-DG alone and in combination. Tamoxifen was used as inducer of autophagy (10 µM, 18h) The western blot represents one of three independent experiments. n = 3

3.7.1 Discussion

In the present study ESE-15-ol was observed to increase the expression of LC3-II relative to the untreated control after 24 hours in Figure 3.11. In Figure 3.12 however it was observed that treatment of ESE-15-ol for a single run resulted in a LC3-II expression similar to the untreated control. This data parallels previous findings where gene expression analysis reported that of the 399 genes assessed in MDA-MB-231 after treatment with ESE-15-ol, the differentially expressed genes observed were linked to genes associated with autophagy (Stander *et al.*, 2012).

The increased expression of LC3-II after treatment with ESE-15-ol was amplified after combination with 2-DG (Figure 3.12). These findings are similar to results previously reported after treatment with the oestrone analogue EMBS. The combination of ESE-15-ol and 2-DG in the present study did not increase the overall LC3-II expression (Figure 3.11) as significantly as reported in previous studies. Previously, a statistically significant increase in LC3-II

118

expression of 23.2% in MCF-7 cells was reported relative to the untreated control and ESE-15-one alone after treatment with ESE-15-one (130 nM, 24 h) in combination with DCA (7.5 mM) following flow cytometric analysis. These findings suggested the increased induction of autophagy when MCF-7 cells were treated in combination with ESE-15-one and DCA. In Section 3.2 it was observed that ESE-15-ol in combination with 2-DG had little effect on the induction of late stage apoptosis. In the present study, it was however observed that ESE15-ol and 2-DG resulted in the induction of autophagy. Previous data has reported that the increased autophagy could explain the protective effect against late stage apoptosis previously observed after 24 hour exposure of the experimental compounds (Stander *et al.*, 2015).

Treatment with 2-DG in the present study increased LC3-II expression relative to the untreated control. The increase in LC3-II expression parallels previous studies that report that 2-DG (10 mM, 36 h) on mouse embryo fibroblast (MEF) cells results in the induction of autophagy as a possible mechanism of cellular death (D'Eletto *et al.*, 2009). The experimetal conditions between the present study and previous studies differ to an extent that the results cannot be directly compared however the data obtained in the present study can confirm the induction of autophagy previously reported.

A previous study also observed the effect of 5 mM 2-DG on bovine aortic endothelial cells (BAEC) after 24 hours where western blot anaysis of LC3-II expression was shown to increase. These results suggested possible induction of autophagy as a response to 2-DG treatment. The increase in LC3-II expression observed in the present study suggests that 2-DG is capable of inducing autophagy. As previously observed in Section 3.6, treatment with 2-DG was observed to result in the formation of autophagosomes. This parallels previous studies which have suggested that another possible mechanism of 2-DG is through the inhibition of the fusion of autophagosomes with lysosomes. Previous studies reported that 2-DG in combination with the lysosomal activity disrupter bafilomycin A, increased increased LC3-II expression in BAEC cells indicating that 2-DG functions by inducing the formation of autophagosomes (Wang *et al.*, 2011). The induction of autophagy noted in the present study confirmed results previously obtained after treatment of 2-DG (25 mM, 72 h) on human androgen insensitive prostate cancer (PC-3) cells (DiPaola *et al.*, 2008). The method of detection however differed from the present study as previously the fluorescent autophagic marker, green fluorescent protein microtubule-associated protein 1 light chain 3 (GFP-LC3) was utilized to detect the induction of autophagy. The results obtained in the present study further confirm previous findings where the anti-MAP

119

LC3 antibody measured an increase in LC3-II expression in human glioblastoma cell lines T98G and LN-229 after treatment of 2-DG (1.6 mM) for 24 hours. Previously it has been reported that the expression of LC3-II is evident after treatment of 1.6 mM 2-DG and increased with increasing concentration up to 50 mM 2-DG in both cell lines (Wu *et al.*, 2009). The high concentration (50 mM) of 2-DG treated would however not be physiologically or clinically relevant and therefore would nt warrant further investigation.

Treatment with ESE-16 was observed to increase the expression of LC3-II relative to the untreated control however the combined averaged effect (mean results) (Figure 3.11) was less than that of ESE-15-ol. Combination of ESE-16 and 2-DG was observed to increase LC3-II expression however it was apparent that 2-DG in combination with ESE-15-ol increased LC3-II expression to a greater extent. The results obtained in the present study support literature where the treatment of ESE-16 was reported to induce autophagy. The induction of autophagy in SNO cells after 24 hour treatment with 0.18 µM ESE-16 was also reported. This was performed via flow cytometric analysis via the Cyto-ID autophagy kit which uses a cationic amphiphilic tracer (CAT) dye and aggresome detection assay which utilizes the PROTEOSTAT dye (Enzo Life Sciences). The Cyto-ID autophagy kit functions via a fluorescent dye that selectively labels autophagosomes and evaluates autophagic flux in live cells (Www.enzolifesciences.com, 2016). The aggresome detection kit utilizes a fluorescent molecular rotor dye to determine the formation of aggresomes indicative of autophagy (www.enzolifesciences.com, 2015). Data reported an increase in the number of autophagic vacuoles and increase aggresome formation after treatment with ESE-16 for 24 hours. This confirmed morphological results previously obtained concluding that ESE-16 induces autophagy in SNO cells (Wolmarans *et al.*, 2014).

The increased LC3-II expression observed after treatment of ESE-15-ol, ESE-16 and 2-DG implies the induction of autophagy as a possible mechanism of cell death. ESE-15-ol was observed to have higher LC3-II expression than ESE-16. The combination of ESE-15-ol and 2-DG increased the expression of LC3-II by 32% relative to the combination of ESE-16 and 2-DG. From the data observed in the present study, ESE-15-ol induced the expression of LC3-II to a greater extent than ESE-16, however these experimental compounds as well as 2-DG resulted in the induction of autophagy. This further supports the morphological changes observed in Section 3.6 where morphological attributes of MCF-7 treated cells showed attributes characteristic of the induction of autophagy. From the increased LC3-II expression
120

reported as well as the autophagy like morphological attributes induced in MCF-7 cells (Section 3.6) it can be implied that treatment with the experimental compounds results in the induction of the autophagic pathway.

121

Chapter 4: Conclusion

The prevalence of cancer is rapidly increasing and multi-drug resistance to existing treatment regimens often occurs. There are currently several treatment regimens available to cancer patients however, multidrug resistance is markedly increasing leading to decreased patient five year survival rates due to therapeutic inefficacy. Patient survival can be increased through the use of combination chemotherapy. This is a useful treatment regimen to improve therapeutic efficacy of chemotherapeutic agents currently on the market and can aid in reducing side effect profiles. Drug induced toxicity can be reduced via combination therapy as chemotherapeutic agents can be used at a lower dose in combination than required for single agent dosing regimens.

The aim of this study was to investigate two oestrone analogues and the glycolysis inhibitor 2-deoxyglucose alone and in combination by measuring the effects on cytotoxicity, mitochondrial membrane potential, cell cycle arrest, cell death mechanisms through necrosis, apoptosis and autophagy using breast adenocarcinoma MCF-7 and non-tumorigenic MCF-12A cell lines in an *in vitro* setting to assess possible synergistic effects.

The aim to determine the cytotoxicity of the oestrogen analogue combinations with 2-deoxyglucose on the breast cancer MCF-7cell line and non-tumorigenic MCF-12A cell line was obtained. The compounds induced dose dependent decreases in cell number with ESE-15-ol and ESE-16 treatments which were both observed to interact synergistically with 2-DG resulting in an enhanced decrease in cell number when treated with these experimental combinations. The SRB assay was effective and gave small variance in replicate assays where a significant decrease in cell number after 72 hours treatment with ESE-15-ol, ESE-16 and 2-DG administered as single compounds was observed. ESE-16 appeared to be more cytotoxic to MCF-7 cells than ESE-15-ol and although these experimental compounds elicited cytotoxic effects on the non-tumorigenic MCF-12A cell line, the effect was less pronounced than for the MCF-7 cell line. Combination therapy of the experimental compounds with 2-DG had a marked effect on MCF-7 cells and the efficacy of these compounds in combination resulted in greater cytotoxic effect in comparison to the compounds alone. This supports previous findings where the compounds were observed to exhibit a synergistic cytotoxic effect in combination.

122

Cytotoxic effects following treatment with the experimental compounds for 72 hours appeared to follow induction of apoptosis. This leads to the aim of investigating the mechanistic properties of the synergistic combinations with regards to the mode of cell death. Treatment with ESE-15-ol had no significant effect on the decrease of cell viability however, the effect was remarkably increased after addition of 2-DG. A necrotic as well as apoptotic response was noted after treatment with ESE-16 and the combination of ESE-16 and 2-DG not only significantly decreased cell viability but also increased apoptosis in MCF-7 treated cells. MCF-12A cells were less sensitive to treatment with ESE-15-ol and 2-DG however, the combination of ESE-16 and 2-DG resulted in a significant decline in cell viability of MCF-12A cells in comparison to MCF-7 cells. The majority of anti-neoplastics induce apoptosis and it has been proposed that defects in this pathway could be linked to treatment failure in cancer patients. Within a clinical setting, chemotherapy and radiation have been observed to result in cell death that is morphologically characteristic of apoptosis (Lowe and Lin, 2000). In the present study, treatment of ESE-16 in combination with 2-DG resulted in the induction of apoptosis as a mechanism of cell death. This induction of apoptosis could possibly be a promising anti-cancer treatment regimen to overcome treatment failure observed in current patients.

The induction of apoptosis was further illustrated morphologically after light and PlasDIC microscopy where cell density was compromised to a larger extent in ESE-16 treated cells in contrast to ESE-15-ol cells. The combination of the oestrone analogues with 2-DG induced several morphological changes that were indicative of apoptosis and cell stress. Cell density was severely compromised in combination treatment groups relative to isolated treatment groups.

The mechanistic properties of the synergistic combinations were investigated with regards to cell cycle arrest. Percentage viability of MCF-7 and MCF-12A cells were observed to have altered relative to the untreated control and shifts in cell cycle progression were noted. Following treatment with ESE-15-ol, an increase in the G1 phase was noted which could possibly be attributed to a G1 block however, this increase was not significant enough to confirm this.

In contrast to ESE-15-ol possibly inducing a G1 block, when treated in combination with 2-DG a G2/M block was induced. The ability to induce a shift from a G1 to a G2 block is important in anti-cancer therapy as cells that overcome or evade the G1 block will be arrested

123

in G2 resulting in halted cell proliferation. Treatment of ESE-16 resulted in a higher accumulation of the sub-G1 phase paralleling the increased percentage of cells in the apoptotic phase of apoptosis/necrosis studies. Further, ESE-16 alone and in combination with 2-DG resulted in accumulation in the S/G2 phase of the cell cycle. From this it can be hypothesized that the combination of 2-DG with the oestrone analogues is a more effective cell cycle inhibitor than the compounds in isolation.

The initiation of the intrinsic apoptotic pathway is marked by the release of cytochrome c from the mitochondria resulting from depolarisation of the mitochondrial membrane potential providing a direct link between mitochondrial membrane potential and the apoptotic pathway. Apoptosis studies performed after 72 hours treatment demonstrated apoptotic effects for the experimental compounds in combination. The possible involvement of the mitochondria as a mechanistic property of the synergistic combinations was therefore assessed. Mitochondrial membrane potential studies were performed at 24 and 48 hours treatment periods in order to observe the effect the compounds elicited on the membrane potential over an extended exposure time. Slight depolarisation in membrane potential was apparent after treatment for 24 hours with ESE-15-ol, ESE-16 and 2-DG alone and in combination. After 48 hours, further depolarisation was noted however to a lesser extent than expected relative to the percentages of apoptosis previously observed. Significant depolarisation of the membrane potential was however observed after 48 hour exposure of the experimental compounds on the MCF-12A cell line. It is a possibility that the induction of apoptosis following treatment of the experimental compounds only partially initiates the intrinsic pathway and mitochondrial involvement, however, this would need to be confirmed through further studies. This aims at further experimental studies to examine the possibility that the experimental compounds could elicit their effects via extrinsic apoptotic and autophagic pathways.

Due to the possible involvement of autophagy as a mechanistic property, transmission electron microscopy was performed in order to identify morphological changes in the cells after treatment with the experimental compounds. The involvement of autophagic pathways was observed after relative quantitative and morphological analysis of the MCF-7 breast cancer cell line after 24 hours treatment period. Ultrastructural changes in MCF-7 cells included the increased formation of multi-membranous vacuoles indicative of autophagosomes after treatment with ESE-15-ol, ESE-16 and 2-DG. Supporting the effect elicited in apoptosis, and cell cycle results in the present study, the combination of the oestrone analogues with 2-DG

124

were observed to elicit a synergistic effect. LC3-II expression was increased in all treatment groups and interestingly, a more pronounced effect was noted after treatment with ESE-15-ol in combination with 2-DG in contrast to ESE-16. This could possibly suggest that ESE-15-ol elicits its cytotoxic effects via autophagic pathways in contrast to ESE-16 which appeared to favour apoptotic/necrotic pathways, however based on the experiments performed in the present study, this claim cannot be confirmed. The combination of the oestrone analogues with 2-DG did not appear to result in a marked increased LC3-II expression relative to that previously observed in cell viability and apoptotic studies.

Studies have previously described the link between autophagic and apoptotic pathways (Wolmarans *et al.*, 2014). It has been reported that apoptotic machinery regulating apoptosis can control autophagy and visa versa. Previous studies have claimed that this can possibly result in combined autophagy and apoptosis or that the cells are capable of mutually exclusively switching between these two mechanisms. This mechanistic switching is therefore a possible explanation for the initiation of apoptosis and autophagy after treatment with ESE-15-ol and ESE-16 and could possibly explain the preference for autophagy in ESE-15-ol treated cells and for apoptosis/necrosis in ESE-16 treated cells.

The cytotoxicity of the oestrogen analogue combinations with 2-deoxyglucose on the breast cancer MCF-7cell line and non-tumorigenic MCF-12A cell line were established and the mechanistic properties of the synergistic combinations with regards to the involvement of the mitochondria, the induction of autophagy, cell cycle phase arrest and mode of cell death were established.

The data reported in this study provides potential insights into the combination of oestrone analogues with the glycolytic inhibitor, 2-DG as an effective treatment regimen for targeted therapy. The combination of anti-mitotic compounds with glycolytic inhibitors leads to the possibility of not only inducing several pathways of cell death but resulting in a shift from G1 to a G2 arrest of the cell cycle. Often the G1-cyclins are not destroyed and their accumulation results in an increase in the G1-Cdk activity. This results in the escape of cells from the G1 to the S phase of the cell cycle. This plays a significant role as cells that are capable of overcoming a G1 block will undergo further arrest.

The synthesis and use of novel compounds is a grower area within research and the basis of many studies. It is however important that these novel treatment regimens are optimised
125

enabling effective treatment regimens and ultimately so that the desired therapeutic responses can be obtained (Yaacob *et al.*, 2014). The combination of novel compounds with existing compounds offers a beneficial prospective to chemotherapeutic development however the efficacy of the compounds in relation to the side effects profile needs to be consistently monitored and optimised. The oestrone analogues ESE-15-ol and ESE-16 have displayed promising mechanistic properties for the treatment of cancer cells and warrant further investigation.

4.1 Study limitations

A major limitation in the present study was the 2% FCS concentration used. The low FCS concentration was introduced due to the effect of the steroid binding effects. The lower concentration of FCS used could account for the increased sensitivity of the cells to the experimental compounds and the differences noted between the present study and previous studies. The increased sensitivity is possibly due to the decreased growth factors which affects the cells capability to grow optimally. The effect could also be due to less binding by the steroid binding proteins in the media. The MCF-7 cell line was very susceptible to changes in the concentration of FCS in the growth media. The initial 2% FCS concentration was not sufficient to sustain the cells prior to and following synchronisation. After a 48 hour nutrient deprivation the cells did not recover and were not able to reattach. Cell viability significantly decreased after nutrient deprivation and a low number of cells were available that did not meet the cell concentration required for the assay.

A complete and more accurate representation of the efficacy of the treatment combinations could be attained via the addition of a third cell line such as the MDA-MB-231 cell line. This is an estrogen receptor negative cell line in contrast to the estrogen receptor positive MCF-7 cell line that was used in this study. The addition of an extra non-tumorigenic cell line such as the human umbilical vein endothelial EA.HY926 cell line would be beneficial as the effect that the compounds elicit on normal cells could be further investigated.

The induction of the apoptotic pathway was observed after treatment with the experimental compounds. The involvement of the mitochondria was however not as expected suggesting the possible role of the induction of the extrinsic apoptotic pathway in contrast to the intrinsic pathway. 2-ME has been shown to result in the induction of the extrinsic pathway (LaVallee *et*

126

al., 2003) and ESE-15-ol and ESE-16 are analogues of this compound which could suggest possibly similar mechanisms of action. From Annexin V-FITC and PI the results obtained did not initiate apoptosis at a rate that was expected however the concentration of ESE-15-ol tested was lower than that tested in previous studies and as previously mentioned, the concentration of FCS was lower. In addition to this, Annexin V-FITC and PI it cannot be used to determine which pathway is being initiated. The investigation of caspases and caspase activity or inhibition could be a useful additive to this study in order to obtain further insight into the exact pathway that is triggered in response to the experimental compounds.

Data indicated autophagy could be involved as a cell response after treatment with the experimental compounds however it cannot be distinguished whether treatment results in autophagosome upregulation or whether the recycling of autophagic components is blocked. The addition of lysosomal protease inhibitors would allow for this parameter to be distinguished as the accumulation of LC3-II would then imply the upregulation of autophagosomes (Barth *et al.*, 2010). If LC3-II levels remain constant in the presence of these inhibitors it can then be distinguished that that autophagosome accumulation occurred due to the break down process being inhibited (Barth *et al.*, 2010).

Despite the limitations encountered in this study, the results produced were reproducible, consistent and provided various prospectives for future research.

4.2 Future prospective for research

Studies conducted on the mechanistic properties of the oestrone analogues, ESE-15-ol and ESE-16 are still premature in nature. Although extensive research has already been done there are many future prospectives for these compounds. The ideal concentration to elicit therapeutic efficacy is an important aspect for the future development of these compounds. Although there is a basic understanding of the mechanistic properties of these novel oestrone analogues, their use *in vivo* needs to be elucidated.

Animal models provide information that is translatable to a clinical environment and the pharmacokinetic profiles of these compounds needs to be attained. Animal studies must be carried out prior to clinical trials and provides important benefits due to the fact that it provides a basis to significantly improve the status of human health care. From this, no unnecessary suffering results and data obtained from such studies can then further be translated into a

127

clinical setting (Perel *et al.*, 2007). Potent antitumor activity has previously been demonstrated in tumour-bearing mice using this method at doses of 2-ME ranging from 50-400 mg/kg/day (Perel *et al.*, 2007). The most sensitive quantitative method to analyse samples extracted from such studies is liquid chromatography mass spectrometry (LC-MS/MS) whereby analytes are separated on a mass to charge ratio (Matuszewski *et al.*, 1998). This technique has been identified as the method of choice to support *in vitro*, as well as *in vivo* pharmacokinetic studies (Matuszewski *et al.*, 1998).

The data reported in this study provide potential insights into the combination of novel oestrone analogues with the glycolytic inhibitor 2-DG as an effective treatment regimen for targeted therapy. The combination of anti-mitotic compounds with glycolytic inhibitors leads to the possibility of not only inducing several pathways as a mechanism of cell death but initiating a G2 arrest instead of a G1 arrest. The *in vitro* efficacy of new drug-like compounds appears to be extensively studied however treatment regimens need to be optimised for the effective treatment of cancer. The combination of novel compounds with existing compounds offers a beneficial prospective to chemotherapeutic development however, the efficacy of the compounds versus the potential side effects need to be monitored and optimised. For this reason together with the data reported in this study, the novel oestrone analogues ESE-15-ol and ESE-16 warrant further investigation.

128

References

Abou-Jawde, R., Choueiri, T., Alemany, C. & Mekhail, T. 2003. An overview of targeted treatments in cancer. *Clinical therapeutics,* 25 number**,** 2121-2137.

Adams, J. M. & Cory, S. 1998. The bcl-2 protein family: Arbiters of cell survival. *Science,* 281 number**,** 1322-1326.

Agarwal, R., Gonzalez-Angulo, A.-M., Myhre, S., Carey, M., Lee, J.-S., Overgaard, J., Alsner, J., Stemke-Hale, K., Lluch, A. & Neve, R. M. 2009. Integrative analysis of cyclin protein levels identifies cyclin b1 as a classifier and predictor of outcomes in breast cancer. *Clinical Cancer Research,* 15 number**,** 3654-3662.

Akilesh, S., Juaire, N., Duffield, J. S. & Smith, K. D. 2014. Chronic ifosfamide toxicity: Kidney pathology and pathophysiology. *American Journal of Kidney Diseases,* 63 number**,** 843-850.

Alayev, A., Berger, S. M., Kramer, M. Y., Schwartz, N. S. & Holz, M. K. 2015. The combination of rapamycin and resveratrol blocks autophagy and induces apoptosis in breast cancer cells. *Journal of cellular biochemistry,* 116 number**,** 450-457.

Aloia, T., Sebagh, M., Plasse, M., Karam, V., Lévi, F., Giacchetti, S., Azoulay, D., Bismuth, H., Castaing, D. & Adam, R. 2006. Liver histology and surgical outcomes after preoperative chemotherapy with fluorouracil plus oxaliplatin in colorectal cancer liver metastases. *Journal of Clinical Oncology,* 24 number**,** 4983-4990.

Amorino, G. P., Freeman, M. L. & Choy, H. 2000. Enhancement of radiation effects in vitro by the estrogen metabolite 2-methoxyestradiol. *Radiation research,* 153 number**,** 384-391.

Arnold, L. D., Ji, Q.-S., Buck, E., Haley, J. D. & Mulvihill, M. J. 2013. Combination cancer therapy. Google Patents.

Arstila, A. U. & Trump, B. F. 1968. Studies on cellular autophagocytosis. The formation of autophagic vacuoles in the liver after glucagon administration. *The American journal of pathology,* 53 number**,** 687.

Baehrecke, E. H. 2005. Autophagy: Dual roles in life and death? *Nature reviews Molecular cell biology,* 6 number**,** 505-510.

Barth, S., Glick, D. & Macleod, K. F. 2010. Autophagy: Assays and artifacts. *The Journal of pathology,* 221 number**,** 117-124.

Bauer, K. R., Brown, M., Cress, R. D., Parise, C. A. & Caggiano, V. 2007. Descriptive analysis of estrogen receptor (er)-negative, progesterone receptor (pr)-negative, and her2-negative invasive breast cancer, the so-called triple-negative phenotype. *Cancer,* 109 number**,** 1721-1728.

Beier, R., Bürgin, A., Kiermaier, A., Fero, M., Karsunky, H., Saffrich, R., Möröy, T., Ansorge, W., Roberts, J. & Eilers, M. 2000. Induction of cyclin e–cdk2 kinase activity, e2f-dependent

129

transcription and cell growth by myc are genetically separable events. *The EMBO journal,* 19 number**,** 5813-5823.

Ben Sahra, I., Tanti, J.-F. & Bost, F. 2010. The combination of metformin and 2 deoxyglucose inhibits autophagy and induces ampk-dependent apoptosis in prostate cancer cells. *Autophagy,* 6 number**,** 670-671.

Binkhathlan, Z. & Alshamsan, A. 2012. Emerging nanodelivery strategies of rnai molecules for colon cancer therapy: Preclinical developments. *Therapeutic delivery,* 3 number**,** 1117-1130.

Birsoy, K., Wang, T., Chen, W. W., Freinkman, E., Abu-Remaileh, M. & Sabatini, D. M. 2015. An essential role of the mitochondrial electron transport chain in cell proliferation is to enable aspartate synthesis. *Cell,* 162 number**,** 540-551.

Bissell, M. J. & Radisky, D. 2001. Putting tumours in context. *Nature Reviews Cancer,* 1 number**,** 46-54.

Blackmore, J. K., Karmakar, S., Gu, G., Chaubal, V., Wang, L., Li, W. & Smith, C. L. 2014. The smrt coregulator enhances growth of estrogen receptor-α-positive breast cancer cells by promotion of cell cycle progression and inhibition of apoptosis. *Endocrinology,* 155 number**,** 3251-3261.

Blecher, E., Chaney-Graves, K., Desantis, C., Ferlay, J., Forman, D., Grey, N., Mcmikel, A., Mcneal, B., O'brien, M. & Loyce Pace. 2008. *Cancer in africa* [Online]. Available: http://www.cancer.org/acs/groups/content/@epidemiologysurveilance/documents/document/acspc-031574.pdf [Accessed 26 April 2016].

Boatright, K. M., Renatus, M., Scott, F. L., Sperandio, S., Shin, H., Pedersen, I. M., Ricci, J.-E., Edris, W. A., Sutherlin, D. P. & Green, D. R. 2003. A unified model for apical caspase activation. *Molecular cell,* 11 number**,** 529-541.

Boatright, K. M. & Salvesen, G. S. 2003. Mechanisms of caspase activation. *Current opinion in cell biology,* 15 number**,** 725-731.

Bokemeyer, C., Berger, C. C., Kuczyk, M. A. & Schmoll, H.-J. 1996. Evaluation of long-term toxicity after chemotherapy for testicular cancer. *Journal of Clinical Oncology,* 14 number**,** 2923-2932.

Boon, T., Coulie, P. G. & Van Den Eynde, B. 1997. Tumor antigens recognized by t cells. *Immunology today,* 18 number**,** 267-268.

Bray, F., Jemal, A., Grey, N., Ferlay, J. & Forman, D. 2012. Global cancer transitions according to the human development index (2008–2030): A population-based study. *The lancet oncology,* 13 number**,** 790-801.

Brodows, R. G., Pi-Sunyer, F. X. & Campbell, R. G. 1975. Sympathetic control of hepatic glycogenolysis during glucopenia in man. *Metabolism,* 24 number**,** 617-624.

130

Bubert, C., Leese, M. P., Mahon, M. F., Ferrandis, E., Regis-Lydi, S., Kasprzyk, P. G., Newman, S. P., Ho, Y. T., Purohit, A. & Reed, M. J. 2007. 3, 17-disubstituted 2-alkylestra-1, 3, 5 (10)-trien-3-ol derivatives: Synthesis, in vitro and in vivo anti-cancer activity. *Journal of medicinal chemistry,* 50 number**,** 4431-4443.

Burghardt, R. C. & Droleskey, R. 2006. Transmission electron microscopy. *Current protocols in microbiology,* number**,** 2B. 1.1-2B. 1.39.

Cadenas, E. & Davies, K. J. 2000. Mitochondrial free radical generation, oxidative stress, and aging. *Free Radical Biology and Medicine,* 29 number**,** 222-230.

Cairns, R. A., Harris, I. S. & Mak, T. W. 2011. Regulation of cancer cell metabolism. *Nature Reviews Cancer,* 11 number**,** 85-95.

Carothers, A., Hughes, S., Ortega, D. & Bertagnolli, M. 2002. 2-methoxyestradiol induces p53-associated apoptosis of colorectal cancer cells. *Cancer letters,* 187 number**,** 77-86.

Chaabane, W., User, S. D., El-Gazzah, M., Jaksik, R., Sajjadi, E., Rzeszowska-Wolny, J. & Łos, M. J. 2013. Autophagy, apoptosis, mitoptosis and necrosis: Interdependence between those pathways and effects on cancer. *Archivum immunologiae et therapiae experimentalis,* 61 number**,** 43-58.

Chander, S., Foster, P., Leese, M. P., Newman, S., Potter, B. V., Purohit, A. & Reed, M. 2007. In vivo inhibition of angiogenesis by sulphamoylated derivatives of 2-methoxyoestradiol. *British journal of cancer,* 96 number**,** 1368-1376.

Charlot, J., Pretet, J., Haughey, C. & Mougin, C. 2004. Mitochondrial translocation of p53 and mitochondrial membrane potential ($\delta\psi$m) dissipation are early events in staurosporine-induced apoptosis of wild type and mutated p53 epithelial cells. *Apoptosis,* 9 number**,** 333-343.

Chen, V., Staub, R. E., Fong, S., Tagliaferri, M., Cohen, I. & Shtivelman, E. 2012. Bezielle selectively targets mitochondria of cancer cells to inhibit glycolysis and oxphos. *PloS one,* 7 number**,** e30300.

Chen, W. W., Birsoy, K., Mihaylova, M. M., Snitkin, H., Stasinski, I., Yucel, B., Bayraktar, E. C., Carette, J. E., Clish, C. B. & Brummelkamp, T. R. 2014. Inhibition of atpif1 ameliorates severe mitochondrial respiratory chain dysfunction in mammalian cells. *Cell reports,* 7 number**,** 27-34.

Chen, Z., Lu, W., Garcia-Prieto, C. & Huang, P. 2007. The warburg effect and its cancer therapeutic implications. *Journal of bioenergetics and biomembranes,* 39 number**,** 267-274.

Cheng, G., Zielonka, J., Dranka, B. P., Mcallister, D., Mackinnon, A. C., Joseph, J. & Kalyanaraman, B. 2012. Mitochondria-targeted drugs synergize with 2-deoxyglucose to trigger breast cancer cell death. *Cancer Research,* 72 number**,** 2634-2644.

131

Cheong, J.-H., Park, E. S., Liang, J., Dennison, J. B., Tsavachidou, D., Nguyen-Charles, C., Cheng, K. W., Hall, H., Zhang, D. & Lu, Y. 2011. Dual inhibition of tumor energy pathway by 2-deoxyglucose and metformin is effective against a broad spectrum of preclinical cancer models. *Molecular cancer therapeutics,* 10 number**,** 2350-2362.

Chicheportiche, Y., Bourdon, P. R., Xu, H., Hsu, Y.-M., Scott, H., Hession, C., Garcia, I. & Browning, J. L. 1997. Tweak, a new secreted ligand in the tumor necrosis factor family that weakly induces apoptosis. *Journal of Biological Chemistry,* 272 number**,** 32401-32410.

Chinnaiyan, A. M. 1999. The apoptosome: Heart and soul of the cell death machine. *Neoplasia,* 1 number**,** 5-15.

Chipuk, J. 2014. Anti-apoptotic bcl-2 proteins govern cellular outcome following b-raf v600e inhibition and can be targeted to reduce resistance. *Oncogene,* 1 number**,** 11.

Chou, T.-C. 2006. Theoretical basis, experimental design, and computerized simulation of synergism and antagonism in drug combination studies. *Pharmacological reviews,* 58 number**,** 621-681.

Chu, R. L., Post, D. E., Khuri, F. R. & Van Meir, E. G. 2004. Use of replicating oncolytic adenoviruses in combination therapy for cancer. *Clinical Cancer Research,* 10 number**,** 5299-5312.

Codogno, P. & Meijer, A. J. 2005. Autophagy and signaling: Their role in cell survival and cell death. *Cell Death & Differentiation,* 12 number**,** 1509-1518.

Coley, H. M. 2010. Overcoming multidrug resistance in cancer: Clinical studies of p-glycoprotein inhibitors. *Multi-drug resistance in cancer.* Springer.

Colotta, F., Allavena, P., Sica, A., Garlanda, C. & Mantovani, A. 2009. Cancer-related inflammation, the seventh hallmark of cancer: Links to genetic instability. *Carcinogenesis,* 30 number**,** 1073-1081.

Conte, P. & Guarneri, V. 2004. Safety of intravenous and oral bisphosphonates and compliance with dosing regimens. *The oncologist,* 9 number**,** 28-37.

Cossarizza, A., Baccaranicontri, M., Kalashnikova, G. & Franceschi, C. 1993. A new method for the cytofluorometric analysis of mitochondrial membrane potential using the j-aggregate forming lipophilic cation 5, 5′, 6, 6′-tetrachloro-1, 1′, 3, 3′-tetraethylbenzimidazolcarbocyanine iodide (jc-1). *Biochemical and biophysical research communications,* 197 number**,** 40-45.

Costa, R., Romagna, C., Pereira, J. & Souza-Pinto, N. 2011. The role of mitochondrial DNA damage in the citotoxicity of reactive oxygen species. *Journal of bioenergetics and biomembranes,* 43 number**,** 25-29.

D'amato, S. 2008. Improving patient adherence with oral chemotherapy. Available: https://www.accc-cancer.org/oncology_issues/articles/JA08/JA08-Improving-Patient-Adherence-with-Oral-Chemotherapy.pdf [Accessed 12 February 2016].

132

D'eletto, M., Grazia Farrace, M., Falasca, L., Reali, V., Oliverio, S., Melino, G., Griffin, M., Fimia, G. M. & Piacentini, M. 2009. Transglutaminase 2 is involved in autophagosome maturation. *Autophagy,* 5 number**,** 1145-1154.

Dahut, W. L., Lakhani, N. J., Gulley, J. L., Arlen, P. M., Kohn, E. C., Kotz, H., Mcnally, D., Parr, A., Parr, A. & Nguyen, D. 2006. Phase i clinical trial of oral 2-methoxyestradiol, an antiangiogenic and apoptotic agent, in patients with solid tumors. *Cancer biology & therapy,* 5 number**,** 22-27.

Danial, N. N. & Korsmeyer, S. J. 2004. Cell death: Critical control points. *Cell,* 116 number**,** 205-219.

Darzynkiewicz, Z., Bruno, S., Del Bino, G., Gorczyca, W., Hotz, M., Lassota, P. & Traganos, F. 1992. Features of apoptotic cells measured by flow cytometry. *Cytometry,* 13 number**,** 795-808.

Darzynkiewicz, Z., Traganos, F. & Melamed, M. R. 1980. New cell cycle compartments identified by multiparameter flow cytometry. *Cytometry,* 1 number**,** 98-108.

Davey, H. M. & Hexley, P. 2011. Red but not dead? Membranes of stressed saccharomyces cerevisiae are permeable to propidium iodide. *Environmental microbiology,* 13 number**,** 163-171.

De Jong, S., Holtrop, M., De Vries, H., De Vries, E. & Mulder, N. 1992. Increased sensitivity of an adriamycin-resistant human small cell lung carcinoma cell line to mitochondrial inhibitors. *Biochemical and biophysical research communications,* 182 number**,** 877-885.

Deberardinis, R. J., Lum, J. J., Hatzivassiliou, G. & Thompson, C. B. 2008. The biology of cancer: Metabolic reprogramming fuels cell growth and proliferation. *Cell metabolism,* 7 number**,** 11-20.

Dipaola, R. S., Dvorzhinski, D., Thalasila, A., Garikapaty, V., Doram, D., May, M., Bray, K., Mathew, R., Beaudoin, B. & Karp, C. 2008. Therapeutic starvation and autophagy in prostate cancer: A new paradigm for targeting metabolism in cancer therapy. *The Prostate,* 68 number**,** 1743.

Doweiko, H. 2011. *Concepts of chemical dependency*, Nelson Education.

Dröse, S. & Brandt, U. 2012. Molecular mechanisms of superoxide production by the mitochondrial respiratory chain. *Mitochondrial oxidative phosphorylation.* Springer.

Dröse, S., Hanley, P. J. & Brandt, U. 2009. Ambivalent effects of diazoxide on mitochondrial ros production at respiratory chain complexes i and iii. *Biochimica et Biophysica Acta (BBA)-General Subjects,* 1790 number**,** 558-565.

Duke, W., Hirschowitz, B. & Sachs, G. 1965. Vagal stimulation of gastric secretion in man by 2-deoxy-d-glucose. *The Lancet,* 286 number**,** 871-876.

Dunn, W. 1990. Studies on the mechanisms of autophagy: Formation of the autophagic vacuole. *The Journal of cell biology,* 110 number**,** 1923-1933.

133

Dwarakanath, B., Singh, D., Banerji, A. K., Sarin, R., Venkataramana, N., Jalali, R., Vishwanath, P., Mohanti, B., Tripathi, R. & Kalia, V. 2009. Clinical studies for improving radiotherapy with 2-deoxy-d-glucose: Present status and future prospects. *Journal of cancer research and therapeutics,* 5 number**,** 21.

Ebato, C., Uchida, T., Arakawa, M., Komatsu, M., Ueno, T., Komiya, K., Azuma, K., Hirose, T., Tanaka, K. & Kominami, E. 2008. Autophagy is important in islet homeostasis and compensatory increase of beta cell mass in response to high-fat diet. *Cell metabolism,* 8 number**,** 325-332.

Edsall, A. B., Mohanakrishnan, A. K., Yang, D., Fanwick, P. E., Hamel, E., Hanson, A. D., Agoston, G. E. & Cushman, M. 2004. Effects of altering the electronics of 2-methoxyestradiol on cell proliferation, on cytotoxicity in human cancer cell cultures, and on tubulin polymerization. *Journal of medicinal chemistry,* 47 number**,** 5126-5139.

Elger, W., Schwarz, S., Hedden, A., Reddersen, G. & Schneider, B. 1995. Sulfamates of various estrogens are prodrugs with increased systemic and reduced hepatic estrogenicity at oral application. *The Journal of steroid biochemistry and molecular biology,* 55 number**,** 395-403.

Elledge, S. J. 1996. Cell cycle checkpoints: Preventing an identity crisis. *Science,* 274 number**,** 1664-1672.

Elmore, S. 2007. Apoptosis: A review of programmed cell death. *Toxicologic pathology,* 35 number**,** 495-516.

Emamzadeh, R., Nazari, M. & Najafzadeh, S. 2014. Adherent state apoptosis assay (asa): A fast and reliable method to detect apoptosis in adherent cells. *Analytical Methods,* 6 number**,** 4199-4204.

Eskelinen, E.-L. 2005. Maturation of autophagic vacuoles in mammalian cells. *Autophagy,* 1 number**,** 1-10.

Eskelinen, E.-L. 2008. New insights into the mechanisms of macroautophagy in mammalian cells. *International review of cell and molecular biology,* 266 number**,** 207-247.

Eskelinen, E.-L. 2008. To be or not to be? Examples of incorrect identification of autophagic compartments in conventional transmission electron microscopy of mammalian cells. *Autophagy,* 4 number**,** 257-260.

Esslinger, M. & Gross, H. 2015. Simulation of differential interference contrast microscopy and influence of aberrations. *Journal of Microscopy,* number.

Facchini, L. M. & Penn, L. Z. 1998. The molecular role of myc in growth and transformation: Recent discoveries lead to new insights. *The FASEB Journal,* 12 number**,** 633-651.

134

Fagius, J. & Berne, C. 1989. Changes of sympathetic nerve activity induced by 2-deoxy-d-glucose infusion in humans. *American Journal of Physiology-Endocrinology And Metabolism,* 256 number**,** E714-E720.

Fendt, S.-M., Bell, E. L., Keibler, M. A., Davidson, S. M., Wirth, G. J., Fiske, B., Mayers, J. R., Schwab, M., Bellinger, G. & Csibi, A. 2013. Metformin decreases glucose oxidation and increases the dependency of prostate cancer cells on reductive glutamine metabolism. *Cancer research,* 73 number**,** 4429-4438.

Foote Jr, F. W. & Stewart, F. W. 1941. Lobular carcinoma in situ: A rare form of mammary cancer. *The American journal of pathology,* 17 number**,** 491.

Foulkes, W. D., Stefansson, I. M., Chappuis, P. O., Bégin, L. R., Goffin, J. R., Wong, N., Trudel, M. & Akslen, L. A. 2003. Germline brca1 mutations and a basal epithelial phenotype in breast cancer. *Journal of the National Cancer Institute,* 95 number**,** 1482-1485.

Funderburk, S. F., Wang, Q. J. & Yue, Z. 2010. The beclin 1–vps34 complex–at the crossroads of autophagy and beyond. *Trends in cell biology,* 20 number**,** 355-362.

Galluzzi, L., Zamzami, N., Rouge, T. D. L. M., Lemaire, C., Brenner, C. & Kroemer, G. 2007. Methods for the assessment of mitochondrial membrane permeabilization in apoptosis. *Apoptosis,* 12 number**,** 803-813.

Gao, L., Laude, K. & Cai, H. 2008. Mitochondrial pathophysiology, reactive oxygen species, and cardiovascular diseases. *Veterinary Clinics of North America: Small Animal Practice,* 38 number**,** 137-155.

Garner, D. L., Thomas, C. A., Joerg, H. W., Dejarnette, J. M. & Marshall, C. E. 1997. Fluorometric assessments of mitochondrial function and viability in cryopreserved bovine spermatozoa. *Biology of reproduction,* 57 number**,** 1401-1406.

Gasic, G., Gasic, T. & Jimenez, S. 1977. Platelet aggregating material in mouse tumor cells. Removal and regeneration. *Laboratory investigation; a journal of technical methods and pathology,* 36 number**,** 413-419.

Gatenby, R. A. & Gillies, R. J. 2004. Why do cancers have high aerobic glycolysis? *Nature Reviews Cancer,* 4 number**,** 891-899.

Gillies, R. J., Robey, I. & Gatenby, R. A. 2008. Causes and consequences of increased glucose metabolism of cancers. *Journal of Nuclear Medicine,* 49 number**,** 24S-42S.

Goldenberg, I., Moss, A. J. & Zareba, W. 2006. Qt interval: How to measure it and what is "normal". *Journal of cardiovascular electrophysiology,* 17 number**,** 333-336.

Gottesman, M. M. 2002. Mechanisms of cancer drug resistance. *Annual review of medicine,* 53 number**,** 615-627.

135

Gottesman, M. M., Fojo, T. & Bates, S. E. 2002. Multidrug resistance in cancer: Role of atp–dependent transporters. *Nature Reviews Cancer,* 2 number**,** 48-58.

Grandori, C., Cowley, S. M., James, L. P. & Eisenman, R. N. 2000. The myc/max/mad network and the transcriptional control of cell behavior. *Annual review of cell and developmental biology,* 16 number**,** 653-699.

Greenough, R. B. 1925. Varying degrees of malignancy in cancer of the breast. *The Journal of Cancer Research,* 9 number**,** 453-463.

Grever, M. R., Schepartz, S. A. & Chabner, B. A. The national cancer institute: Cancer drug discovery and development program. Seminars in oncology, 1992. WB SAUNDERS CO INDEPENDENCE SQUARE WEST CURTIS CENTER, STE 300, PHILADELPHIA, PA 19106-3399, 622-638.

Group, E. B. C. T. C. 2000. Favourable and unfavourable effects on long-term survival of radiotherapy for early breast cancer: An overview of the randomised trials. *The Lancet,* 355 number**,** 1757-1770.

Gudjonsson, T., Adriance, M. C., Sternlicht, M. D., Petersen, O. W. & Bissell, M. J. 2005. Myoepithelial cells: Their origin and function in breast morphogenesis and neoplasia. *Journal of mammary gland biology and neoplasia,* 10 number**,** 261-272.

Gusterson, B. A., Warburton, M. J., Mitchell, D., Ellison, M., Neville, A. M. & Rudland, P. S. 1982. Distribution of myoepithelial cells and basement membrane proteins in the normal breast and in benign and malignant breast diseases. *Cancer research,* 42 number**,** 4763-4770.

Haga, N., Naito, M., Seimiya, H., Tomida, A., Dong, J. & Tsuruo, T. 1998. 2-deoxyglucose inhibits chemotheapeutic drug-induced apoptosis in human monocytic leukemia u937 cells ith inhibition of c-jun n-terminal kinase 1/stress-activated protein kinase activation. *International journal of cancer,* 76 number**,** 86-90.

Hagerling, C., Casbon, A.-J. & Werb, Z. 2015. Balancing the innate immune system in tumor development. *Trends in cell biology,* 25 number**,** 214-220.

Hamada, H. & Tsuruo, T. 1986. Functional role for the 170-to 180-kda glycoprotein specific to drug-resistant tumor cells as revealed by monoclonal antibodies. *Proceedings of the National Academy of Sciences,* 83 number**,** 7785-7789.

Hamada, H. & Tsuruo, T. 1988. Purification of the 170-to 180-kilodalton membrane glycoprotein associated with multidrug resistance. 170-to 180-kilodalton membrane glycoprotein is an atpase. *Journal of Biological Chemistry,* 263 number**,** 1454-1458.

Hanahan, D. & Weinberg, R. A. 2000. The hallmarks of cancer. *Cell,* 100 number**,** 57-70.

Hanahan, D. & Weinberg, R. A. 2011. Hallmarks of cancer: The next generation. *Cell,* 144 number**,** 646-674.

Harris, J. R., Lippman, M. E., Osborne, C. K. & Morrow, M. 2012. *Diseases of the breast*, Lippincott Williams & Wilkins.

Hayes, D. F., Bast, R. C., Desch, C. E., Fritsche, H., Kemeny, N. E., Jessup, J. M., Locker, G. Y., Macdonald, J. S., Mennel, R. G. & Norton, L. 1996. Tumor marker utility grading system: A framework to evaluate clinical utility of tumor markers. *Journal of the National Cancer Institute,* 88 number**,** 1456-1466.

Henderson, B. E., Ross, R. & Bernstein, L. 1988. Estrogens as a cause of human cancer: The richard and hinda rosenthal foundation award lecture. *Cancer research,* 48 number**,** 246-253.

Henriksson, E., Kjellén, E., Wahlberg, P., Wennerberg, J. & Kjellström, J. H. 2006. Differences in estimates of cisplatin-induced cell kill in vitro between colorimetric and cell count/colony assays. *In Vitro Cellular & Developmental Biology-Animal,* 42 number**,** 320-323.

Henry, C. M., Hollville, E. & Martin, S. J. 2013. Measuring apoptosis by microscopy and flow cytometry. *Methods,* 61 number**,** 90-97.

Hirt, B. V. 2013. *Mathematical modelling of cell cycle and telomere dynamics.* University of Nottingham.

Ho, Y., Purohit, A., Vicker, N., Newman, S., Robinson, J., Leese, M., Ganeshapillai, D., Woo, L., Potter, B. & Reed, M. 2003. Inhibition of carbonic anhydrase ii by steroidal and non-steroidal sulphamates. *Biochemical and biophysical research communications,* 305 number**,** 909-914.

Holland, R., Peterse, J. L., Millis, R. R., Eusebi, V., Faverly, D., Van De Vijver, M., And & Zafrani, B. Ductal carcinoma in situ: A proposal for a new classification. Seminars in diagnostic pathology, 1994. 167-180.

Holliday, D. L. & Speirs, V. 2011. Choosing the right cell line for breast cancer research. *Breast Cancer Res,* 13 number**,** 215.

Hortobagyi, G. N., Ames, F., Buzdar, A., Kau, S., Mcneese, M., Paulus, D., Hug, V., Holmes, F., Romsdahl, M. & Fraschini, G. 1988. Management of stage iii primary breast cancer with primary chemotherapy, surgery, and radiation therapy. *Cancer,* 62 number**,** 2507-2516.

Hsu, H., Xiong, J. & Goeddel, D. V. 1995. The tnf receptor 1-associated protein tradd signals cell death and nf-κb activation. *Cell,* 81 number**,** 495-504.

Hunt, T. 1989. Embryology. Under arrest in the cell cycle. *Nature,* 342 number**,** 483-484.

Huo, Y., Yin, S., Yan, M., Win, S., Than, T., Aghajan, M., Hu, H., Kaplowitz, N. 2017. Protective role of p53 in acetaminophen hepatotoxicity. Free radical biology and medicine, volume 106, 111-117.

Hurrell, T. & Outhoff, K. 2013. Human epidermal growth factor receptor 2-positive breast cancer: Which cytotoxic agent best complements trastuzumab's efficacy in vitro? *OncoTargets and therapy,* 6 number**,** 693.

137

Hurrell, T. & Za, T. H. U. A. 2013. *The in vitro influences of epidermal growth factor and heregulin-β1 on the efficacy of trastuzumab used in her-2 positive breast adenocarcinoma*, BioMed Central.

Ibrahim, A., Sobeh, M., Ismail, A., Alaa, A., Sheashaa, H., Sobh, M. & Badria, F. 2014. Free‑b‑ring flavonoids as potential lead compounds for colon cancer therapy. *Molecular and clinical oncology,* 2 number**,** 581-585.

Igney, F. H. & Krammer, P. H. 2002. Death and anti-death: Tumour resistance to apoptosis. *Nature Reviews Cancer,* 2 number**,** 277-288.

Israels, E. & Israels, L. 2000. The cell cycle. *The oncologist,* 5 number**,** 510-513.

Jain, V. 1996. Modifications of radiation responses by 2-deoxy-d-glucose in normal and cancer cells. *Ind J Nucl Med,* 11 number**,** 8-17.

James, J., Murry, D. J., Treston, A. M., Storniolo, A. M., Sledge, G. W., Sidor, C. & Miller, K. D. 2007. Phase i safety, pharmacokinetic and pharmacodynamic studies of 2-methoxyestradiol alone or in combination with docetaxel in patients with locally recurrent or metastatic breast cancer. *Investigational new drugs,* 25 number**,** 41-48.

Jemal, A., Siegel, R., Xu, J. & Ward, E. 2010. Cancer statistics, 2010. *CA: a cancer journal for clinicians,* 60 number**,** 277-300.

Jing, K. & Lim, K. 2012. Why is autophagy important in human diseases? *Experimental & molecular medicine,* 44 number**,** 69-72.

Jinushi, M., Baghdadi, M., Chiba, S. & Yoshiyama, H. 2012. Regulation of cancer stem cell activities by tumor-associated macrophages. *American journal of cancer research,* 2 number**,** 529.

Johansen, T. & Lamark, T. 2011. Selective autophagy mediated by autophagic adapter proteins. *Autophagy,* 7 number**,** 279-296.

Kabeya, Y., Mizushima, N., Ueno, T., Yamamoto, A., Kirisako, T., Noda, T., Kominami, E., Ohsumi, Y. & Yoshimori, T. 2000. Lc3, a mammalian homologue of yeast apg8p, is localized in autophagosome membranes after processing. *The EMBO journal,* 19 number**,** 5720-5728.

Kanzawa, T., Germano, I., Komata, T., Ito, H., Kondo, Y. & Kondo, S. 2004. Role of autophagy in temozolomide-induced cytotoxicity for malignant glioma cells. *Cell Death & Differentiation,* 11 number**,** 448-457.

Kaplan, O., Navon, G., Lyon, R. C., Faustino, P. J., Straka, E. J. & Cohen, J. S. 1990. Effects of 2-deoxyglucose on drug-sensitive and drug-resistant human breast cancer cells: Toxicity and magnetic resonance spectroscopy studies of metabolism. *Cancer research,* 50 number**,** 544-551.

138

Karim, M. R., Kanazawa, T., Daigaku, Y., Fujimura, S., Miotto, G. & Kadowaki, M. 2007. Cytosolic lc3 ratio as a sensitive index of macroautophagy in isolated rat hepatocytes and h4-ii-e cells. *Autophagy,* 3 number**,** 553-560.

Karoui, M., Penna, C., Amin-Hashem, M., Mitry, E., Benoist, S., Franc, B., Rougier, P. & Nordlinger, B. 2006. Influence of preoperative chemotherapy on the risk of major hepatectomy for colorectal liver metastases. *Annals of surgery,* 243 number**,** 1.

Katzenellenbogen, B. S. 1991. Antiestrogen resistance: Mechanisms by which breast cancer cells undermine the effectiveness of endocrine therapy. *Journal of the National Cancer Institute,* 83 number**,** 1434-1435.

Kaufmann, S. H., Ewing, C. M. & Shaper, J. H. 1987. The erasable western blot. *Analytical biochemistry,* 161 number**,** 89-95.

Keepers, Y. P., Pizao, P. E., Peters, G. J., Van Ark-Otte, J., Winograd, B. & Pinedo, H. M. 1991. Comparison of the sulforhodamine b protein and tetrazolium (mtt) assays for in vitro chemosensitivity testing. *European Journal of Cancer and Clinical Oncology,* 27 number**,** 897-900.

Kitamura, M., Murakami, K., Yamada, K., Kawai, K. & Kunishima, M. 2013. Binding of sulforhodamine b to human serum albumin: A spectroscopic study. *Dyes and Pigments,* 99 number**,** 588-593.

Klionsky, D. J., Abdalla, F. C., Abeliovich, H., Abraham, R. T., Acevedo-Arozena, A., Adeli, K., Agholme, L., Agnello, M., Agostinis, P. & Aguirre-Ghiso, J. A. 2012. Guidelines for the use and interpretation of assays for monitoring autophagy. *Autophagy,* 8 number**,** 445-544.

Klionsky, D. J., Cuervo, A. M. & Seglen, P. O. 2007. Methods for monitoring autophagy from yeast to human. *Autophagy,* 3 number**,** 181-206.

Klionsky, D. J. & Emr, S. D. 2000. Autophagy as a regulated pathway of cellular degradation. *Science,* 290 number**,** 1717-1721.

Kluck, R. M., Degli Esposti, M., Perkins, G., Renken, C., Kuwana, T., Bossy-Wetzel, E., Goldberg, M., Allen, T., Barber, M. J. & Green, D. R. 1999. The pro-apoptotic proteins, bid and bax, cause a limited permeabilization of the mitochondrial outer membrane that is enhanced by cytosol. *The Journal of cell biology,* 147 number**,** 809-822.

Köhler, A. 1893. Zeitschrift für wissenschaftliche. *Mikroskopie X,* number**,** 433-440.

Kuma, A. & Mizushima, N. Physiological role of autophagy as an intracellular recycling system: With an emphasis on nutrient metabolism. Seminars in cell & developmental biology, 2010. Elsevier, 683-690.

Kumar, S. N., Visagie, M., Hood, M. & Joubert, A. 2015. In vitro effects exerted by an in silico-designed compound and 2-methoxyestradiol on cell morphology and cell death induction via apoptosis in cervical tumorigenic cells. number.

Kurtoglu, M., Gao, N., Shang, J., Maher, J. C., Lehrman, M. A., Wangpaichitr, M., Savaraj, N., Lane, A. N. & Lampidis, T. J. 2007. Under normoxia, 2-deoxy-d-glucose elicits cell death in select tumor types not by inhibition of glycolysis but by interfering with n-linked glycosylation. *Molecular cancer therapeutics,* 6 number**,** 3049-3058.

Kussmaul, L. & Hirst, J. 2006. The mechanism of superoxide production by nadh: Ubiquinone oxidoreductase (complex i) from bovine heart mitochondria. *Proceedings of the National Academy of Sciences,* 103 number**,** 7607-7612.

Kwan, M. L., Kushi, L. H., Weltzien, E., Maring, B., Kutner, S. E., Fulton, R. S., Lee, M. M., Ambrosone, C. B. & Caan, B. J. 2009. Epidemiology of breast cancer subtypes in two prospective cohort studies of breast cancer survivors. *Breast Cancer Res,* 11 number**,** R31.

Lakhani, N. J., Sarkar, M. A., Venitz, J. & Figg, W. D. 2003. 2-methoxyestradiol, a promising anti-cancer agent. *Pharmacotherapy: The Journal of Human Pharmacology and Drug Therapy,* 23 number**,** 165-172.

Landau, B. R., Laszlo, J., Stengle, J. & Burk, D. 1958. Certain metabolic and pharmacologic effects in cancer patients given infusions of 2-deoxy-d-glucose. number.

Lavallee, T. M., Burke, P. A., Swartz, G. M., Hamel, E., Agoston, G. E., Shah, J., Suwandi, L., Hanson, A. D., Fogler, W. E. & Sidor, C. F. 2008. Significant antitumor activity in vivo following treatment with the microtubule agent enmd-1198. *Molecular cancer therapeutics,* 7 number**,** 1472-1482.

Lavallee, T. M., Zhan, X. H., Johnson, M. S., Herbstritt, C. J., Swartz, G., Williams, M. S., Hembrough, W. A., Green, S. J. & Pribluda, V. S. 2003. 2-methoxyestradiol up-regulates death receptor 5 and induces apoptosis through activation of the extrinsic pathway. *Cancer research,* 63 number**,** 468-475.

Leese, M. P., Leblond, B., Smith, A., Newman, S. P., Di Fiore, A., De Simone, G., Supuran, C. T., Purohit, A., Reed, M. J. & Potter, B. V. 2006. 2-substituted estradiol bis-sulfamates, multitargeted antitumor agents: Synthesis, in vitro sar, protein crystallography, and in vivo activity. *Journal of medicinal chemistry,* 49 number**,** 7683-7696.

Leese, M. P., Newman, S. P., Purohit, A., Reed, M. J. & Potter, B. V. 2004. 2-alkylsulfanyl estrogen derivatives: Synthesis of a novel class of multi-targeted anti-tumour agents. *Bioorganic & medicinal chemistry letters,* 14 number**,** 3135-3138.

Letai, A. & Kutuk, O. 2008. Regulation of bcl-2 family proteins by posttranslational modifications. *Current molecular medicine,* 8 number**,** 102-118.

140

Lin, X., Zhang, F., Bradbury, C. M., Kaushal, A., Li, L., Spitz, D. R., Aft, R. L. & Gius, D. 2003. 2-deoxy-d-glucose-induced cytotoxicity and radiosensitization in tumor cells is mediated via disruptions in thiol metabolism. *Cancer research,* 63 number**,** 3413-3417.

Linette, G. P., Li, Y., Roth, K. & Korsmeyer, S. J. 1996. Cross talk between cell death and cell cycle progression: Bcl-2 regulates nfat-mediated activation. *Proceedings of the National Academy of Sciences,* 93 number**,** 9545-9552.

Liu, H., Hu, Y., Savaraj, N., Priebe, W. & Lampidis, T. 2001. Hypersensitization of tumor cells to glycolytic inhibitors. *Biochemistry,* 40 number**,** 5542-5547.

Livasy, C. A., Karaca, G., Nanda, R., Tretiakova, M. S., Olopade, O. I., Moore, D. T. & Perou, C. M. 2006. Phenotypic evaluation of the basal-like subtype of invasive breast carcinoma. *Modern pathology,* 19 number**,** 264-271.

Lowe, S. W. & Lin, A. W. 2000. Apoptosis in cancer. *Carcinogenesis,* 21 number**,** 485-495.

Lumachi, F., Brunello, A., Maruzzo, M., Basso, U. & Mm Basso, S. 2013. Treatment of estrogen receptor-positive breast cancer. *Current medicinal chemistry,* 20 number**,** 596-604.

Maher, J. C., Krishan, A. & Lampidis, T. J. 2004. Greater cell cycle inhibition and cytotoxicity induced by 2-deoxy-d-glucose in tumor cells treated under hypoxic vs aerobic conditions. *Cancer chemotherapy and pharmacology,* 53 number**,** 116-122.

Mahmood, T. & Yang, P.-C. 2012. Western blot: Technique, theory, and trouble shooting. *North American journal of medical sciences,* 4 number**,** 429.

Mantovani, A. 2009. Cancer: Inflaming metastasis. *Nature,* 457 number**,** 36-37.

Maschek, G., Savaraj, N., Priebe, W., Braunschweiger, P., Hamilton, K., Tidmarsh, G. F., De Young, L. R. & Lampidis, T. J. 2004. 2-deoxy-d-glucose increases the efficacy of adriamycin and paclitaxel in human osteosarcoma and non-small cell lung cancers in vivo. *Cancer research,* 64 number**,** 31-34.

Matuszewski, B., Constanzer, M. & Chavez-Eng, C. 1998. Matrix effect in quantitative lc/ms/ms analyses of biological fluids: A method for determination of finasteride in human plasma at picogram per milliliter concentrations. *Analytical chemistry,* 70 number**,** 882-889.

Mazurek, S., Boschek, C. B., Hugo, F. & Eigenbrodt, E. Pyruvate kinase type m2 and its role in tumor growth and spreading. Seminars in cancer biology, 2005. Elsevier, 300-308.

Mcpherson, K., Steel, C. & Dixon, J. 2000. Abc of breast diseases: Breast cancer—epidemiology, risk factors, and genetics. *BMJ: British Medical Journal,* 321 number**,** 624.

Mehta, S. B. & Sheppard, C. J. 2008. Partially coherent image formation in differential interference contrast (dic) microscope. *Optics express,* 16 number**,** 19462-19479.

Mitchell, P. 1961. Coupling of phosphorylation to electron and hydrogen transfer by a chemi-osmotic type of mechanism. *Nature,* 191 number**,** 144-148.

141

Mizushima, N., Yamamoto, A., Matsui, M., Yoshimori, T. & Ohsumi, Y. 2004. In vivo analysis of autophagy in response to nutrient starvation using transgenic mice expressing a fluorescent autophagosome marker. *Molecular biology of the cell,* 15 number**,** 1101-1111.

Mooberry, S. L. 2003. Mechanism of action of 2-methoxyestradiol: New developments. *Drug Resistance Updates,* 6 number**,** 355-361.

Mosmann, T. 1983. Rapid colorimetric assay for cellular growth and survival: Application to proliferation and cytotoxicity assays. *Journal of immunological methods,* 65 number**,** 55-63.

Murphy, D. B. 2002. *Fundamentals of light microscopy and electronic imaging*, John Wiley & Sons.

Murray, A. 1994. Cell cycle checkpoints. *Current opinion in cell biology,* 6 number**,** 872-876.

Murray, A. W. 1992. Creative blocks: Cell-cycle checkpoints and feedback controls. *Nature,* 359 number**,** 599-604.

Nedelsky, N. B., Todd, P. K. & Taylor, J. P. 2008. Autophagy and the ubiquitin-proteasome system: Collaborators in neuroprotection. *Biochimica et Biophysica Acta (BBA)-Molecular Basis of Disease,* 1782 number**,** 691-699.

Newman, S. P., Ireson, C. R., Tutill, H. J., Day, J. M., Parsons, M. F., Leese, M. P., Potter, B. V., Reed, M. J. & Purohit, A. 2006. The role of 17β-hydroxysteroid dehydrogenases in modulating the activity of 2-methoxyestradiol in breast cancer cells. *Cancer research,* 66 number**,** 324-330.

Nicholls, D. G. 2004. Mitochondrial membrane potential and aging. *Aging cell,* 3 number**,** 35-40.

Nicoletti, I., Migliorati, G., Pagliacci, M., Grignani, F. & Riccardi, C. 1991. A rapid and simple method for measuring thymocyte apoptosis by propidium iodide staining and flow cytometry. *Journal of immunological methods,* 139 number**,** 271-279.

Nicolson, G. L. 1988. Organ specificity of tumor metastasis: Role of preferential adhesion, invasion and growth of malignant cells at specific secondary sites. *Cancer and Metastasis Reviews,* 7 number**,** 143-188.

Nigam, M., Ranjan, V., Srivastava, S., Sharma, R. & Balapure, A. K. 2008. Centchroman induces g 0/g 1 arrest and caspase-dependent apoptosis involving mitochondrial membrane depolarization in mcf-7 and mda mb-231 human breast cancer cells. *Life sciences,* 82 number**,** 577-590.

Ning, X., Shu, J., Du, Y., Ben, Q. & Li, Z. 2013. Therapeutic strategies targeting cancer stem cells. *Cancer biology & therapy,* 14 number**,** 295-303.

Nkandeu, D. S., Mqoco, T. V., Visagie, M. H., Stander, B. A., Wolmarans, E., Cronje, M. J. & Joubert, A. M. 2013. In vitro changes in mitochondrial potential, aggresome formation and caspase activity by a novel 17-β-estradiol analogue in breast adenocarcinoma cells. *Cell biochemistry and function,* 31 number**,** 566-574.

142

Nuydens, R., Novalbos, J., Dispersyn, G., Weber, C., Borgers, M. & Geerts, H. 1999. A rapid method for the evaluation of compounds with mitochondria-protective properties. *Journal of neuroscience methods,* 92 number**,** 153-159.

Paget, S. 1889. The distribution of secondary growths in cancer of the breast. *The Lancet,* 133 number**,** 571-573.

Papazisis, K., Geromichalos, G., Dimitriadis, K. & Kortsaris, A. 1997. Optimization of the sulforhodamine b colorimetric assay. *Journal of immunological methods,* 208 number**,** 151-158.

Pastorekova, S., Ratcliffe, P. J. & Pastorek, J. 2008. Molecular mechanisms of carbonic anhydrase ix-mediated ph regulation under hypoxia. *BJU international,* 101 number**,** 8-15.

Pathania, D., Millard, M. & Neamati, N. 2009. Opportunities in discovery and delivery of anti-cancer drugs targeting mitochondria and cancer cell metabolism. *Advanced drug delivery reviews,* 61 number**,** 1250-1275.

Perel, P., Roberts, I., Sena, E., Wheble, P., Briscoe, C., Sandercock, P., Macleod, M., Mignini, L. E., Jayaram, P. & Khan, K. S. 2007. Comparison of treatment effects between animal experiments and clinical trials: Systematic review. *Bmj,* 334 number**,** 197.

Perou, C. M., Sørlie, T., Eisen, M. B., Van De Rijn, M., Jeffrey, S. S., Rees, C. A., Pollack, J. R., Ross, D. T., Johnsen, H. & Akslen, L. A. 2000. Molecular portraits of human breast tumours. *Nature,* 406 number**,** 747-752.

Perry, S. W., Norman, J. P., Barbieri, J., Brown, E. B. & Gelbard, H. A. 2011. Mitochondrial membrane potential probes and the proton gradient: A practical usage guide. *Biotechniques,* 50 number**,** 98.

Petersen, O. W., Rønnov-Jessen, L., Howlett, A. R. & Bissell, M. J. 1992. Interaction with basement membrane serves to rapidly distinguish growth and differentiation pattern of normal and malignant human breast epithelial cells. *Proceedings of the National Academy of Sciences,* 89 number**,** 9064-9068.

Pietras, K. & Östman, A. 2010. Hallmarks of cancer: Interactions with the tumor stroma. *Experimental cell research,* 316 number**,** 1324-1331.

Pozarowski, P. & Darzynkiewicz, Z. 2004. Analysis of cell cycle by flow cytometry. *Checkpoint controls and cancer.* Springer.

Pravettoni, G., Yoder, W. R., Riva, S., Mazzocco, K., Arnaboldi, P. & Galimberti, V. 2016. Eliminating "ductal carcinoma in situ" and "lobular carcinoma in situ"(dcis and lcis) terminology in clinical breast practice: The cognitive psychology point of view. *The Breast,* 25 number**,** 82-85.

143

Pribluda, V. S., Gubish, E. R., Lavallee, T. M., Treston, A., Swartz, G. M. & Green, S. J. 2000. 2-methoxyestradiol: An endogenous antiangiogenic and antiproliferative drug candidate. *Cancer and Metastasis Reviews,* 19 number**,** 173-179.

Qu, X., Zou, Z., Sun, Q., Luby-Phelps, K., Cheng, P., Hogan, R. N., Gilpin, C. & Levine, B. 2007. Autophagy gene-dependent clearance of apoptotic cells during embryonic development. *Cell,* 128 number**,** 931-946.

Rabinowitz, J. D. & White, E. 2010. Autophagy and metabolism. *Science,* 330 number**,** 1344-1348.

Radi, E., Formichi, P., Battisti, C. & Federico, A. 2014. Apoptosis and oxidative stress in neurodegenerative diseases. *Journal of Alzheimer's disease: JAD,* 42 number**,** S125-52.

Raez, L. E., Papadopoulos, K., Ricart, A. D., Chiorean, E. G., Dipaola, R. S., Stein, M. N., Lima, C. M. R., Schlesselman, J. J., Tolba, K. & Langmuir, V. K. 2013. A phase i dose-escalation trial of 2-deoxy-d-glucose alone or combined with docetaxel in patients with advanced solid tumors. *Cancer chemotherapy and pharmacology,* 71 number**,** 523-530.

Robbins, E. & Gonatas, N. K. 1964. The ultrastructure of a mammalian cell during the mitotic cycle. *The Journal of cell biology,* 21 number**,** 429-463.

Ronnov-Jessen, L., Petersen, O. W. & Bissell, M. J. 1996. Cellular changes involved in conversion of normal to malignant breast: Importance of the stromal reaction. *Physiological reviews,* 76 number**,** 69-125.

Roy, S. S. & Hajnóczky, G. 2009. Fluorometric methods for detection of mitochondrial membrane permeabilization in apoptosis. *Apoptosis: Methods and Protocols, Second Edition,* number**,** 173-190.

Sahra, I. B., Laurent, K., Giuliano, S., Larbret, F., Ponzio, G., Gounon, P., Le Marchand-Brustel, Y., Giorgetti-Peraldi, S., Cormont, M. & Bertolotto, C. 2010. Targeting cancer cell metabolism: The combination of metformin and 2-deoxyglucose induces p53-dependent apoptosis in prostate cancer cells. *Cancer research,* 70 number**,** 2465-2475.

Santini, D., Vincenzi, B., Massacesi, C., Picardi, A., Gentilucci, U., Esposito, V., Liuzzi, G., La Cesa, A., Rocci, L. & Marcucci, F. 2002. S-adenosylmethionine (adomet) supplementation for treatment of chemotherapy-induced liver injury. *Anti-cancer research,* 23 number**,** 5173-5179.

Saslow, D., Boetes, C., Burke, W., Harms, S., Leach, M. O., Lehman, C. D., Morris, E., Pisano, E., Schnall, M. & Sener, S. 2007. American cancer society guidelines for breast screening with mri as an adjunct to mammography. *CA: a cancer journal for clinicians,* 57 number**,** 75-89.

Sawai, H. & Domae, N. 2011. Discrimination between primary necrosis and apoptosis by necrostatin-1 in annexin v-positive/propidium iodide-negative cells. *Biochemical and biophysical research communications,* 411 number**,** 569-573.

144

Seeger, H., Diesing, D., Gückel, B., Wallwiener, D., Mueck, A. & Huober, J. 2003. Effect of tamoxifen and 2-methoxyestradiol alone and in combination on human breast cancer cell proliferation. *The Journal of steroid biochemistry and molecular biology,* 84 number**,** 255-257.

Sella, A. & Ro, J. Y. 1987. Renal cell cancer: Best recipient of tumor-to-tumor metastasis. *Urology,* 30 number**,** 35-38.

Semenza, G. L., Artemov, D., Bedi, A., Bhujwalla, Z., Chiles, K., Feldser, D., Laughner, E., Ravi, R., Simons, J. & Taghavi, P. 'The metabolism of tumours': 70 years later. The Tumour Microenvironment: Causes and Consequences of Hypoxia and Acidity: Novartis Foundation Symposium 240, 2001. Wiley Online Library, 251-264.

Shrotriya, S., Deep, G., Lopert, P., Patel, M., Agarwal, R. & Agarwal, C. 2014. Grape seed extract targets mitochondrial electron transport chain complex iii and induces oxidative and metabolic stress leading to cytoprotective autophagy and apoptotic death in human head and neck cancer cells. *Molecular carcinogenesis,* number.

Siegel, R., Miller, K. & Jemal, A. 2016. Cancer facts and figures 2016. *American Cancer society,* number.

Siegel, R., Naishadham, D. & Jemal, A. 2013. Cancer statistics, 2013. *CA: a cancer journal for clinicians,* 63 number**,** 11-30.

Siegel, R. L., Miller, K. D. & Jemal, A. 2016. Cancer statistics 2016. *Cancer Journal for Clinicians,* number.

Simonnet, H., Alazard, N., Pfeiffer, K., Gallou, C., Béroud, C., Demont, J., Bouvier, R., Schägger, H. & Godinot, C. 2002. Low mitochondrial respiratory chain content correlates with tumor aggressiveness in renal cell carcinoma. *Carcinogenesis,* 23 number**,** 759-768.

Sionov, R. V. & Haupt, Y. 1999. The cellular response to p53: The decision between life and death. *Oncogene,* 18 number**,** 6145-6157.

Skehan, P., Storeng, R., Scudiero, D., Monks, A., Mcmahon, J., Vistica, D., Warren, J. T., Bokesch, H., Kenney, S. & Boyd, M. R. 1990. New colorimetric cytotoxicity assay for anti-cancer-drug screening. *Journal of the National Cancer Institute,* 82 number**,** 1107-1112.

Slee, E. A., Harte, M. T., Kluck, R. M., Wolf, B. B., Casiano, C. A., Newmeyer, D. D., Wang, H.-G., Reed, J. C., Nicholson, D. W. & Alnemri, E. S. 1999. Ordering the cytochrome c–initiated caspase cascade: Hierarchical activation of caspases-2,-3,-6,-7,-8, and-10 in a caspase-9–dependent manner. *The Journal of cell biology,* 144 number**,** 281-292.

Song, K.-S., Kim, J.-S., Yun, E.-J., Kim, Y.-R., Seo, K.-S., Park, J.-H., Jung, Y.-J., Park, J.-I., Kweon, G.-R. & Yoon, W.-H. 2008. Rottlerin induces autophagy and apoptotic cell death

145

through a pkc-delta-independent pathway in ht1080 human fibrosarcoma cells: The protective role of autophagy in apoptosis. *Autophagy,* 4 number**,** 650-658.

Sørlie, T., Perou, C. M., Tibshirani, R., Aas, T., Geisler, S., Johnsen, H., Hastie, T., Eisen, M. B., Van De Rijn, M. & Jeffrey, S. S. 2001. Gene expression patterns of breast carcinomas distinguish tumor subclasses with clinical implications. *Proceedings of the National Academy of Sciences,* 98 number**,** 10869-10874.

Sørlie, T., Tibshirani, R., Parker, J., Hastie, T., Marron, J., Nobel, A., Deng, S., Johnsen, H., Pesich, R. & Geisler, S. 2003. Repeated observation of breast tumor subtypes in independent gene expression data sets. *PNAS,* 100 number.

Span, L., Pennings, A., Vierwinden, G., Boezeman, J., Raymakers, R. & De Witte, T. 2002. The dynamic process of apoptosis analyzed by flow cytometry using annexin-v/propidium iodide and a modified in situ end labeling technique. *Cytometry,* 47 number**,** 24-31.

Spencer, C. A. & Groudine, M. 1991. Control of c-myc regulation in normal and neoplastic cells. *Adv Cancer Res,* 56 number**,** 1-48.

Stander, A., Joubert, F. & Joubert, A. 2011. Docking, synthesis, and in vitro evaluation of antimitotic estrone analogs. *Chemical biology & drug design,* 77 number**,** 173-181.

Stander, B. A., Joubert, F., Tu, C., Sippel, K. H., Mckenna, R. & Joubert, A. M. 2012. In vitro evaluation of ese-15-ol, an estradiol analogue with nanomolar antimitotic and carbonic anhydrase inhibitory activity. number.

Stander, B. A., Joubert, F., Tu, C., Sippel, K. H., Mckenna, R. & Joubert, A. M. 2013. Signaling pathways of ese-16, an antimitotic and anticarbonic anhydrase estradiol analog, in breast cancer cells. *PloS one,* 8 number**,** e53853.

Stander, X. X., Stander, B. A. & Joubert, A. M. 2011. In vitro effects of an in silico-modelled 17β-estradiol derivative in combination with dichloroacetic acid on mcf-7 and mcf-12a cells. *Cell Proliferation,* 44 number**,** 567-581.

Stander, X. X., Stander, B. A. & Joubert, A. M. 2015. Synergistic anti-cancer potential of dichloroacetate and estradiol analogue exerting their effect via ros-jnk-bcl-2-mediated signalling pathways. *Cellular Physiology and Biochemistry,* 35 number**,** 1499-1526.

Stein, M., Lin, H., Jeyamohan, C., Dvorzhinski, D., Gounder, M., Bray, K., Eddy, S., Goodin, S., White, E. & Dipaola, R. S. 2010. Targeting tumor metabolism with 2-deoxyglucose in patients with castrate-resistant prostate cancer and advanced malignancies. *The Prostate,* 70 number**,** 1388-1394.

Stengel, C., Newman, S., Day, J., Chander, S., Jourdan, F., Leese, M., Ferrandis, E., Regis-Lydi, S., Potter, B. & Reed, M. 2014. In vivo and in vitro properties of stx2484: A novel non-steroidal

146

anti-cancer compound active in taxane-resistant breast cancer. *British journal of cancer,* 111 number**,** 300-308.

Stephens, D. J. & Allan, V. J. 2003. Light microscopy techniques for live cell imaging. *Science,* 300 number**,** 82-86.

Stewart, B. & Wild, C. P. 2015. World cancer report 2014. *World,* number.

Stockler, M. R., Wilcken, N. J. & Coates, A. S. 2003. Chemotherapy for advanced breast cancer–how long should it continue? *Breast Cancer Research and Treatment,* 81 number**,** 49-52.

Subik, K., Lee, J.-F., Baxter, L., Strzepek, T., Costello, D., Crowley, P., Xing, L., Hung, M.-C., Bonfiglio, T. & Hicks, D. G. 2010. The expression patterns of er, pr, her2, ck5/6, egfr, ki-67 and ar by immunohistochemical analysis in breast cancer cell lines. *Breast cancer: basic and clinical research,* 4 number**,** 35.

Sugarbaker, E. 1981. Patterns of metastasis in human malignancies. *Cancer Biol Rev,* 2 number**,** 235-278.

Sun, Y., Kucej, M., Fan, H.-Y., Yu, H., Sun, Q.-Y. & Zou, H. 2009. Separase is recruited to mitotic chromosomes to dissolve sister chromatid cohesion in a DNA-dependent manner. *Cell,* 137 number**,** 123-132.

Tagg, S., Foster, P., Leese, M., Potter, B., Reed, M., Purohit, A. & Newman, S. 2008. 2-methoxyoestradiol-3, 17-o, o-bis-sulphamate and 2-deoxy-d-glucose in combination: A potential treatment for breast and prostate cancer. *British journal of cancer,* 99 number**,** 1842-1848.

Tagg, S. L. C., Foster, P. A., Newman, S. P., Reed, J. M., Purohit, A. & Potter, B. V. L. 2008. Composition comprising a glycolytic inhibitor and a ring system comprising a sulphamate group for the treatment of cancer. Google Patents.

Tait, S. W. & Green, D. R. 2010. Mitochondria and cell death: Outer membrane permeabilization and beyond. *Nature reviews Molecular cell biology,* 11 number**,** 621-632.

Takano, S., Shiomoto, S., Inoue, K. Y., Ino, K., Shiku, H. & Matsue, T. 2014. Electrochemical approach for the development of a simple method for detecting cell apoptosis based on caspase-3 activity. *Analytical chemistry,* 86 number**,** 4723-4728.

Takizawa, C. G. & Morgan, D. O. 2000. Control of mitosis by changes in the subcellular location of cyclin-b1–cdk1 and cdc25c. *Current opinion in cell biology,* 12 number**,** 658-665.

Tanaka, K., Kohga, S., Kinjo, M. & Kodama, Y. 1977. Tumor metastasis and thrombosis, with special reference to thromboplastic and fibrinolytic activities of tumor cells. *Gann Monogr Cancer Res,* 20 number**,** 97-119.

Tanida, I., Ueno, T. & Kominami, E. 2008. Lc3 and autophagy. *Autophagosome and phagosome.* Springer.

147

Tavassoli, F. A. & Devilee, P. 2003. *Pathology and genetics of tumours of the breast and female genital organs*, Iarc.

Theron, A. E., Nolte, E. M., Lafanechère, L. & Joubert, A. M. 2013. Molecular crosstalk between apoptosis and autophagy induced by a novel 2-methoxyestradiol analogue in cervical adenocarcinoma cells. *Cancer cell international,* 13 number**,** 87.

Thorburn, A., Thamm, D. H. & Gustafson, D. L. 2014. Autophagy and cancer therapy. *Molecular pharmacology,* 85 number**,** 830-838.

Tonder, A. V. 2016. *Exploiting drug synergism to extend the application of oestrone analogues.* PhD, University of Pretoria.

Tong, G.-H., Tong, W.-W., Qin, X.-S., Lu, L.-P. & Liu, Y. 2015. Dbd-f induces apoptosis in gastric cancer-derived cells through suppressing hif2α expression. *Cellular Oncology,* number**,** 1-6.

Troy, C. M. & Jean, Y. Y. 2015. Caspases: Therapeutic targets in neurologic disease. *Neurotherapeutics,* 12 number**,** 42-48.

Tsuruo, T., Iida, H., Tsukagoshi, S. & Sakurai, Y. 1981. Overcoming of vincristine resistance in p388 leukemia in vivo and in vitro through enhanced cytotoxicity of vincristine and vinblastine by verapamil. *Cancer research,* 41 number**,** 1967-1972.

Tsuruo, T., Naito, M., Tomida, A., Fujita, N., Mashima, T., Sakamoto, H. & Haga, N. 2003. Molecular targeting therapy of cancer: Drug resistance, apoptosis and survival signal. *Cancer science,* 94 number**,** 15-21.

Tyson, J. J., Csikasz-Nagy, A. & Novak, B. 2002. The dynamics of cell cycle regulation. *Bioessays,* 24 number**,** 1095-1109.

Van Engeland, M., Nieland, L. J., Ramaekers, F. C., Schutte, B. & Reutelingsperger, C. P. 1998. Annexin v-affinity assay: A review on an apoptosis detection system based on phosphatidylserine exposure. *Cytometry,* 31 number**,** 1-9.

Van Tonder, J. J., Gulumian, M., Cromarty, A. D. & Steenkamp, V. 2014. In vitro effect of n-acetylcysteine on hepatocyte injury caused by dichlorodiphenyltrichloroethane and its metabolites. *Human & experimental toxicology,* 33 number**,** 41-53.

Van Vuuren, R. J., Visagie, M. H., Theron, A. E. & Joubert, A. M. 2015. Antimitotic drugs in the treatment of cancer. *Cancer chemotherapy and pharmacology,* 76 number**,** 1101-1112.

Van Zijl, C., Lottering, M. L., Steffens, F. & Joubert, A. 2008. In vitro effects of 2-methoxyestradiol on mcf-12a and mcf-7 cell growth, morphology and mitotic spindle formation. *Cell biochemistry and function,* 26 number**,** 632-642.

Vander Heiden, M. G., Cantley, L. C. & Thompson, C. B. 2009. Understanding the warburg effect: The metabolic requirements of cell proliferation. *Science,* 324 number**,** 1029-1033.

Vermeulen, K., Berneman, Z. N. & Van Bockstaele, D. R. 2003. Cell cycle and apoptosis. *Cell proliferation,* 36 number**,** 165-175.

Vermeulen, K., Van Bockstaele, D. R. & Berneman, Z. N. 2003. The cell cycle: A review of regulation, deregulation and therapeutic targets in cancer. *Cell proliferation,* 36 number**,** 131-149.

Vichai, V. & Kirtikara, K. 2006. Sulforhodamine b colorimetric assay for cytotoxicity screening. *Nature protocols,* 1 number**,** 1112-1116.

Visagie, M., Mqoco, T. & Joubert, A. 2012. Sulphamoylated estradiol analogue induces antiproliferative activity and apoptosis in breast cell lines. *Cellular and Molecular Biology Letters,* 17 number**,** 549-558.

Visagie, M., Theron, A., Mqoco, T., Vieira, W., Prudent, R., Martinez, A., Lafanechère, L. & Joubert, A. 2013. Sulphamoylated 2-methoxyestradiol analogues induce apoptosis in adenocarcinoma cell lines. *PloS one,* 8 number**,** e71935.

Visagie, M. H., Birkholtz, L.-M. & Joubert, A. M. 2015. A 2-methoxyestradiol bis-sulphamoylated derivative induces apoptosis in breast cell lines. *Cell & bioscience,* 5 number**,** 19.

Visagie, M. H., Birkholtz, L. M. & Joubert, A. M. 2014. 17-beta-estradiol analog inhibits cell proliferation by induction of apoptosis in breast cell lines. *Microscopy research and technique,* 77 number**,** 236-242.

Visagie, M. H., Stander, B. A., Birkholtz, L.-M. & Margaretha, A. 2013. Short communication: Effects of a 17-beta estradiol analogue on gene expression and morphology in a breast epithelial adenocarcinoma cell line: A potential antiproliferative agent. *Biomedical Research,* 24 number**,** 525-530.

Voigt, W. 2005. Sulforhodamine b assay and chemosensitivity. *Chemosensitivity.* Springer.

Wallace, D. C. 1999. Mitochondrial diseases in man and mouse. *Science,* 283 number**,** 1482-1488.

Wang, C. & Youle, R. J. 2009. The role of mitochondria in apoptosis*. *Annual review of genetics,* 43 number**,** 95-118.

Wang, Q., Liang, B., Shirwany, N. A. & Zou, M.-H. 2011. 2-deoxy-d-glucose treatment of endothelial cells induces autophagy by reactive oxygen species-mediated activation of the amp-activated protein kinase. *PloS one,* 6 number**,** e17234.

Warburg, O. 1956. On the origin of cancer cells. *Science,* 123 number**,** 309-314.

Wehner, E. 2003. Plasdic, an innovative relief contrast for routine observation in cell biology. *Imaging Microsc,* 4 number**,** 23.

Weiss, L. & Ward, P. M. 1983. Cell detachment and metastasis. *Cancer and Metastasis Reviews,* 2 number**,** 111-127.

149

Wen, J.-J. & Garg, N. J. 2010. Mitochondrial complex iii defects contribute to inefficient respiration and atp synthesis in the myocardium of trypanosoma cruzi–infected mice. *Antioxidants & redox signaling,* 12 number**,** 27-37.

White, E. & Dipaola, R. S. 2009. The double-edged sword of autophagy modulation in cancer. *Clinical Cancer Research,* 15 number**,** 5308-5316.

Wolmarans, E., Mqoco, T., Stander, A., Nkandeu, S., Sippel, K., Mckenna, R. & Joubert, A. 2014. Novel estradiol analogue induces apoptosis and autophagy in esophageal carcinoma cells. *Cellular and Molecular Biology Letters,* 19 number**,** 98-115.

Wolmarans, E., Sippel, K., Mckenna, R. & Joubert, A. 2014. Induction of the intrinsic apoptotic pathway via a new antimitotic agent in an esophageal carcinoma cell line. *Cell & bioscience,* 4 number**,** 1-14.

Wong, K.-K., Engelman, J. A. & Cantley, L. C. 2010. Targeting the pi3k signaling pathway in cancer. *Current opinion in genetics & development,* 20 number**,** 87-90.

Wu, H., Zhu, H., Liu, D. X., Niu, T.-K., Ren, X., Patel, R., Hait, W. N. & Yang, J.-M. 2009. Silencing of elongation factor-2 kinase potentiates the effect of 2-deoxy-d-glucose against human glioma cells through blunting of autophagy. *Cancer research,* 69 number**,** 2453-2460.

Www.Atcc.Org. 2014. *Mcf7 (atcc htb-22)* [Online]. Available: http://www.atcc.org/products/all/HTB-22.aspx#characteristics [Accessed 12 February 2016 2016].

Www.Biocat.Com. *Apoptosis detection (mitochondrial)* [Online]. Available: http://www.biocat.com/cell-biology/apoptosis/apoptosis-detection-mitochondrial [Accessed 12 February 2016 2016].

Www.Breastcancer.Org. 2015. *Options by cancer stage* [Online]. Available: http://www.breastcancer.org/treatment/planning/cancer_stage [Accessed 2 February 2016 2016].

Www.Cancer.Org. 2015. *Planning chemotherapy treatments* [Online]. Available: http://www.cancer.org/treatment/treatmentsandsideeffects/treatmenttypes/chemotherapy/chemotherapyprinciplesanin-depthdiscussionofthetechniquesanditsroleintreatment/chemotherapy-principles-planning-drug-doses-and-schedules [Accessed 20 January 2016 2016].

Www.Cansa.Org.Za. 2010. *Prevalence cancer* [Online]. Available: http://www.cansa.org.za/south-african-cancer-statistics/ [Accessed 25 January 2016 2016].

Www.Enzolifesciences.Com. 2015. *Proteostat aggreresome detection kit* [Online]. Available: http://www.enzolifesciences.com/ENZ-51035/proteostat-aggresome-detection-kit/ [Accessed 15 February 2016 2016].

150

Www.Enzolifesciences.Com. 2016. *Cyto-id autophagy detection kit* [Online]. Available: http://www.enzolifesciences.com/ENZ-51031/cyto-id-autophagy-detection-kit/ [Accessed 15 February 2016 2016].

Www.Who.Int. 2015. *Cancer* [Online]. Available: http://www.who.int/mediacentre/factsheets/fs297/en/ [Accessed 25 January 2016 2016].

Yaacob, N. S., Kamal, N. N. & Norazmi, M. N. 2014. Synergistic anti-cancer effects of a bioactive subfraction of strobilanthes crispus and tamoxifen on mcf-7 and mda-mb-231 human breast cancer cell lines. *BMC complementary and alternative medicine,* 14 number**,** 252.

Ylä-Anttila, P., Vihinen, H., Jokitalo, E. & Eskelinen, E. L. 2009. Monitoring autophagy by electron microscopy in mammalian cells. *Methods in enzymology,* 452 number**,** 143-164.

Yu, L., Wan, F., Dutta, S., Welsh, S., Liu, Z., Freundt, E., Baehrecke, E. H. & Lenardo, M. 2006. Autophagic programmed cell death by selective catalase degradation. *Proceedings of the National Academy of Sciences of the United States of America,* 103 number**,** 4952-4957.

Yu, Q., Geng, Y. & Sicinski, P. 2001. Specific protection against breast cancers by cyclin d1 ablation. *Nature,* 411 number**,** 1017-1021.

Zeiss, C. *Axio observer* [Online]. Available: http://qb3.berkeley.edu/qb3/sscf-htsf/docs/Zeiss%20AxioObserver_A1_detailed%20description.pdf [Accessed 12 February 2016 2016].

Zhang, X. D., Deslandes, E., Villedieu, M., Poulain, L., Duval, M., Gaduchon, P., Schwartz, L. & Icard, P. 2006. Effect of 2-deoxy-d-glucose on various malignant cell lines in vitro. *Anticancer research,* 26 number**,** 3561-3566.

Zhu, Z., Jiang, W., Mcginley, J. N. & Thompson, H. J. 2005. 2-deoxyglucose as an energy restriction mimetic agent: Effects on mammary carcinogenesis and on mammary tumor cell growth in vitro. *Cancer research,* 65 number**,** 7023-7030.

Zou, H., Li, Y., Liu, X. & Wang, X. 1999. An apaf-1· cytochrome c multimeric complex is a functional apoptosome that activates procaspase-9. *Journal of Biological Chemistry,* 274 number**,** 11549-11556.

151

Appendix:

UNIVERSITEIT VAN PRETORIA
UNIVERSITY OF PRETORIA
YUNIBESITHI YA PRETORIA

Faculty of Health Sciences Research Ethics Committee

26/06/2014

Approval Certificate
New Application

Ethics Reference No.: 230/2014

Title: Improving breast cancer therapy through oestrone analogue and glycolysis inhibitor synergism

Dear Ms Roxette Anderson

The **New Application** as supported by documents specified in your cover letter for your research received on the 4/04/2014, was approved, by the Faculty of Health Sciences Research Ethics Committee on the 25/06/2014.

Please note the following about your ethics approval:
- Ethics Approval is valid for 2 years.
- Please remember to use your protocol number (**230/2014**) on any documents or correspondence with the Research Ethics Committee regarding your research.
- Please note that the Research Ethics Committee may ask further questions, seek additional information, require further modification, or monitor the conduct of your research.

Ethics approval is subject to the following:
- The ethics approval is conditional on the receipt of 6 monthly written Progress Reports, and
- The ethics approval is conditional on the research being conducted as stipulated by the details of all documents submitted to the Committee. In the event that a further need arises to change who the investigators are, the methods or any other aspect, such changes must be submitted as an Amendment for approval by the Committee.

We wish you the best with your research.

Yours sincerely

Dr R Sommers; MBChB; MMed (Int); MPharMed.
Deputy Chairperson of the Faculty of Health Sciences Research Ethics Committee, University of Pretoria

The Faculty of Health Sciences Research Ethics Committee complies with the SA National Act 61 of 2003 as it pertains to health research and the United States Code of Federal Regulations Title 45 and 46. This committee abides by the ethical norms and principles for research, established by the Declaration of Helsinki, the South African Medical Research Council Guidelines as well as the Guidelines for Ethical Research: Principles Structures and Processes 2004 (Department of Health).

- Tel:012-3541330
- Web: //www.healthethics-up.co.za
- Fax:012-3541367 Fax2Email: 0866515924
- H W Snyman Bld (South) Level 2-34
- E-Mail: fhsethics@up.ac.za
- Private Bag x 323, Arcadia, Pta, S.A., 0007

152